INVESTIGATIONS OF HIGH ALTITUDE GEOMAGNETIC PHENOMENA USING A RUBIDIUM VAPOUR SYSTEM

THESIS

Submitted by

WILLIAM FORBES STUART, B.Sc., D.I.C.,

for the

Degree of Doctor of Philosophy

in the

Faculty of Science

UNIVERSITY OF LONDON

February 1965

Department of Geophysics
Imperial College,
London, S.W.7.

ERRATA

Fig. 2.5. For $\underline{\mu}_J$ read total $\underline{\mu}$

Fig. 2.6. For $\underline{\mu}_F$ read total $\underline{\mu}$

ABSTRACT

The electrical properties of atomic particles, and the absolute nature of the constants involved in their behaviour in magnetic fields, suggest that some of the nuclear resonance techniques of atomic physics might present new methods of measuring the magnetic field phenomena of importance in geophysics. To this end "Optical Pumping" of Rubidium vapour is considered in detail and the experimental development of a magnetometer using the principle is discussed.

The construction of two forms of instrument is described. One, which operates in fields between 1 gauss and 0.05 gauss is applicable to ionosphere rocket probe experiments and ground studies. The other, operating in fields from 10^{-1} gauss to 10^{-4} gauss, is designed for satellite payloads in the study of the magnetosphere and extra-terrestrial magnetic fields.

In order to provide a comprehensive assessment of the capabilities of optically pumped magnetometers a field study into the nature and occurrence of micropulsations was undertaken. Micropulsations are small, regular variations in the geomagnetic field, whose origin lies in the interaction of Solar emanations with the earth's magnetic field

at high altitude. Their properties may indicate the structure of the exosphere and of the magnetic field at the magnetosphere boundary.

Measurements of micropulsation periods were made at Kiruna (Sweden), Lerwick, Eskdalemuir and Hartland (U.K.) in an attempt to establish a correlation between latitude and the period of the events.

The results of the observations and an analysis of the performance of the rubidium vapour magnetometer are discussed, with recommendations regarding the further development of the instrument and its application in geomagnetism.

CONTENTS

CHAPTER 1

INTRODUCTION

General Review.

The study of the outer regions of the Earth's atmosphere has a relatively short history, the direct examination of high altitude phenomena beginning largely with the discovery of cosmic rays, and the inference that charged particles enter the Earth's environment from the space beyond. Immediately, the magnetic field configuration was recognised as a controlling influence, by virtue of the interaction between it and the moving electric charges. Optical observations of Aurora presented a general picture of their form and occurrence, and the theoretical work of Störmer, together with the experimental research of Birkeland, suggested a connection between auroral phenomena and particles entering the Earth's atmosphere under the control of the geomagnetic field.

The existence of a continuous stream of charged particles emanating from the sun and impinging on the Earth was suggested, and formed the basis of the Chapman-Ferraro theory of magnetic storms, in which an impulse within the charged stream was constrained by the geomagnetic field, and

established a circulating current around the Earth. The treatment described some features of magnetic storm disturbance well, but failed to complete the model. The success of the theory established the existence of the solar wind, and demonstrated that the magnetic field of the Earth formed a cavity with a radius of 6.E.R. within the particle stream, and that, at the boundary, interaction between the magnetic field and the particle flux was responsible, to a great extent, for some observed geomagnetic phenomena.

The ionosphere, which occurs in altitude between 80 Km and 500 Km, is a phenomenon established by the direct ionisation of local atmospheric particles by radiant emission from the sun. Although its form is affected by the geomagnetic field and it is responsible for many geomagnetic variations, the ionosphere is not a product of the control exerted by the magnetic field of the Earth on the solar particle stream, and may be regarded as a distinct low altitude phenomenon.

Stimulated by the success of the Chapman-Ferrarro theory considerable effort has been applied to the theoretical analysis of the properties of the solar stream, its interaction with the magnetosphere at its boundary, and the form of control exerted by the magnetic field upon the entry of particles into the exosphere and their motions therein. The general equations of magnetohydrodynamics, which govern the

flow of charged particles in the presence of a magnetic field are complex, and explicit solutions are not usually possible for real situations. Accepted features of the models used to describe the Earth's environment show the broad results of the general theory, supplemented by particular results of the motion of individual particles, whose properties and motion can be defined. Some fundamental properties of the situation have been established. The solar wind is taken to be electrically neutral, consisting of protons and electrons. It is regarded as a streamline flow and the distortion it produces in the Earth's magnetic field and which the Earth's field produces in it has been examined (e.g. Beard 1960). Mathematical treatments describe the sunlit side of the interaction boundary well, for suitably chosen parameter values, but fail to evaluate the dark side with sufficient accuracy to permit a complete description.

Particles entering the magnetosphere are believed (Singer 1957) to be trapped in orbits by the lines of magnetic field, where they travel in a spiral motion along the lines of force. The direction of motion along the line of force is reversed near the poles, where the field strength increases, and the particles oscillate between corresponding points in each hemisphere. It is pointed out by most authors that the motions of individual particles do not necessarily indicate the particular properties of large groups of particles under

the same influence.

The experiments carried out by Cahill and Van Allen (1956) and later workers provided the first detailed measurements of upper atmosphere parameters. The rocket flights of Cahill (1958) established the existence of an equatorial ring current in the E region of the ionosphere and which is responsible for the abnormal diurnal variation of the geomagnetic field near the magnetic equator. Later rockets launched at Fort Churchill by Meredith, Davies, Heppner and Berg (1958), in which magnetic field measurements were made in conjunction with electron density measurements, established the existence of sharply defined current sheets which occur at E region ionospheric altitudes and are associated with simultaneous auroral displays. These were thought to be responsible for some magnetic bay occurrences.

With the advent of Earth satellites accurate measurements of the outer atmosphere could be made, and the prospect stimulated research in all aspects of the new technique. In particular the problem most urgent in geomagnetism was the production of a magnetometer able to withstand the environment of a rocket launch, and capable of making the required field measurements with sufficient reliability. The main restrictions on a satellite instrument are in size, power consumption and mechanical strength. Considerable loss of efficiency in the experimental payload would occur

if the instrument could not operate over a wide field range, including low field values, with a high resolution and without being unduly affected by its orientation with respect to the field vector. The problem, in satellite geomagnetism, of acquiring measurements of very small variations in time and space of a large quantity, makes instrumental techniques very complicated. The difficulties encountered by Cahill, in his rockoon experiments, and of Singer, Maple and Bowen (1951), who used component instruments, illustrate the problem.

The development, by Varian Associates, of the proton precession magnetometer, devised by Packard, was the first step toward solving the difficulties. The instrument has been extensively used in rocket flights, with some success, and, installed in Vaguard III, was the first geomagnetic survey instrument carried in a satellite (Cain, Shapiro, Stolarik and Heppner 1962). The technical advantages of total scalar field measurements were shown to outweigh the loss of detail, and theoretical effort was applied to geomagnetic harmonic analysis in terms of scalar values (Zmuda 1958). The shortcomings of the proton magnetometer when applied to the study of the exosphere and its boundary lie in its power consumption which for continuous operation is high, and in the time, restricted by the polarising-counting cycle of the instrument, taken to acquire a measure-

ment. Also the signal amplitude from the proton magnetometer decreases with ambient field strength and imposes a severe limitation upon the lowest field in which it can operate successfully.

In 1960 Coleman, Davis and Sonnet reported the use of an induction coil sensor, consisting of a permalloy core surmounted by a multi-turn coil of wire. The core was mounted in the plane perpendicular to the satellite spin axis so that in operation the flux change, as the probe rotated, induced an electrical signal in the coil. The peak amplitude and phase with respect to the satellite spin coordinate system indicate magnetic field magnitude and its direction in the plane of rotation of the sensor. The experiment is reported to have observed a ring current at 6.5 E.R. and an interplanetary field strength of 2γ in a direction perpendicular to the ecliptic. The shortcomings of the system lie mainly in electronic problems of drift, the range of the instrument and the lack of complete information it yields. Since it requires to be rotated the necessity for either a spinning satelite or an acceptable motor on a stabilised satellite detract from its applicability.

In 1958 Varian Associates suggested that "optically pumped" atomic resonance could be used to make an atomic oscillator whose frequency, controlled by the Larmor

precession of the atoms, would be linearly dependant on the magnetic field magnitude. Such an instrument using Rubidium vapour was developed under contract to N.A.S.A. and versions have been flown in 1960 in a Javelin rocket and in 1961 in the probe Explorer 10. Rubidium magnetometers were installed in the first two Ranger Lunar probes which failed to exit from their 'parking' orbits round the earth. The instrument carried in the rocket was a complete success. In Explorer 10 the surfaces designed to maintain the correct thermal environment were destroyed during the launching with the result that the instrument became overheated and failed to operate after several hours. In the Ranger series, in which the experiment was designed to make interplanetary and Lunar field measurements, the magnetic field values at the parking orbit produced magnetometer signal frequencies outside the telemetry bandwidth and no measurements were made. However, the ancilliary telemetry information indicated that the magnetometer was, in fact, operational.

The unfortunate history of the Rubidium magnetometer in* satellite work to date has been due to causes which were

*The Rubidium Magnetometer has been used successfully by Dr. Ness and his colleagues in the IMP-1 satellite (Interplanetary Monitoring Platform) launched on November 27, 1963 and still in operation on May 30th 1964. Data has been acquired about the solar origin of the interplanetary magnetic field. (Ness and Wilcox 1964).

altogether external to the instrument. In all cases where it was permitted to operate properly it behaved satisfactorily. Explorer 10, which contained flux-gates as additional apparatus and which were calibrated against the rubidium magnetometer, provided a great deal of information about the dark side of the interaction boundary of the deformed magnetosphere (Heppner at al 1963). However, the limits of thermal environment within which the Rubidium magnetometer operates present technical difficulties in its use in satellite payloads.

The properties of the self-oscillating magnetometer which make it suitable for consideration as a satellite instrument are listed in Table I with the main features of the other useful instruments. It is possible to make general comparisons between types of magnetometer from Table I, but it is not intended to prove the absolute superiority of the Rubidium system. The experimental observations, together with the technical requirements in the aquisition of complete information, preclude the choice of a unique magnetometer for satellite work. A detailed description of the errors of magnetic measurement, their significance in field analysis, and their bearing on measuring technique is contained in A Review of the World Magnetic Survey by Heppner.

TABLE I

	Flux-gate	Induction coil	Proton	Rubidium
Resolution	1 in 10^3	1 in 10^3	1 in 10^5	1 in 10^6
Weight	1 lb	2 lb	5 lb	1 lb
Power	1 watt	5 watts	25 watts	2.3 watts
Range	limited	limited	high fields	wide
Output	voltage	voltage	frequency	frequency
Scalar or Vector	Vector	Partial vector	scalar	scalar
Calibration required	in flight possible	in flight not possible	not reqd.	not reqd.
Temp. Range	wide	wide	wide	limited

The Origin of Micropulsations

Micropulsations are regular fluctuations of the geomagnetic field which have peak to peak amplitudes from a few tenths of a gamma to several tens of gammas and periods between 1 second and several minutes. They represent the very low frequency extension of the electromagnetic spectrum and the period limits are arbitrary, usually defined by the frequency response of the detection equipment used. It is

thought that the pulsations are generated at high altitude within the magnetosphere and propagated by various modes to the Earth's surface. The propagation equations for these waves are similar in principle to the propagation of electromagnetic waves in an ionised gas with the additional complication that, because of the low frequency, the interaction between the wave and ions as well as electrons and the interaction between the ions and neutral atoms must be taken into account. The variation of these parameters and of the magnetic field further complicate the matter.

In 1954 J.W. Dungey considered in detail the electrodynamics of outer atmosphere and showed that, although extremely complex, the interaction between the magnetic field, and its variations, and the particles in the exosphere permitted the transmission of very low frequency fluctuations. He indicated that the system possesses certain natural frequencies of oscillation and suggested a way by which solar plasma striking the boundary could excite these frequencies.

It is not intended here to give any detail of the mathematical treatment and only the essential equations are quoted. In 1954 Dungey uses Maxwell's equations,

$$\nabla \times \underline{H} = \underline{j}, \quad \nabla . \underline{H} = 0, \qquad \nabla \times \underline{E} = -\frac{d\underline{B}}{dt}, \qquad \underline{B} = \mu \underline{H}$$

together with $\underline{E} = \underline{V} \times \underline{B}$, which describes the dynamo electric field, with $\underline{V}$ the bulk velocity of the charged particles,

to derive

$$\frac{\partial \underline{H}}{\partial t} = \nabla \times (\underline{V} \times \underline{H})$$

By considering the disturbance field h, defined by

$\underline{H} = \underline{H}o + h$, $|\underline{H}o| \gg |h|$ and $\nabla \times \underline{H}o = 0$,

it is possible to arrive at the equation

$$4\pi\rho \frac{\partial^2 \underline{E}}{\partial t^2} = - \underline{H} \times (\nabla \times \nabla \times \underline{E}) \times \underline{H} \qquad (1)$$

which is the general equation for the propagation of transverse waves transmitted along the direction of the line of force with a wave velocity $2H\sqrt{\frac{\pi\rho}{\mu}}$ in a non-uniform field, where ρ is the mass density of the gas. These waves are called Alfvén waves after their discoverer who investigated their transmission within plasma streams under simplified conditions.

The mathematical treatment proceeds by expanding equation (1) in spherical coordinates and results in two coupled partial differential equations governing $E\phi$ and $V\phi$, the components of electric field and particle velocity in the azimuthal direction. By assuming axial symmetry, when $\frac{\partial}{\partial \phi} = 0$, the two equations become independent, permitting each to be carried to a solution. The boundary conditions cannot be readily presented, with the exception of the lower boundary, represented by the Earth's surface and the lower ionosphere which Dungey (1954B) shows to be a good reflector.

Two simplified modes are suggested by the form of the equations. The first is defined by $E_\phi = 0$, i.e. the component of electric field perpendicular to the meridian is zero. This implies that the magnetic vibration is perpendicular to the meridian and it is possible to interpret the equation as one where the disturbance propagates along a line of force, and to show that each surface of revolution of a line of force may oscillate independently. Thus the two points at which a line intersects the Earth's surface are considered to be the boundaries of the vibrating section. Using a dipole field geometry and a value of $\rho = 10^{-21}$ gm/cc, Dungey arrives at the approximate formula $T = 0.6 \sec^8\lambda$ to describe the periods of normal modes observed at latitude λ on the ground. The values calculated from this formula are shown by curve A in Fig I.1.

Another mode suggested by Dungey's analysis is described by $U_\phi = 0$, ie. magnetic oscillation occurs in the meridian plane and may extend over the whole of the outer atmosphere. The boundary conditions cannot be obtained explicitly for this mode and this type of oscillation is discussed qualitatively. Periods of the order of one hour are indicated.

Dungey's work in 1954, although unable to produce periods corresponding to observed phenomena, made a

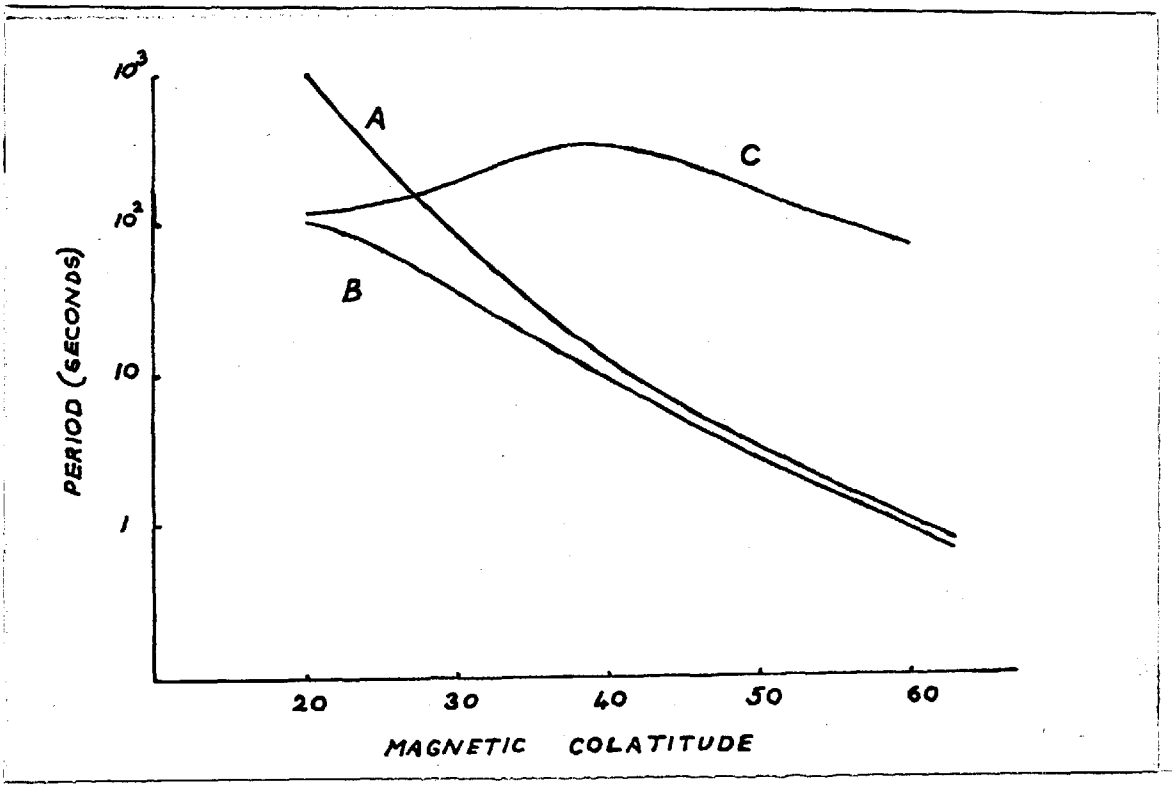

Fig. 1.1 The calculated variation of period of the Torsional mode with latitude. A) Dungey. B)Westphal and Jacobs confined dipole. C) Confined dipole, variable plasma density.

realistic evaluation of the exosphere and the fundamental properties of low frequency propagation. Further development of the theory has not provided a significant increase in explicit knowledge of the origin of micropulsations and a largely intuitive attitude would seem to prevail.

The two types of oscillation described above have been supported in theory by several authors (Kato, Watanabe, Westphal and Jacobs 1962) and are usually referred to by the names Toroidal, or torsional, to describe the twisting

vibrations of lines of force, and Poloidal to describe the oscillation taking place in the meridian.

Torsional waves have been the only waves capable of explicit solution and consist of vibrations where the disturbance magnetic field is perpendicular to a line of force and transmitted along the line of force to the Earth's surface. The period of the fundamental mode of the vibrations observed at ground level increases with latitude due to the change in length and field strength of the corresponding lines of force. The period is also affected by the particle density of the regions in the exosphere through which the line passes, a matter which is not considered by Dungey. The rapid increase in period at high latitude suggested by the $\sec^8\lambda$ term is due to the simple geometry of the dipole model.

The Poloidal vibrations, for which Dungey could not state the boundary conditions, are represented by the magnetic disturbance vector oscillating in the meridian plane, and the propagation, not constrained to one direction, is sometimes called isotropic propagation. For this reason micropulsations arising from this mode are expected to exhibit a greater range of geographical occurrence than those due to the toroidal mode. Dungey estimated a typical period for such oscillations to be of the order of one hour, Kato and Watanabe estimate the fundamental period to be 10-20 minutes.

It is clear from experimentally derived values of period that neither type of oscillation fits observed pulsations very well. Westphal and Jacobs have attempted to modify the solution of the equations of toroidal oscillations, firstly by correcting the geometrical model to take account of the restriction of the dipole magnetic field within a cavity, and secondly to take account of the variation of particle density in the exosphere. A spherical cavity was used, and its effect was to reduce the high latitude periods considerably, the greater reduction being associated with the smaller radius of the confining sphere. Low latitude values of period did not deviate to any great extent from the values of Dungey. When the variable plasma density profile was introduced in conjunction with the confined geometry an increase in low latitude periods was achieved. Fig. 1.1 shows the curves calculated by Westphal and Jacobs using these two methods, and compared with Dungey's. The radius of the confining field is taken to be 6 Earth radii for the curve B, and 4 E.R. for C which has the particle density distribution taken into account. It may be noted that if the cavity radius in Curve C is increased an increase in the high latitude periods should result from the dilation of the lines of force.

The plasma profile is illustrated in Fig. 1.2 B, and the corresponding Alfvèn velocity profile is shown in Fig.1.2A.

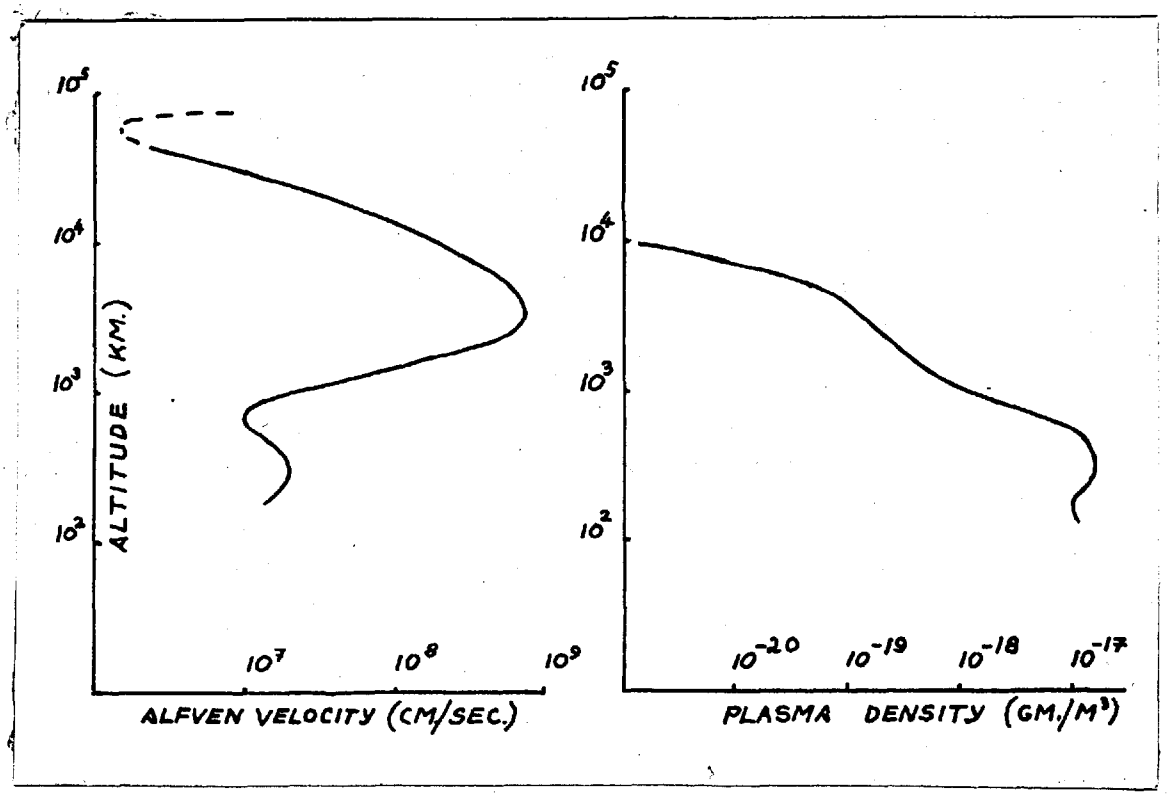

Fig. 1.2. Illustrating the variation of Alfvèn velocity, and particle density with altitude.

Kato and Watanabe have reported that, in middle and low latitudes, the disturbance vector is mainly in the meridian plane, whereas the vector at high latitudes predominates in a direction perpendicular to the meridian. Since no phase difference was detected between events at different stations Dungey suggested that the pulsations recorded represented standing waves, a fact which is taken to indicate that at middle and low latitudes poloidal resonance is the source. The long periods of poloidal waves expected in

theory negate this inference, until the plasma profile is considered. Watanabe argues that since the Alfvèn velocity profile is that shown in Fig. 1.2A, waves propagated vertically down through the region of high velocity at 3000 Km will be reflected at the base of the ionosphere and again be partly reflected at the high velocity region. Thus a resonant cavity exists at a much lower altitude than the exosphere boundary and which does not vary greatly in properties over the surface of the Earth. This feature is in agreement with experiment, where observations show that periods do not vary greatly with latitude.

Review of Micropulsations

Micropulsations occur throughout the world, with the possible exception of polar regions, and display several forms exhibiting different characteristics. The classification below lists three main types and agrees in essence with the generally accepted scheme.

Large Pulsations

These pulsations have amplitudes generally within the range of 5 - 20% and are observed to have a limited occurrence near auroral latitudes. Their period is within the range 2 - 10 minutes and they are mainly a night time event, often associated with disturbances. Their periods

agree well with those calculated by Dungey for torsional vibrations.

Included in this category are the Giant pulsations (P_G) which are thought to be special events in which a very clear sinusoidal large pulsation occurs over a small area, usually near auroral latitudes.

Continuous Pulsations (P_c)

Continuous pulsations occur mainly in the daylight hemisphere and include periods from 1 sec. to two minutes. The amplitude is typically one gamma and occurrence is world wide. The duration and continuity of the wave train is variable, but often continuous activity can be detected for 10 - 12 hours. Jacobs and Sinno indicate that the occurrence of Pc's increases considerably at auroral latitudes.

Transient Pulsations (P_t)

These pulsations, which occur mainly in the night hemisphere, consist of bursts of pulsation. Amplitude and period are typically larger than corresponding P_c's and continuity is not often displayed. The idealised form associated with P_t events is a decaying burst lasting several tens of minutes containing pulsations of, typically, 100 seconds period. This type of event is somewhat rare, and short bursts of varying shape are more common.

Other forms of pulsation activity exist in less clearly defined groups. Long period oscillation occurs throughout the day, with periods of the order of 30 minutes - 1 hour. The amplitude is generally low and often the phenomenon is accompanied by disturbance. In general it is thought that there is insufficient knowledge to classify pulsations other than the three distinct types above.

Experimental work has been carried out largely using observatory magnetograms, which in general do not yield sufficient resolution for detailed comparison. However, several groups have designed instruments and experiments for precise observations of micropulsation events. Synoptic measurements are not yet available to indicate the actual variation of period with latitude. Component measurements have indicated a lack of pulsation activity in the vertical component which may confirm Dungey's suggestion, to establish one boundary condition, that the Earth's surface is a good conductor.

Kato suggests, on the basis of component measurements, that Pc's and P_t's occurring in low and middle latitudes are poloidal in origin. His work with Watanabe produces correct period values for Pc's using the Alfven velocity barrier as a boundary of the resonant cavity and he modifies the solution of the poloidal mode so that the line of force with equatorial radius = 6 E.R., which corresponds to a line

within the auroral zone, produces the correct order of period for observed P_t's. He suggests that the torsional vibrations have too short a period to occur at low latitudes and that the mode is represented by the large pulsations occurring in auroral zones. This fact is confirmed by Sugiura who observed that large amplitude transient pulsations observed near the auroral zone are observed simultaneously at the magnetic conjugate point.

Troitskaya (1961) has made observations of pulsations occurring in the period range 1 - 10 seconds. A regular modulation of the amplitude of continuous activity was observed and named 'pearls' appropriately. It was remarked that 'pearl' behaviour rarely occurred in pulsations having periods greater than 4 seconds. This phenomenon has been shown by Tepley (1961) and Heacock (1963) to consist of several discrete trains of pulsation, each with periods increasing approximately linearly with time, and which begin at the same period at slightly different times. The intermodulation of the two waves produces the 'pearl' effect.

McNicol (1962) has established a direct proportionality between the amplitude of Pc occurrence and the Kp figure for the day, supporting evidence to this effect, produced by Jacobs (1961). McNicol making observations at approximately 35°S, indicates a decrease of Pc period during the course of the day, and has been able to show a correspondence between

the upper frequency of pulsation activity and the Kp index.

Recent work, carried out by Voclker and Jaeschke, at 53°N, has indicated a variation of the period of some types of pulsations with latitude and also with time of day. This work covered a relatively short traverse of latitude (600 Km) and is being at present extended. Their results show an increase in the period of observed pulsations during the morning (Siebert 1964).

Ness (1961), who observed micropulsations with a self-oscillating rubidium magnetometer at Fredericksburg, during the flight of Explorer 10, reports a daily variation of period of the pulsations observed, which were about 10 seconds. It was not possible to discover any precise dependence of the period upon time of day.

Remarks

It is clear that the theoretical groundwork on the origin of pulsations has scored a direct success in establishing the modes and propagation of the vibrations of the magnetosphere believed to be responsible for this phenomena. A reliable model has been suggested from which experimental investigation can be planned with some hope of success.

It has been assumed, provided that a resonant cavity exists, that suitable stimulus is available to excite oscillation. There is no doubt that the stimulus is associated

with the solar plasma stream, and Dungey has shown how waves may be formed on the magnetosphere boundary by the solar wind, in a manner entirely analogous to the way waves are generated on the surface of a lake. It is not difficult to imagine a situation where slight irregularities in the constitution of the solar wind may be transferred to the exosphere in a manner sufficient to excite oscillation. A distinct 27 day recurrence period has been detected in the occurrence of Pc's (Jacobs and Westphal 1964), and is taken to confirm the direct connection between Pc's and the solar wind.

Direct confirmation of the theory has not been possible in any simple way and, as yet, there is an inadequate statistical mass of data, of sufficient detail to suggest the correct modifications to the basic model. Definite information about the period structure of pulsations, their vector properties, and their phase relationships are essential before further manipulation of exosphere parameters is attempted.

At the same time it is necessary to consider other prospective ways in which the pulsations may be generated and propagated. For example the oscillation between mirror points of bunches of trapped electrons, originally suggested by Störmer as a source of micropulsations and discarded because the behaviour of the trapped gas was insufficiently

known, has been invoked as the explanation of pearls by Tepley.

Detailed measurements of the exosphere and the Earth's magnetic field, at present being carried out, will improve the working model considerably. For example Cahill and Amazeen (1963) report having observed the magnetosphere boundary on the daylight side of the Earth to be at 10 E.R. The observations were made using saturable core magnetometers, and indicated a disturbed magnetic field immediately beyond the presumed boundary. Such a position for the boundary would modify curve B in Fig. 1.1 and result in an improved fit with experiment at high latitudes. Heppner has shown a similar disturbance in the field external to the magnetosphere boundary, and also indicates that the extension of the magnetosphere due to the tear drop is as great as 22 E.R. on the dark side of the Earth. Bridges (1961) has shown, from plasma measurements made with Explorer X, that the fluctuating magnetic field is often associated with variations of the energy and number of particles in the solar stream.

In order to complement this work, detailed synoptic measurements of pulsation phenomena should be carried out to establish the relevant features of similarity and dissimilarity between the main types of pulsation. If possible direct correlation between pulsations observed on the ground and

pulsations detected at source by satellite experiments should be attempted.

CHAPTER 2

THE OPERATING PRINCIPLES OF THE MAGNETOMETER

Introduction

The magnetometer employs a radio frequency resonance method of detecting the Zeeman splitting of the hyperfine strucutre of a line of the spectrum of a sample of rubidium vapour in weak magnetic fields. In this section the physical processes of the resonance, and of the method by which it is detected are described in a semi-classical way, details of the atomic physics involved may be found in Kopfermann 1958.

Before describing the resonant interaction it is convenient to discuss the term "optical pumping", which is used to describe the technique by which suitable resonance of the observed atoms is made available. The technique, first suggested by Kastler (1950) and demonstrated by Dehmelt (1957A),was developed considerably as a research tool in fine structure spectroscopy, and formed the basis of the first rubidium magnetometer suggested by Bell and Bloom (1957), and reported by Skillman and Bender (1958).

Naturally occurring rubidium has two main isotopes Rb^{85} and Rb^{87}, in the ratio of abundance 7 to 3. They

differ in the magnitude of their nuclear spin, and except where nuclear spin magnitude affects a measured quantity e.g. in the value of the "splitting factor", the discussion for Rb^{85} applies to Rb^{87}.

In the semi-classical models of the atom used by Sommerfeld and by Larmor the quantum numbers may be described as follows:

$\underline{L}$ represents the orbital angular momentum of the electrons, and may only have values which are integral multiples of $\hbar$.

$\underline{S}$ represents the spin angular momentum of the electrons and may only have values which are integral or half integral multiples of $\hbar$.

$\underline{I}$ represents the nuclear spin, and may only have values which are integral or half integral multiples of $\hbar$,

where $\hbar = \frac{h}{2\pi}$, is a rationalised form of the action quantum used by Plank to derive the laws of black-body radiation. In the purely quantum mechanical treatment the quantum numbers appear directly in the discrete solutions of the wave equation, with the additional feature that the magnitude of an angular momentum $\underline{A}$ is given by $\underline{A} = \sqrt{A(A+1)}$.

The total energy of an atom, disregarding its motion, is the sum of the energies associated with $\underline{L}$, $\underline{S}$ and $\underline{I}$. The addition of atomic angular momenta is restricted by the spin-orbital interaction of the electron, which can be

understood classically as the spin magnetic moment of the electron experiencing the magnetic field due to its orbital motion. The constraint thus imposed is that $\underline{L}$ and $\underline{S}$ must be added, and their resultant $\underline{J} = \underline{L} + \underline{S}$, which is quantised, added to $\underline{I}$ to produce the total angular momentum $\underline{F} = \underline{J} + \underline{I}$, which is also quantised.

Fig. 2.1 shows the energy level diagram for Rubidium 85 in a schematic form, based on the vector additions of $\underline{L}$, $\underline{S}$, $\underline{I}$. The ground state denoted by $S_{\frac{1}{2}}$ has $\underline{L} = 0$, $S_{\frac{1}{2}}$. This is split by the action of nuclear spin $\underline{I} = 5/2$ into two levels with $\underline{F} = 3$ and 2 respectively. Similarly the first excited state, P, has $\underline{L} = 1$, $\underline{S} = \frac{1}{2}$ and is split into substates $P_{\frac{1}{2}}$ with $\underline{J} = \frac{1}{2}$, and $P_{3/2}$ with $J = 3/2$, corresponding to the conditions when the angular momenta $\underline{L}$ and $\underline{S}$ are antiparallel and parallel respectively. Each of the substates $P_{\frac{1}{2}}$ and $P_{3/2}$ is split once again by the nuclear spin into $\underline{F}$ levels.

The generalisation of Bohr's quantisation principle leads to the state of affairs where angular momentum is also quantised in any chosen direction to which observations of angular momentum is referred. Hence the sum of $\underline{L}$ and $\underline{S}$ is quantised, and the sum of $\underline{J}$ and $\underline{I}$, and more generally, if the angular momentum of an atom is measured with respect to a chosen axis it may only appear in discrete values. This 'space quantisation' leads to a splitting of the $\underline{F}$ levels, when a reference direction is imposed on the system, into

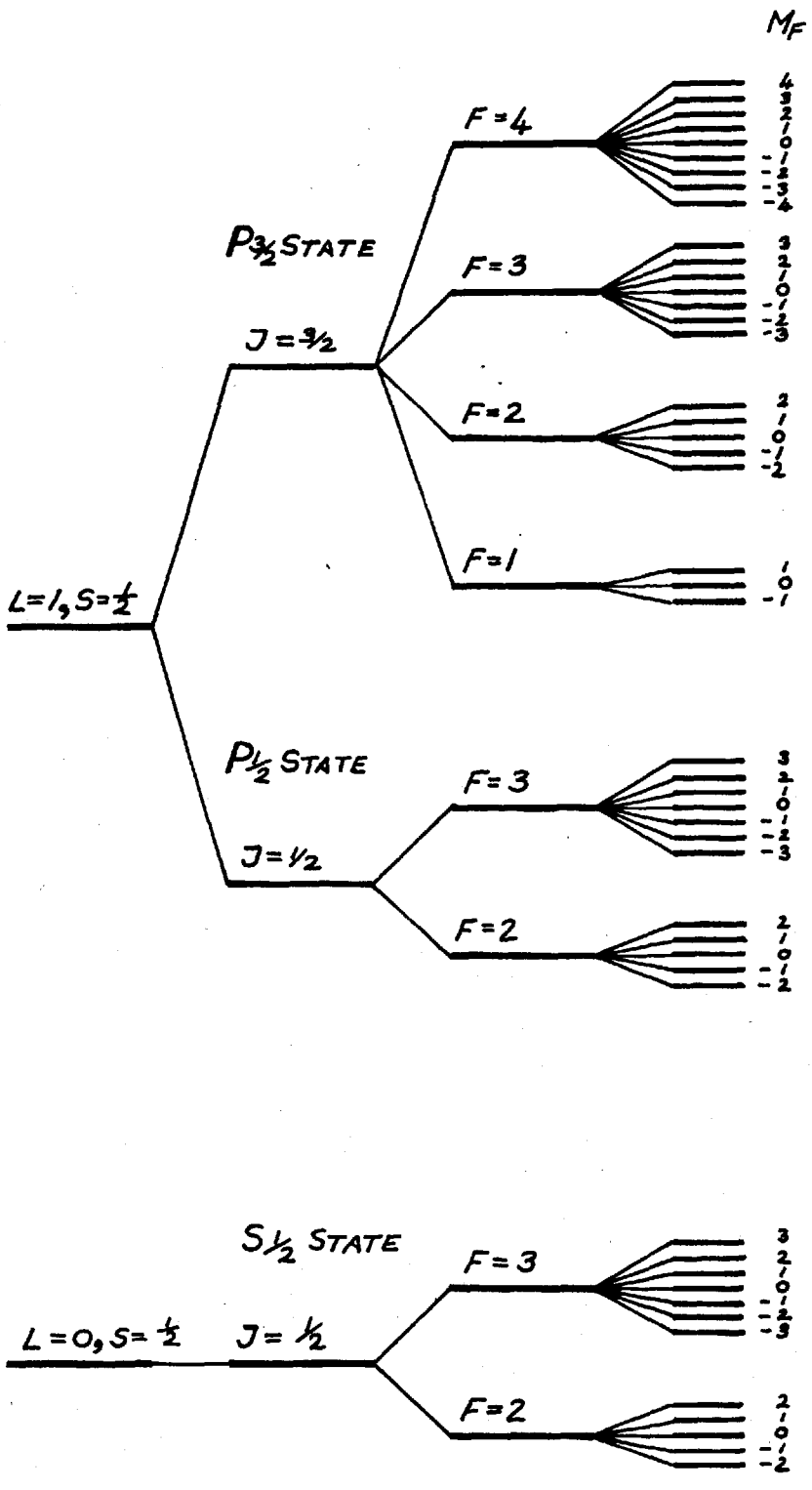

FIG 2.1

ENERGY LEVEL DIAGRAM FOR RUBIDIUM 85, $I = 5/2$.

sublevels denoted by M_F. The angular momentum of an atom measured along a given axis may take one of the values $M_F = F, F - 1 \ldots\ldots 1-F, -F$, corresponding, classically to the permitted projections of F along the chosen direction. The sublevels all have the same energy except when a magnetic field is present, which space quantises the momenta, and because of the magnetic moment associated with the angular momentum of an atom, produces energy differences between adjacent sublevels. The M_F numbers take on the significance of indicating the magnitude of the component of magnetic moment in the field direction and the energy acquired by an atom in the magnetic field.

Optical Pumping

A transition $S \rightarrow P$ takes place when an atom absorbs a photon of light of the energy corresponding to the energy difference between the S and P states. Relaxation $P \rightarrow S$ takes place with the emission of a similar photon by the atom.

Restricting the discussion to transitions between $S_{\frac{1}{2}}$ and $P_{\frac{1}{2}}$ states, it is to be understood that for an individual atom the transition takes place between distinct M_F sublevels of the respective states. Besides other selection rules governing the transitions which are not pertinent to the description, the quantum mechanical treatment permits M_F

to change by $\pm$ 1, 0 in an optical transition, corresponding to the absorption or emission of a photon with spin $\pm$ 1, 0. Classically this is the conservation of angular momentum in the direction of the light beam.

Fig. 2.2 is a simplified description of the state of

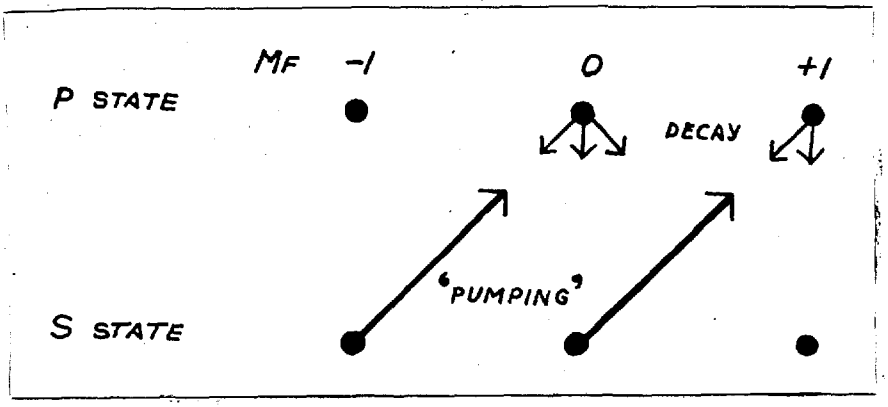

Fig. 2.2.

affairs when an assembly of atoms is irradiated by a collimated beam of light consisting of spin = +1 photons. The collimation of the beam ensures that all the atoms are under the same space quantisation constraint imposed by the axis of the light beam, which is also the axis of rotation of the photon spin. The M_F sublevels of the P state are drawn horizontally above those of the S state for clarity of description.

In a transition S $\rightarrow$ P the absorption of a spin = +1 photon must increase the space quantised value of an atom's angular momentum by 1 unit. Thus transitions corresponding to ΔM_F = +1 are the only ones permissible. These are

indicated by the diagonal arrows in Fig. 2.2. The $M_F = +1$ sublevel of the S state cannot be excited by the optical beam.

The decay $P \rightarrow S$ does not suffer from the restriction on ΔM_F since it does not require the absorption of one of the incident photons, and in the relaxation ΔM_F may be ± 1, 0 with about equal probability, if such a transition is available, allowing some of the atoms excited into the P state to decay to the S state sublevel $M_F = +1$.

The effect of repeated or continuous irradiation is the accumulation of atoms in the $M_F = +1$ sublevel of the ground state. This corresponds to the alignment of the atoms in the assembly along the direction of the light beam.

The pumping of atoms up the M_F scale is very rapid. A casual inspection of the situation in Fig. 2.2 indicates that 90% of the total number of atoms present are in the $M_F = +1$ sublevel of the S state after three cycles of the absorption and decay.

If the P state has a sublevel with $M_F = 2$ the S state sublevel $M_F = +1$ could be excited causing the steady accumulation of atoms there to be dispersed, shuttling back and forth between S and P. Such a condition exists for rubidium, where the $P_{3/2}$ state has a value of F greater than the $S_{\frac{1}{2}}$ state and optical transitions $S_{\frac{1}{2}} \rightarrow P_{3/2}$ may take place as well as $S_{\frac{1}{2}} \longrightarrow P_{\frac{1}{2}}$. The two transitions form a doublet of

the optical line, similar to the well known sodium D lines. Because of its undesirable effect on the optical pumping process it is necessary to remove the line corresponding to $S_{\frac{1}{2}} \rightarrow P_{3/2}$ from the irradiating light beam. This is possible in the case of rubidium because the doublet separation is large. The D_1 line, corresponding to $S_{\frac{1}{2}} \rightarrow P_{\frac{1}{2}}$, has a wavelength of 7945Å and the D_2, corresponding to $S_{\frac{1}{2}} \rightarrow P_{3/2}$, has a wavelength of 7800Å and it is possible to use standard techniques of optical filtering to exclude the D_2 line. It is clear from Fig. 2.1 that even when D_1 light only is used the F = 2 level of the $S_{\frac{1}{2}}$ state may be excited to the F = 3 level of the $P_{\frac{1}{2}}$ state, reducing the optical pumping efficiency of the $S_{\frac{1}{2}}$, F = 2 level. For this reason the F = 2 level is not significant and the resonance observed in rubidium is that of the F = 3 level of the $S_{\frac{1}{2}}$ state (the ground state).

The spin of a photon arises out of its electromagnetic properties and corresponds directly to the polarisation of the associated wave. Thus, it may be taken that spin = +1 photons correspond to a right circularly polarised light beam.

This is the optical pumping process fundamental to the magnetometer. The property used to measure magnetic fields is the energy difference between M_F sublevels of the $S_{\frac{1}{2}}$ state in the presence of a magnetic field. Without optical

pumping the populations of the sublevels would be equal except for a negligible difference due to the Boltzman distribution. In such a case a process used to stimulate $M_F \rightarrow M_F$ transitions would induce as many one way as the other, and while the atoms might be shuffled within the ground state no net change in energy or alignment could take place.

The $M_F \rightarrow M_F$ resonance is most simply detected by irradiating a sample of rubidium vapour by a light beam, polarised as described, collinearwith the field direction so that the quantisation axis for light alignment coincides with that for magnetic energy separation. It is clear that, when all the atoms of the sample have been pumped to the extreme M_F sublevel of the ground state, the light beam is transmitted through the sample without loss of intensity due to absorption by the atoms, because in the extreme M_F sublevel there is no permissible optical transition available to the atoms. If a process may be adopted to dislodge some atoms from the pumped state to a sublevel where optical absorption is possible, its action will be indicated by a decrease in the intensity of the light transmitted through the sample due to the renewed pumping of the disturbed atoms. It is possible to achieve such a situation using the resonant effect upon the atoms of a radio frequency magnetic field. When the frequency of the applied RF field corresponds to

the energy of separation of the M_F sublevels in the magnetic field, atoms may be dislodged from the pumped state by the resonant interaction. The condition governing the resonance is that $h\nu = \Delta E$, where h is Plank's action quantum, ν is the frequency of the RF field and ΔE is the energy between adjacent M_F sublevels due to the magnetic field. ν is approximately 470 Kc/s per gauss for Rb^{85}.

The Self Oscillating System

The significance of space quantisation is that the atomic angular momentum is constrained to precise orientations with respect to the direction of quantisation. It follows classically, from the interaction of a magnetic field with a magnetic moment intrinsically associated with an angular momentum, that the angular momentum vector precesses about the field direction at a constant rate. This is illustrated in Fig. 2.3, where $\underline{H}_o$ is the magnetic field, $\underline{\mu}$ the magnetic moment and $\underline{G}$ the angular momentum associated with $\underline{\mu}$. $\underline{i}$ and $\underline{j}$ are unit vectors describing the component directions of $\underline{G}$ parallel and perpendicular to $\underline{H}_o$

$$\underline{\mu} \times \underline{H}_o = \frac{d}{dt} (\underline{G})$$

describes the situation.

i.e. $$H_o \sin\theta = \frac{d}{dt} (|\underline{G}| \sin\theta . \underline{j})$$

Fig. 2.3.

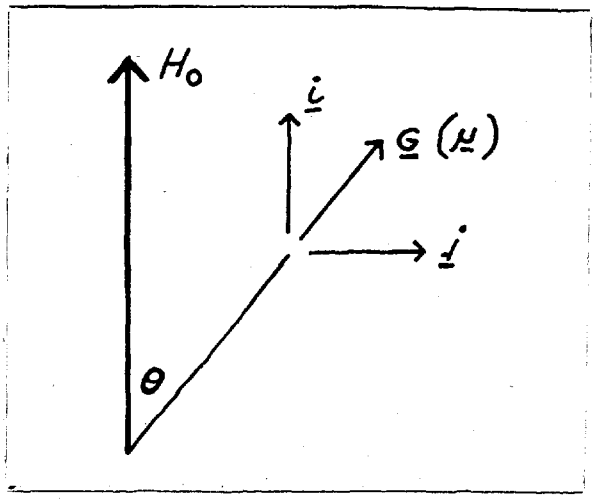

or $$\frac{d\underline{i}}{dt} = \underline{\mu}\frac{H}{G}\ , \qquad (2.1)$$

where θ and G are fixed. This describes the rotation of $\underline{i}$ about $\underline{H}$ at the rate $\underline{\mu}\frac{H}{G}$. This is the precession used by Larmor to build a semi-classical atomic model. $\frac{\mu}{G}$, the ratio of magnetic moment to angular momentum of an atom is called the gyromagnetic ratio and given the symbol .

For a given angular momentum the magnetic moment is fixed, and the significance of the M_F quantum numbers is the allocation of fixed discrete values of θ. Thus, to this order, all M_F levels precess about a magnetic field with the same Larmor frequency.

The splitting of a level by the interaction of angular momenta is best described using the 'splitting factor', g, of Landé. The derivation used here is carried out for the combination of $\underline{L}$ and $\underline{S}$ for clarity, and the nuclear interaction follows.

In the case of an atom with $\underline{L}$ and $\underline{S}$ it should be noted that the magnetic moments associated with an electron are negative and the spin magnetic moment is twice what might be expected in classical terms.

Fig. 2.4 illustrates the calculation. Since $\underline{\mu}_S$ is

Fig. 2.4

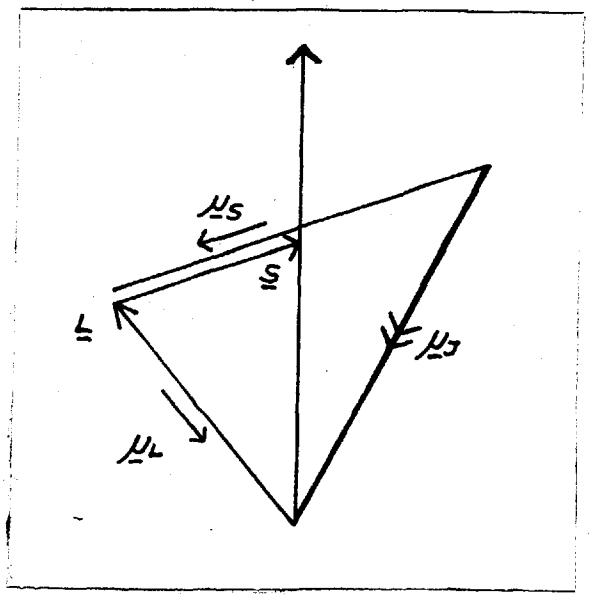

twice the value expected on purely classical grounds, the total moment $\underline{\mu}$ is not collinear with $\underline{J}$. The spin-orbit interaction makes $\underline{L}$ and $\underline{S}$ precess around $\underline{J}$ and the total magnetic moment $\underline{\mu}$ likewise precesses about the $\underline{J}$ direction. This value, $\underline{\mu}$, of the magnetic moment has no real physical significance since its rate of precession is high; its component in the direction of $\underline{J}$ becomes the effective magnetic moment.

$$\mu_J = \mu_L \cos (L, J) + \mu_S \cos (S, J)$$

where (L, J) represents the angle between $\underline{L}$ and $\underline{J}$ etc.

The value of the magnetic moment associated with a particle of mass m and charge e moving in a circle of radius r with velocity v, shown in Fig. 2.5 is given by

$$\mu = \frac{i\,A}{C} \text{ emu, where i is in esu.}$$

Fig. 2.5.

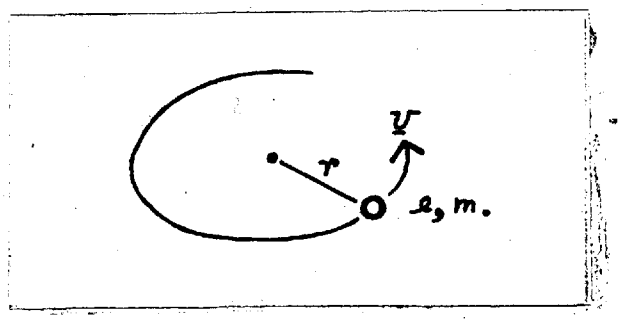

Bearing in mind that the current requires to be averaged over the path of the orbit

$$i = \frac{e\,v}{2\pi r} \quad \text{and} \quad A = \pi r^2$$

Therefore $\mu = \frac{e\,v\,r}{2C}$.

The angular momentum of the particle is given by $G = m\,v\,r$, so that $\mu = \frac{e}{2MC} \times G$.

In this way it can be shown that

$$\mu_L = -\frac{2}{2MC}\,\hbar\sqrt{L(L+1)}$$

$$\mu_S = -\frac{e}{MC}\,\hbar\sqrt{S(S+1)}$$

Thus

$$\mu_J = -\frac{e\hbar}{2MC}\left[\sqrt{L(L+1)}\cos(L,J) + 2\sqrt{S(S+1)}\cos(S,J)\right]$$

The cosine formula, remembering that the quantum mechanical value of $\underline{L}$ is $\sqrt{L(L+1)}$, leads to

$$\mu_J = \beta g_J \sqrt{J(J+1)} \qquad (2.2)$$

where $\beta = \frac{e\hbar}{2mC}$ = Bohr magneton

and $g_J = \left[1 + \frac{J(J+1) + S(S+1) - L(L+1)}{2\,J(J+1)}\right]$

= the splitting factor for the combination.

The derivation of the splitting factor accounting for nuclear spin follows by cominging $\underline{I}$ and $\underline{J}$. This is illustrated in Fig. 2.6.

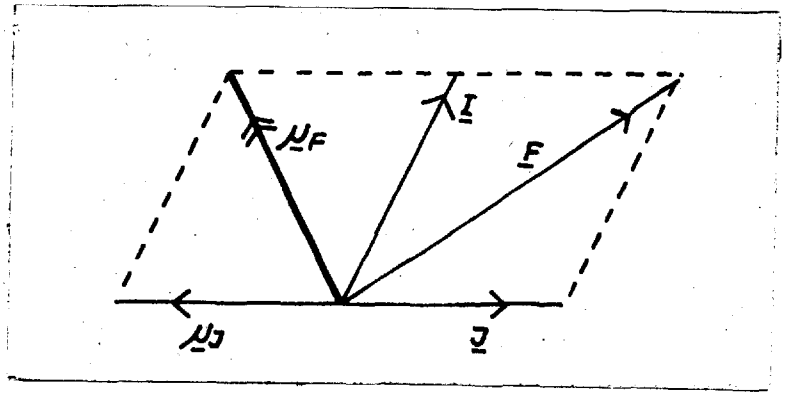

Fig. 2.6

Again the total μ does not lies along $\underline{F}$ and

$$\mu_F = \mu_I \cos(I,F) - \mu_J \cos(J,F)$$

Also
$$\mu_I = \frac{e\hbar}{2MC} g_I \sqrt{I(I+1)}$$

by analogy with the previous section, and replacing the electronic mass m with the proton mass M.

Therefore

$$\mu_F = -\frac{e\hbar}{2mC} \left[g_J \cos(J,F) \sqrt{J(J+1)} - \frac{m}{M} g_I \cos(I,F) \sqrt{I(I+1)} \right]$$

$$= -\beta g_F \sqrt{F(F+1)}$$

where β is the Bohr magneton
and g_F atomic splitting factor.

The energy an atom may acquire in a magnetic field is classically

$$\Delta E = \mu H \cos\theta$$

= H x component of μ in the $\underline{H}$ direction.

Using μ_F derived above,

$$\Delta E = H.\ \beta\ g_F\ .\ "\sqrt{F(F+1)}\ \cos\theta"$$

$$= H\beta g_F.\ M_F$$

Where M_F represents the value of the projection of the angular momentum in the $\underline{H}$ direction.

The energy separation between adjacent M_F sublevels is given by

$$\Delta E = H.\ \beta\ g_F, \text{ since } \Delta M_F = 1.$$

$$= \mu_F.\ \frac{\hbar}{G}\ .\ H. \text{ using (2.3)}$$

$$= h\ .\ \frac{1}{2\pi}\ .\ \frac{di}{dt} \text{ using (2.1)}$$

$$= \underline{\underline{h.\nu}}$$

That is, the energy difference between M_F sublevels is equal, and the frequency of the transition quantum is the same as the Larmor precession frequency of the atom.

A more precise calculation, taking into account the interaction energies of the atomic momenta shows that there exists a small difference between the precession rates of the different M_F sublevels, and correspondingly the transition energies are different. In the case of the $S_{\frac{1}{2}}$ state of rubidium this results in the radio frequency resonance exhibiting a fine structure consisting of six lines, separated by approximately 60 c/s per gauss, corresponding to the six $\Delta M_F = 1$ transitions available. The splitting of this fine structure is proportional to H^2.

The rotating coordinate system

Consider the precession described by

$$\underline{\mu} \times \underline{H}_o = \frac{d}{dt}(\underline{G}) \text{ and the transformation}$$

to a set of axes rotating about H_o with angular velocity $-\underline{\omega}$, described by Rabi, Ramsey and Swinger, 1954.

Then $\frac{d\underline{G}}{dt} = \frac{\partial \underline{G}}{\partial t} - \underline{\omega} \times \underline{G}$

where $\frac{d}{dt}$ is rate of change in the laboratory system,

$\frac{\partial}{\partial t}$ is rate of change in the rotating system.

Thus $\frac{\partial \underline{G}}{\partial t} - \underline{\omega} \times \underline{G} = \underline{\mu} \times \underline{H}_o$

ie. $\frac{\partial \underline{G}}{\partial t} = \underline{\mu} \times \underline{H}_o + \underline{\omega} \times \underline{G}$

$$= \underline{\mu} \times \underline{H}_o - \frac{\underline{\mu}}{\gamma} \times \underline{\omega}$$

$$= \underline{\mu} \times (\underline{H}_o - \frac{\underline{\omega}}{\gamma})$$

This equation describes, in the rotating coordinate system, the precession of $\underline{\mu}$ about an equivalent field $(\underline{H}_o - \frac{\underline{\omega}}{\gamma})$.

Consider the situation where the rotating coordinate system is defined by a magnetic field H_1, perpendicular to H_o, and rotating about it with angular velocity $\underline{\omega}$. This is illustrated in Fig. 2.7. In the rotating system the magnetic field is the resultant, H_R, of H_1 and $(\underline{H}_o - \frac{\underline{\omega}}{\gamma})$. A magnetic moment precesses about H_R when observed in the rotating coordinate system.

If H_1 rotates at the rate W_o about H_o, such that

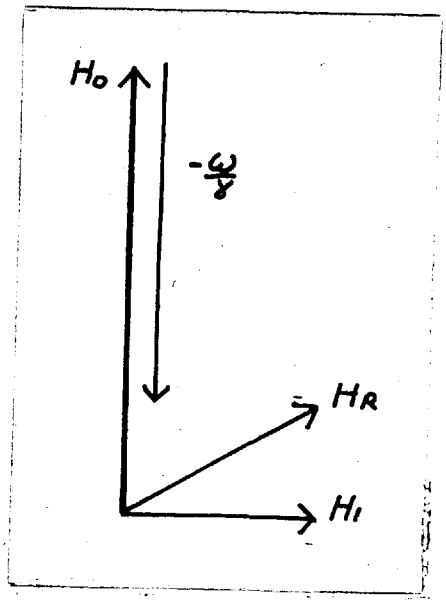

Fig. 2.7.

$H_0 - \frac{\omega_0}{\gamma} = 0$, precession takes place about H_1 alone.

In an optically pumped assembly of atoms it is possible to use the rotating system of coordinates in the description of the operation of the self-oscillating magnetometer. If a light beam, collimated and polarised as before, is shone on to the sample at an inclination to the magnetic field H_0, optical pumping takes place, the direction of the space quantisation being the axis of the light beam (De Zafra 1960). In the rotating system of axes described above the light beam becomes a cone around H_0, which is homogeneous because the light source is not coherent. Thus the alignment of the atoms forms a cone about H_0, producing a net magnetic moment

$\bar{\mu}_o$, which is in the H_o direction, since the components perpendicular to H_o annul each other over the cycle of rotation. $\bar{\mu}_o$ precesses about H_R in the manner described, at the same time decaying under the stimulus of the H_1 radio frequency field. The decay is arrested by the renewed pumping of decay atoms and an equilibrium is reached at a value $\bar{\mu}$. $\bar{\mu}$ is then a fixed vector in the rotating coordinate system. In the simple case where $\omega = \omega_o$ the precession of $\bar{\mu}_o$ takes place about H_1, in the plane perpendicular to H_1, because the initial position of $\bar{\mu}_o$ is along H_o. Transferred back to laboratory coordinates the net magnetic moment $\bar{\mu}$, produced by optical pumping, is stable in magnitude and precesses about H_o at the Larmor frequency and bears a fixed phase relationship of 90^o to the H_1 field's rotation. Thus the applied radio frequency field, rotating about H_o in the correct sense at the resonance frequency produces a phase coherance in the precession of the optically aligned atoms which is one quarter of a cycle different from the phase of the radio frequency field.

Dehmelt suggested that the precession about H_o of the net alignment might be used to detect the resonant precession. (Dehmelt 1957B, Bell & Bloom 1957). The optical absorption coefficient for an atom depends on its orientation with respect to the light beam and the precession of the net moment of the sample corresponds to a variation of the net

orientation with respect to the light axis. When $\vec{\mu}$ is in its nearest position to the direction of the light beam, corresponding to an 'all-pumped' condition, light transmission is high. When $\vec{\mu}$ has precessed 180^{o} to a position corresponding to a largely depumped condition, optical absorption is high resulting in a reduction of the transmitted light. This is most easily envisaged classically when it is remembered that in the stable condition the net magnetic moment consists of atoms in all M_F sublevels precessing in phase to a first order, around the H_o field direction. The change of orientation of $\vec{\mu}$ with respect to the light beam during the precession presents a 'depumped' atom with a modulated opportunity to absorb a photon.

The modulation of the intensity of the transmitted light may be used to monitor the resonance. In the self-oscillating magnetometer the light modulation is detected by photocells, amplified, and fed back as the radio frequency field, H_1, to the sample. The configuration is shown in Fig. 3.8.

Assume that the conditions are such that $\vec{\mu}$ lags H_1 by 90^{o} at the resonance, and consider the moment of first switching on the amplifier, the light having been started previously. The light modulation has the form $L = A \cos \omega_o t$, for this first randomly occurring moment precesses at the true resonant frequency. Suppose the amplifier has a suitable gain, so that H_1 has the form $H_1 = B \cos (\omega_o t + \phi)$

i.e. a phase shift ϕ is produced by the amplifier in converting the light modulation to a magnetic field. The case where $\phi = +90^{\circ}$ is trivial; oscillation takes place precisely at the resonant frequency. When $\phi \neq 90^{\circ}$ the first increment of H_1 leads to the net moment by less than 90° say. The atomic moments attempt to get in step and in doing so have to slow down. This causes the first increment of light modulation to have $\omega_o' < \omega_o$. The implication is that the H_1 frequency is less than that which satisfies $H_o - \frac{\omega_o}{\gamma} = 0$ in the rotating system, and the net moment, precessing in a cone about H_R reaches an equilibrium position which lags H_1 by less than 90°. Thus two effects take place;

1. The net moment decreases its precession frequency in its attempt to lock on to H_1, and
2. The decreased frequency fed back as H_1 causes to precess about an H_R $(= \sqrt{H_1^2 + (H_o - \frac{\omega}{\gamma})^2}\,)$ which is not perpendicular to H_o.

A stable state is reached where the phase change in the amplifier matches that between μ and H_R at some frequency $\neq \omega$ The limit of this oscillation is the line width of the resonance, beyond which self-oscillation cannot occur.

Orientation dependence of the Self-Oscillator.

In the previous discussion it was assumed that μ lags the rotating H_1 field. This involves assuming that the

magnetic moments produced by the optical pumping process precess in a clockwise direction about the positive direction of magnetic field. If this were not true it would only be necessary to reverse the direction of the polarisation of the light beam to produce a net moment of the opposite sign.

Consider the light modulation, the geometry of which is illustrated in Fig. 2.8. This is drawn in the laboratory

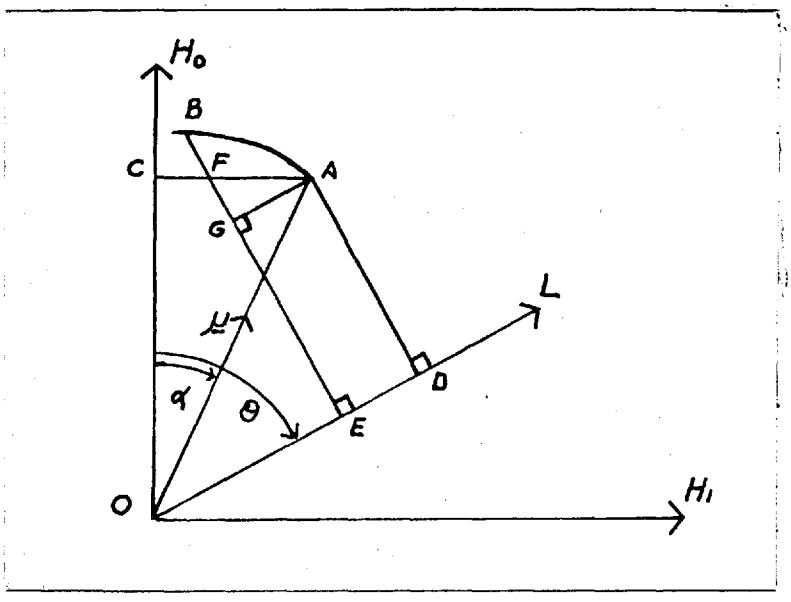

Fig. 2.8.

coordinates in the plane of $\underline{H}_0$ and $\underline{L}$, the light beam, at the moment t = 0, when $\vec{\mu}$ is also in this plane.

OA represents $\vec{\mu}$ at t = 0, and OB lying in some direction other than the plane of the paper represents the position of $\vec{\mu}$ at $t = t^1$.

The angle ACB = ωt^1.

OC is the projection of μ on the H_0 axis.

OD is the projection on the $\underline{L}$ axis of $\vec{\mu}$ at t = 0, and

BFGE represents the plane, perpendicular to L drawn through B. F is the intersection of this plane with CA and AG is drawn parallel to L.

Thus OE represents the projection on the L axis of $\bar{\mu}$ at $t = t'$.

Angle OAC = $90 - \alpha$

Angle GAO = $\theta - \alpha$

Therefore, GAF = $90 - \theta$

$$FA = \bar{\mu} \sin\alpha \, (1 - \cos \omega t')$$

$$GA = FA \cos GAF$$

$$= \bar{\mu} \sin\alpha \sin\theta (1 - \cos \omega t')$$

GA represents the variable part of the component of $\bar{\mu}$ along L.

The magnitude of $\bar{\mu}_o$ is the projection of the net orientation on the H_o direction and is thus proportional to $\cos \theta$. It is therefore possible to write $\bar{\mu} = k \cos \theta$, whence the equation for light modulation takes the form

$$\mathcal{L} = K \sin\alpha \sin 2\theta (1 - \cos\omega t'),$$

where K is a constant.

This indicates a time variation of $\mathcal{L}$ at the precession frequency and also an amplitude dependence of $\mathcal{L}$ upon the value of θ. In particular $\mathcal{L} = 0$, when $\theta = 0, 90^\circ, 180^\circ$. Thus the magnetometer is subject to null zones when the light beam and the magnetic field are collinear or perpendicular to each other. Note also that the sign of $\mathcal{L}$ changes between $\theta < 90^\circ$ and $\theta > 90^\circ$. This means that the light modulation

changes phase between the two ranges of θ. Thus for a magnetometer of the type described, operation is only possible for one of the hemispheres $\theta \lesssim 90^{\circ}$ unless the facility exists for changing the sign of the 90° phase shift as required.

Another feature of the orientation dependence of a magnetometer based upon the type of resonance discussed is illustrated in Fig. 2.9. The fine structure of the

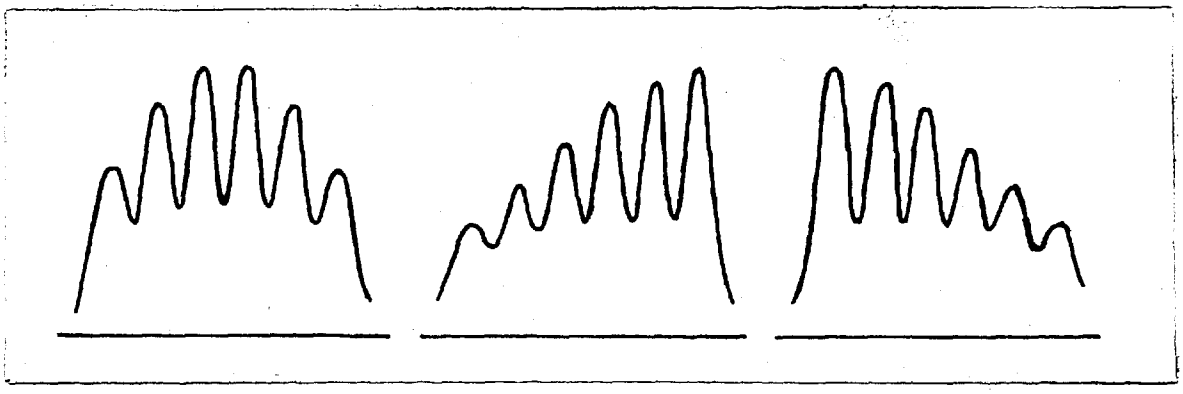

Fig. 2.9. Illustrating the dependence of the self-oscillator frequency upon orientation.

resonance has been mentioned previously and its association with the different M_F sublevels explained. These component lines have been observed using the swept resonance technique. Because of their closeness together a very narrow line width is required for their observation. In the self-oscillator resolution of the lines would present ambiguity in the oscillation, the question arising as to which of the individual lines was responsible for the self-oscillation.

For this reason, and in order to achieve maximum signal-to-noise ratio from the instrument it is preferable to use a broad line width in which the individual components are not resolved. The resultant loss in absolute accuracy is no more than the indeterminacy of which component is sustaining the oscillation.

However, it is found that the relative strengths of the individual lines show a variation dependent on the orientation of the light beam with respect to H_o. This is due to the dependence of the optical absorption coefficient on the alignment with respect to the light beam, in the same way as the light modulation takes place. Thus the angle between $\underline{L}$ and $\underline{\mu}$ specifies one of the M_F sublevel orientations which is in a more favourable position to absorb light.

The result of this condition is to produce a variable assymetry of the composite line, which produces a small variation of the frequency of oscillation of the self-oscillator dependent on the light beam orientation.

CHAPTER 3

DEVELOPMENT OF THE SELF-OSCILLATING MAGNETOMETER

Introduction

A great deal of the interest which prompted the initial investigation of optically pumped systems for measuring magnetic fields lay in their ability to measure low values of field strength, and rapidly changing values of field strength, and in their adaptability to configurations suitable for inclusion into satellite and rocket payloads. The engineering constraints arising from such applications were taken into account from the outset. Wherever possible component parts were chosen and designed to produce a compact, light, yet robust final unit.

The experimental approach was, in general, empirical and followed the order of firstly detecting the resonance signal and using this as a monitor with which to optimise the optical system, so that observations of the radio frequency signal produced by the freely precessing atoms could be made. This leads directly to the study of self-oscillation and the subsequent development.

Component Equipment

Fig. 3.1 shows the basic equipment and the sensor configuration used in the preliminary investigations.

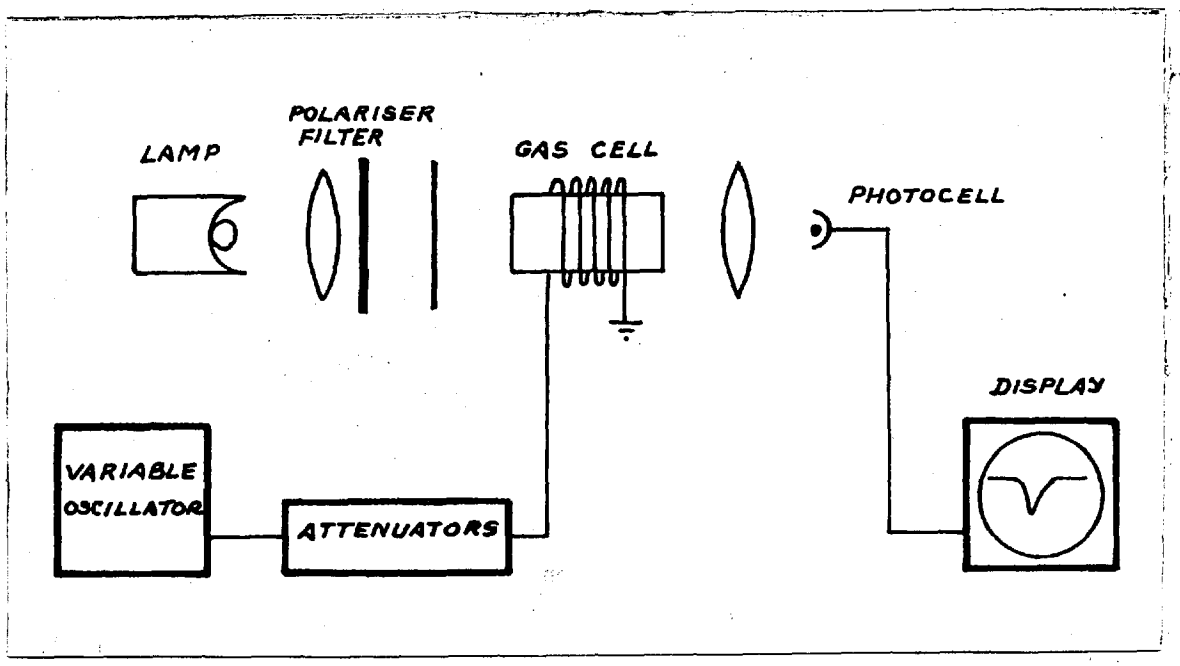

Fig. 3.1. Experimental arrangement for observing the swept resonance.

Lamp

The lamp was supplied by Varian Associates, California. It consists of a single triode high frequency oscillator ($\sim$ 100 Mc/s) the coils of which surround a small glass bulb containing a trace of Rubidium in a low pressure atmosphere of Krypton. The Krypton pressure is its equilibrium pressure at liquid nitrogen temperatures. The valve, a GEC 5718, is a small transmitting valve consuming 3.5 watts. The Rubidium vapour in the bulb is excited into an electrodeless

discharge by the radio frequency field between the coils of the tuned circuit of the oscillator.

Light Filter

The light filter, supplied by Barr and Stroud Ltd., Glasgow, is a high quality multiple interference filter of the metal dielectric type, mounted in glass. It has a peak transmission of 60% at 7948 Å with a 60 Å pass band. This suitably suppresses the unwanted D_2 resonance line.

Circular Polariser

The circular polariser consists of an absorption linear polariser efficient at the wavelength concerned followed by a quarter-wave plate. Various types of polariser were used in the progress toward improved signal strength. A combined polariser supplied by Polaroid Inc., produced the best and most convenient unit.

Lenses

Lenses used in the optical system are manufactured by Kodak Ltd., under the title of Ektachrome filters. They are fresnel zones etched on rigid plastic. Their performance as lenses is suitable for the application, while their lightness and the convenience with which they can be cut and mounted are of considerable advantage. Glass lenses have also

been used.

Gas Cells

Gas cells were manufactured under contract, by the G.E.C. Hirst Research Centre. They are circularly cylindrical soft glass bottles with flat ends, 2" diameter by 3" long, continaing 0.3 milligrams of natural Rubidium in a buffer gas of Helium. In the filling of the cells particular attention was paid to the removal of impurities. The cells were evacuated to a pressure of 10^{-6} mm. of mercury and baked at 350°C for 30 minutes at this pressure before the rubidium, which is a solid at room temperature, was distilled in.

The free relaxation of aligned rubidium vapour is controlled by collisions between the rubidium atoms and other atoms in which the interaction results in a loss of orientation of the rubidium. Bloom (1959) indicates that the processes by which this takes place involve electric and magnetic interaction between the atoms and by spin exchange.

The collision rate between rubidium atoms increases with an increase in the vapour pressure, while the relative frequency of collisions with the walls of the enclosing vessel decreases when the mean free path is smaller than the vessel's dimensions.

Kastler discovered that an artificially high pressure could be achieved by using a noble gas to 'buffer'the

rubidium atoms, allowing a reduction of the frequency of wall collisions without increasing the rate of collisions between rubidium atoms. The requirements for effective buffering are that the buffer atoms should have all electron shells filled and no nuclear spin (Parsons and Wiatr).

Wall coatings having buffering properties have been used to eliminate wall collisions completely and achieve very long relaxation times (Bender 1959). However since reports of their use indicated unsatisfactory long term performance their use was not considered in the construction of a magnetometer.

Bloom (Sci. Amer.) indicates that disorientation due to collisions between rubidium atoms is very small at the low partial pressures used.

Variation of temperature controls the number of rubidium atoms present in the vapour and the rate of their collisions among themselves and with the walls of the vessel. This results in a limited range of temperatures over which the resonance can be observed, since low temperatures do not produce sufficient numbers of rubidium atoms in the vapour and high temperatures produce a high relaxation rate.

Under these conditions the gas-cell dimensions are not critical and were therefore chosen as suitable for the application.

Initially a series of cells was made to determine the optimum buffer gas pressure. It was found that pressures in the range measured (2 mm - 60 mm Hg.) produced a very broad maximum of signal at 25 mm. Hg. Helium and subsequent cells were manufactured at this pressure. The end faces of the gas cells, through which the light beam must pass were made reasonably flat. The specification was that there should be no rings on the end face produced when it is fused to the cylinder. The faces used satisfied this condition. Since optically flat ends, which were in fact tested, proved to be no more efficient they were not employed.

Photocells

Silicon photovoltaic cells, whose peak optical response lies conveniently at 8000 Å, were used. Cells ranging in efficiency from 6% - 11%, and in size from $\frac{1}{2}$ cm x 1 cm to 2 cm x 1 cm were tested. In general the more efficient cells produce greater signals, but are more susceptible to noise from pick up, and fluctuations of light intensity.

Combinations of cells connected in series and in parallel behave in the normal way when their high internal resistance is taken into account. Fig. 3.2 shows the response of four 1 cm x 1 cm cells, connected in series, to a low frequency test signal with varying values of load resistance, and the

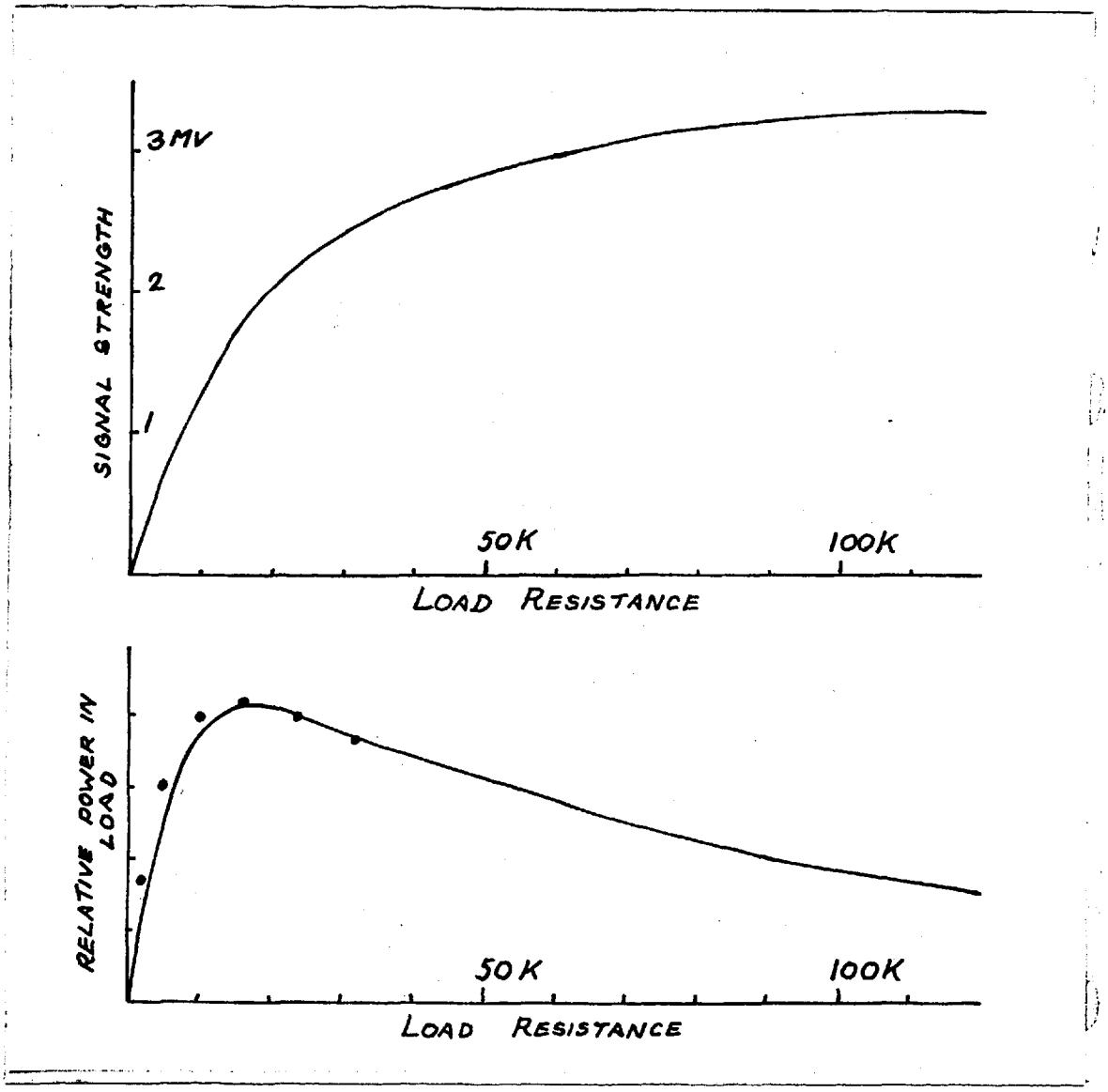

Fig. 3.2. Sighal response of four 1 cm x 1 cm photocells connected in series under load conditions.

corresponding variation of power in the load circuit. The points marked on the power curve represent values calculated from equation (2) of the Note appended to this chapter, and show good agreement with experiment.

The response shown in Fig. 3.2 indicates a source resistance of 4 KΩ per cell and this in combination with the shunt capacitance of 0.03 μf per square centimetre, limits the electrical frequency response of the photocells. Fig. 3.3 illustrates the difference in phase change and

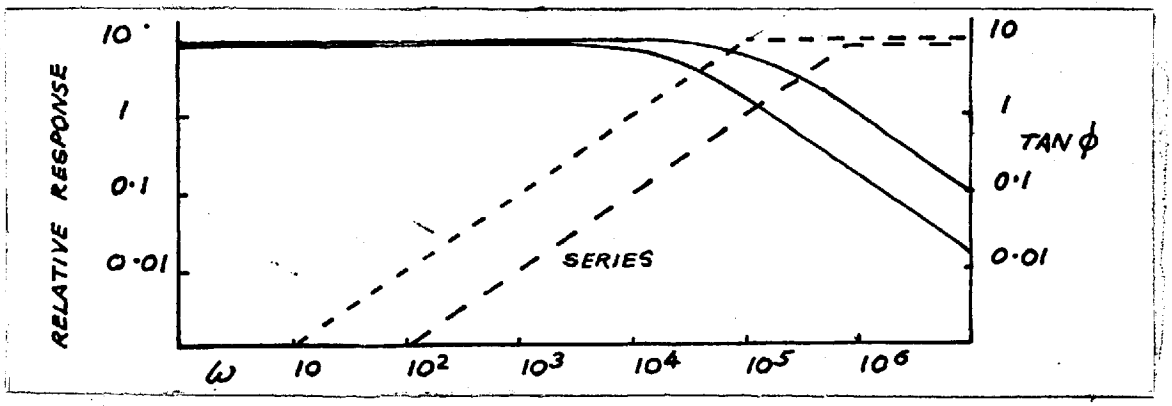

Fig. 3.3. Response and phase-shift of series and parallel photocell connections.

frequency response between configurations with four cells connected in series, and in parallel. Phase curves are shown dotted while those for relative response are solid lines. In each case the curves for series connected cells extend further to the right of the scale, and the phase curves have been flattened out at $\tan\phi = 10$, to indicate the range of effective 90° shift.

Laboratory Equipment

The test equipment used to detect and investigate the resonance is shown in Fig. 3.1 and consisted of a variable

radio frequency generator the output of which was connected via attenuators and a series resistor to the H_1 coil, 80 turns of 22 gauge enamelled copper wire wound coaxially round the gas cell, and an oscilloscope with a high sensitivity D.C. channel.

Suitable temperature conditions in the gas cell during the experimental stage were maintained by keeping the laboratory at as high a temperature as possible and by supplying additional heat directly to the cell by a small hot air blower. A commercial hand hair dryer was sufficient for the purpose and when the gas cell was lagged with glass fibre to maintain the temperature it was only necessary to heat the cell two or three times per day.

Experimental

In the development toward self-oscillation no attempt was made to resolve line structure. The progression was simply that of acquiring the strongest swept signal, detecting and optimising the radio frequency modulation, driving the modulation by the applied field, and finally closing the feedback loop.

The method employed was to set the sensing element in the Earth's field and sweep the generator frequency manually, through the resonance, until the H_1 level was adjusted for maximum signal response. Typical test conditions were:

Photocells: four 1 cm x 1 cm cells in series, connected directly to the oscilloscope.

H_1 strength: 500μa peak-peak through the coil.

The swept signal had a peak of 300μV with a noise level of 40μV peak to peak. It was not considered necessary to study the detail of the noise at this stage.

With this rather poor signal it was possible to detect resonances with Rb^{85} and Rb^{87} and to demonstrate that Rb^{87} produces its optimum signal at a higher temperature than Rb^{85}. Fig. 3.4 shows photographs of the two resonances at different temperatures. In each case the Rb^{87} signal is to the left of the trace.

Improvement in the quality of the optical components, and in the collimation of the light beam, produced a marked improvement in the signal. The collimation of the light beam was found to be achieved most satisfactorily by the lamp reflector alone. A parabolic reflector manufactured from the curve $x = 10\ y^2$ produced good results.

A small set of Helmholtz coils was used to adjust the magnetic field strength and direction for these tests.

These modifications resulted in a signal strength of 5 mV with only a slight increase in noise level due mainly to low frequency noise in the light beam. Signals of this magnitude were achieved with the optical axis within 30° of the field direction, in a field strength of 0.25 gauss. In

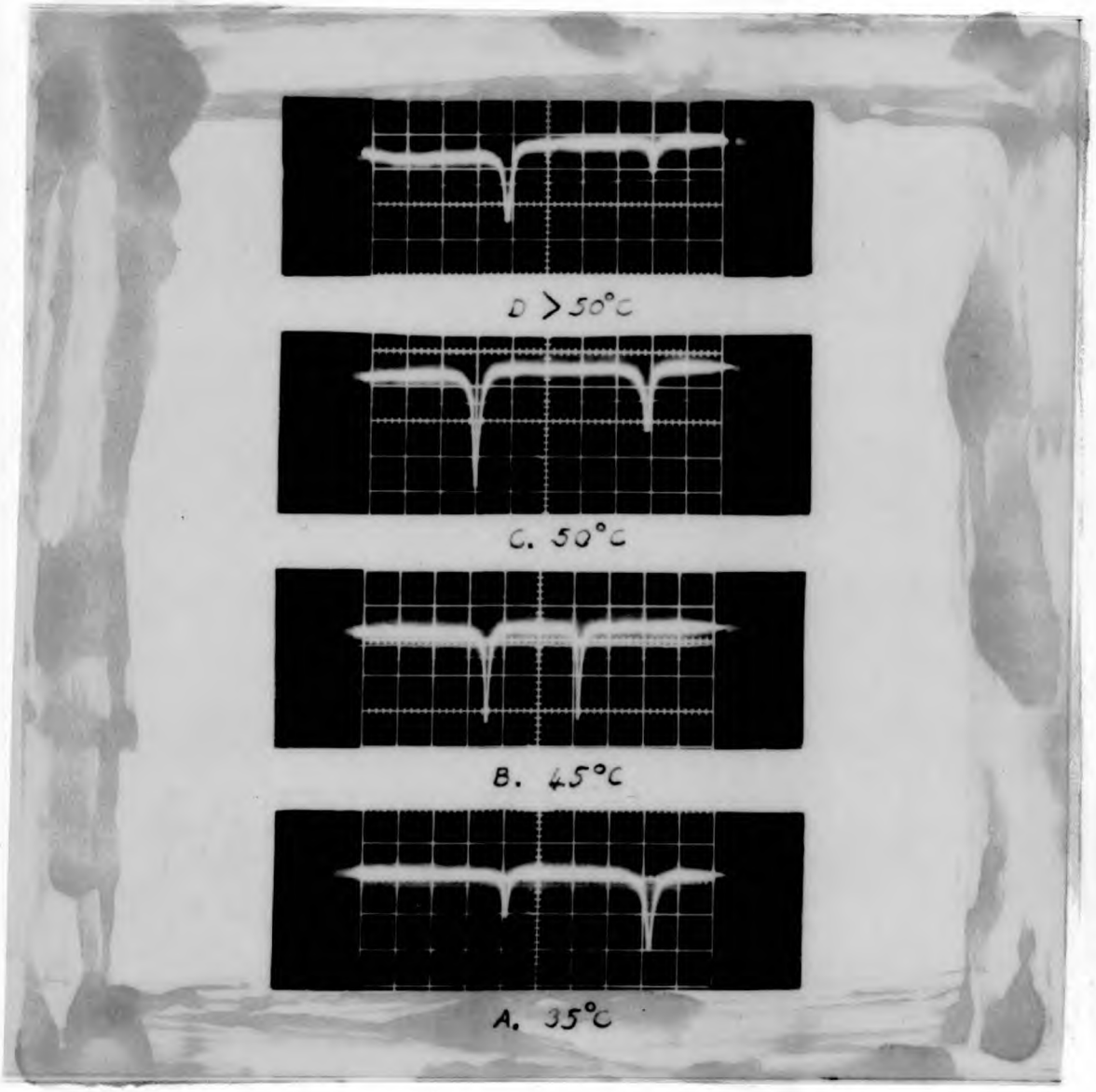

Fig. 3.4. Relative amplitude of the rubidium 87 and rubidium 85 swept resonance A) 35°C. B) 45°C. C) 50°C. D) 50°C. In all cases Rb87 appears on the left.

general, signal strength increased with light intensity, although at a later date it was found that the signal amplitude of the swept resonance reached a maximum, after which an increase in light intensity reduced its amplitude.

The variation of the amplitude of the swept signal with orientation with respect to the field direction is shown in Fig. 3.5. Agreement with a $\cos^2\theta$ law, as suggested by

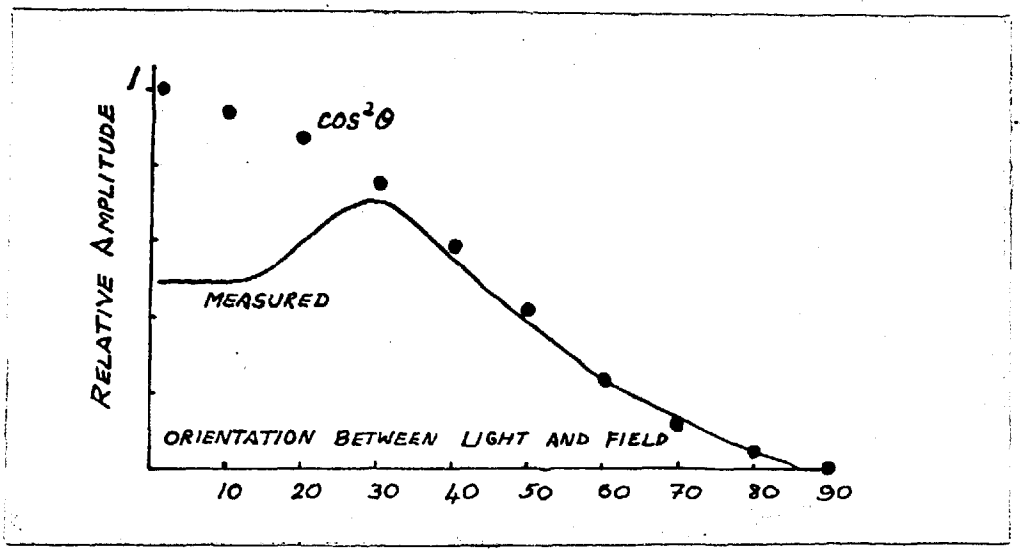

Fig. 3.5. The variation of the amplitude of the swept resonance with orientation.

Bloom is good for $\theta > 30^\circ$. It is possible that the deviation from the law for $\theta < 30^\circ$ is due to a saturation of the swept resonance by the high component of light intensity along the field direction at small angles, in the manner noted above.

It was found possible to excite the resonance by sub-harmonics of the resonant frequency, using a high level of H_1 field strenght.

The line width of the resonance was estimated from readings of the generator scale to be 1000 cycles per second. The method was to set the generator frequency to the points on either side of the line centre at which resonance was just

observable by a decrease in transmitted light intensity. The resultant line width was regarded as a maximum value, because of the error of reading the generator scale, which was of the order of 500 c/s and because of the indeterminacy of the measured points on the resonance line.

Fig. 3.6A shows a photograph of the swept resonance signal

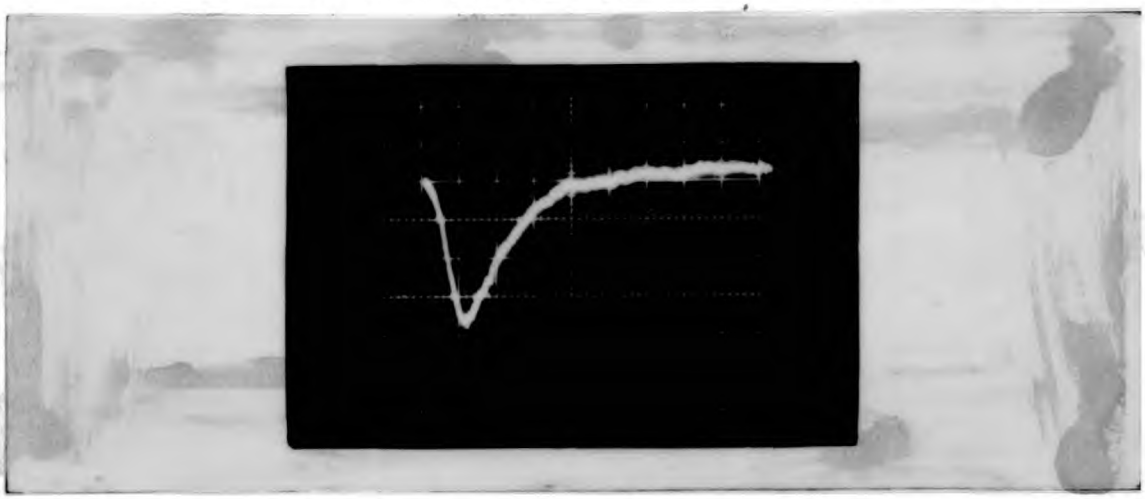

Fig. 3.6A. Photograph of the swept resonance signal. Horizontal scale 1 msec/cm., vertical scale 200 volts/cm.

of Rb^{85}. The trace was triggered by the initiation of the resonance pulse, which was generated by sweeping the generator frequency manually. The downward limb of the pulse represents the disorienting effect on the Rb atoms of the resonant radio frequency field, and the upward limb in the reorientation of the atoms by optical pumping. The time constants T_R and T_P of the relaxation process and the optical absorption are seen to be approximately 10^{-3} seconds and 2×10^{-3} seconds respectively. The value of T_R is to be compared with

relaxation times in the range 20 - 40 x 10^{-3} reported by Franzen and Little (1959), using Argon as the buffer gas, and representing free relaxation without radiofrequency stimulus. In Fig. 3.6A the H_1 field had a maximum value of 500 γ, and was expected to cause a substantial decrease in the relaxation time constant. The pumping time T_P = 2 x 10^{-3} seconds represents a higher optical absorption rate than that expected by Parsons and Wiatr (1962) because of the greater light intensity used here, and required to produce adequate signal-to-noise ratio in the self-oscillator. The line width, given by the formula $\Delta f = \frac{1}{\pi}\left(\frac{1}{T_R} + \frac{1}{T_P}\right)$, is 500 cycles per second, and represents the half width of the resonance line.

The measured time constants, T_R and T_P, are subject to inaccuracies because of the time of passage of the generator frequency across the resonance line, which imposes a time variation of radiofrequency stimulus, and also because optical absorption takes place concurrently with disorientation. It is thought that the value of T_P is a good representation of the pumping time constant. The traverse time of the generator sweep is approximately 10^{-3} seconds, so that the errors which are inevitably produced in T_R by the sweep rate and the error due to optical absorption taking place during relaxation may be neglected during the pumping limb

of the resonance pulse. This is confirmed in Fig. 3.6B

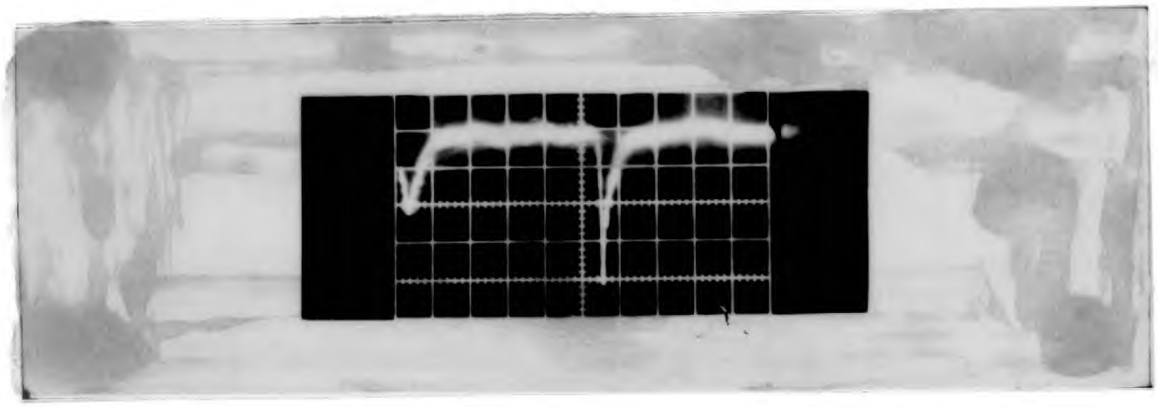

Fig.3.6B. Photograph of swept resonance. Horizontal scale 20 msec/cm. Rb^{87} on left.

where the resonance is shown with a writing speed of 20×10^{-3} seconds per centimetre. Here the passage time is less than 10^{-3} seconds and its effect on T_R is clearly shown, while T_P remains at approximately 2×10^{-3} seconds. It was possible to demonstrate that all sweep rates except the very slow produced values of $T_P \doteqdot 2 \times 10^{-3}$ seconds.

It was not possible to indicate the accuracy of the measured T_R, since a slow sweep through resonance extends the time of relaxation, and a fast sweep curtails it. Because of the H_1 stimulus, values considerably shorter than 20×10^{-3} seconds are to be expected. Also since line structure is not resolved the minimum line width is 200 c/s, corresponding to $T_R = 5 \times 10^{-4}$ seconds, and the indicated maximum value of

1000 c/s represents a $T_R = 2.5 \times 10^{-3}$ seconds.

The generator could be tuned to the frequency of the resonance line centre, indicated by the maximum decrease in transmitted light, and a state of balance achieved between radiofrequency relaxation and optical pumping. Using this condition it was possible to observe the pumping time directly by switching off the radiofrequency field rapidly. This method indicated a value of $T_P = 2 \times 10^{-3}$ seconds. By switching on the radiofrequency field under the same conditions a value of $T_R = 10^{-3}$ seconds was observed.

Another method of display, in which the ambient field is modulated at a convenient low frequency of small amplitude (less than the resonance line width) was used. This method is described in Fig. 3.7 where the effect on the optical transmission of the field modulation, centred at different points on the resonance curve, is shown. This method was used at a later date to make a direct measurement of line width. The technique was to tune the generator frequency to the maximum response at the field modulation frequency. If the modulation amplitude corresponds to half the line width this condition may be taken to represent the half amplitude point of the resonance line. The two resulting frequencies were measured by a frequency counter and showed a line half width of 340 c/s, under the conditions of the previous measurements, which correspond to those of the self-oscillating

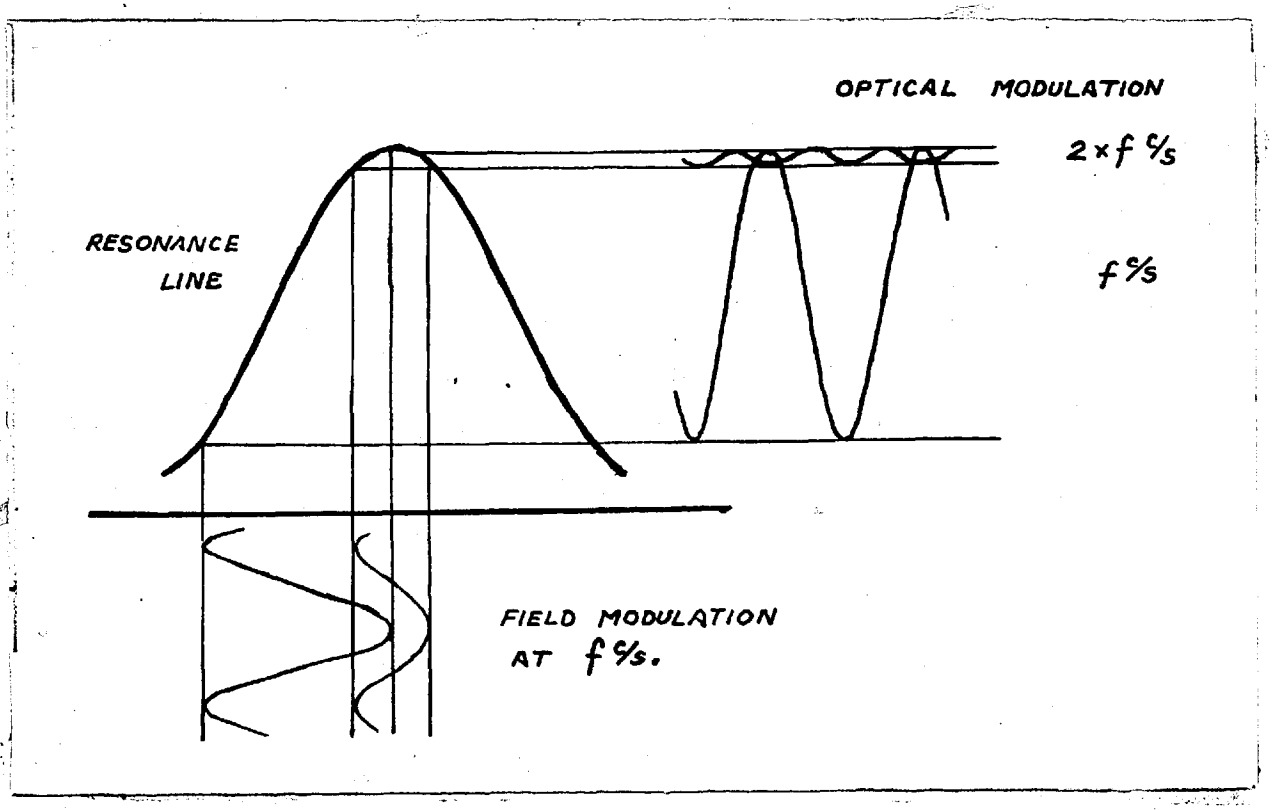

Modulated field method of detecting the swept resonance. On a limb of the resonance line the optical detector responds at the same frequency as the field modulation. At the line centre the optical detector responds to the 2nd harmonic of the field variation.

magnetometer described later. A doubling of the radiofrequency field strength increased the line width by 30%, while a fourfold reduction produced no appreciable reduction. This indicates that the remaining line broadening is largely due to the light beam.

The modulated field method, which is a convenient way of acquiring a repetitive sweep, made it possible to detect the radiofrequency modulation on the flanks of the resonance line.

Using ambient field values of one or two tenths of a gauss it was possible to drive the radiofrequency modulation continuously, by tuning the generator to the resonance frequency, and to monitor the signal with photocells connected directly to the oscilloscope.

Because the signal was marginal low values of magnetic field were necessary in order to minimise the capacitive loss of the photocells. Difficulty was encountered due to direct interaction between the H_1 field and the photocells, and the H_1 field had to be reduced considerably to ensure that the observed signal was due to light modulation.

The driven system was investigated using an amplifier which had been designed to have suitable gain and phase control for self oscillation. A four stage transistor amplifier with a gain of about 90 db and an input impedance of 1 KΩ was used. Two 2 cm x 1 cm., photcells connected in parallel, provided the signal detection and it was expected that the satisfactory input matching would allow reasonable phase control up to 20 Kc/s.

The H_1 field strength required for optimum driven signal, using the amplifier, was one hundredth of that required for the maximum swept signal. However, low H_1 field level was required to prevent direct pick-up.

In general signal strength decreased with increasing field from 0.5 gauss to 0.1 gauss but an accurate measurement

could not be made because the direction of the field vector could not be ascertained with sufficient precision when the bias coils were used.

Self-Oscillation

It remained to connect the amplifier output to the H_1 coil, through a resistance to prevent loading of the amplifier by the coil, and a capacitance to block the direct current from the amplifier. Fig. 3.8 shows the schematic form of the self-oscillating system. The value of the capacitance in series with the H_1 coil

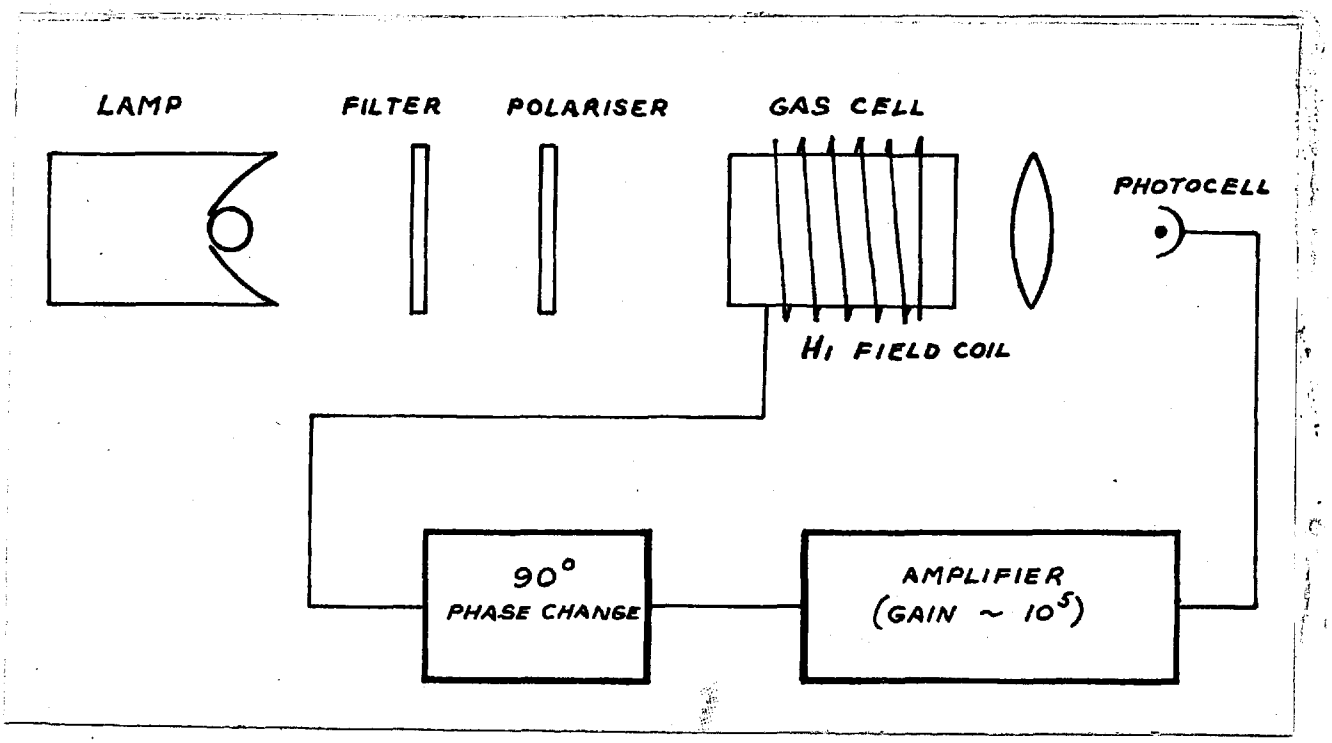

Fig. 3.8. Schematic diagram of the self-oscillating system.

was chosen by test to produce the correct phase condition for self-oscillation. Self oscillation was first observed at a frequency of 5 Kc/s corresponding to a field of 1000 gammas, and it appeared that the signal to noise ratio had improved by a factor of two over the driven condition.

In a field of 250 gammas the line width was found to be 100 c/s. This was measured by varying the phase of the H_1 current by altering the resistance and capacitance mentioned above. The frequencies at which the arrangement could be made just to oscillate in a fixed magnetic field are taken to be the limits of the resonance line in the self-oscillator.

The measured figure, which corresponds to 20 gamma, seems excessive when it is borne in mind that the fine structure of the resonance is virtually zero at this order of field value. It is thought that the field gradients produced by the Helmholtz coils was a contributing factor. This would account for 25 cycles of the measured line, since the field variation over the volume of the gas cell was 5 gammas. Field due to the A.C. mains are thought to have been responsible for a considerable line broadening at low fields. In effect the 50 c/s field modulates the ambient field. Parsons and Wiatr consider that a power field of amplitude 1 gamma produces the same line broadening as a 1 gamma field change over the volume of the gas cell. In previous measurements of the driven system it had been possible

to demonstrate power field modulation of the form described in Fig. 3.7. It is not possible to calculate the total effect of gradient and power field on the line width. For this reason, the value of 100 cycles per second must be regarded as the extreme line width at low fields.

Development

The physical configuration of the sensor was improved so that it could be mounted rigidly inside a fibreglass tube 12" long and 3" diameter. Fig. 3.9 illustrates the mounting assembly and Fig. 3.10 is a photograph of the component parts.

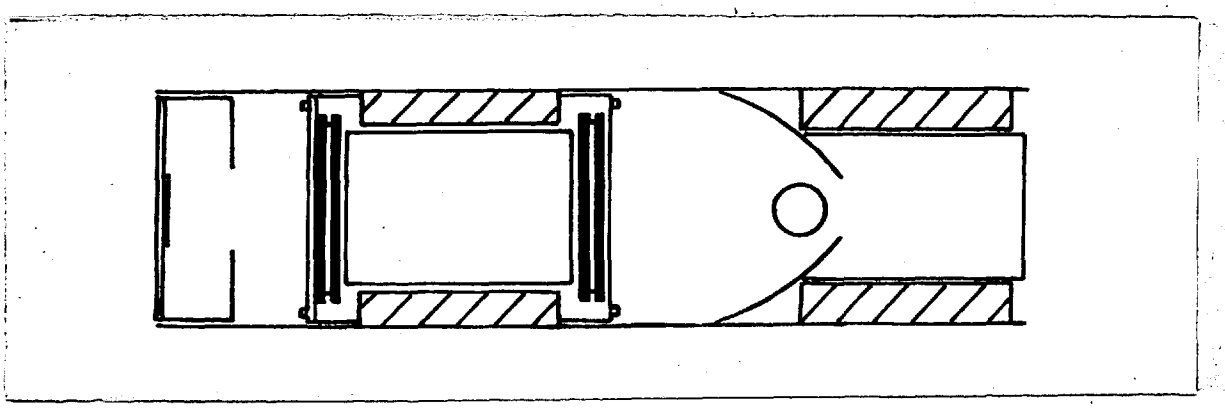

Fig. 3.9. Sensor assembly. Hatched areas represent thermal lagging. Optical components are shown dark.

The lamp, on the right of the diagram, was held in place by a sheath of expanded polystyrene, shown hatched, which acted as a former for the windings of the H_1 coil, and to which polythene end pieces, machined to hold the optical

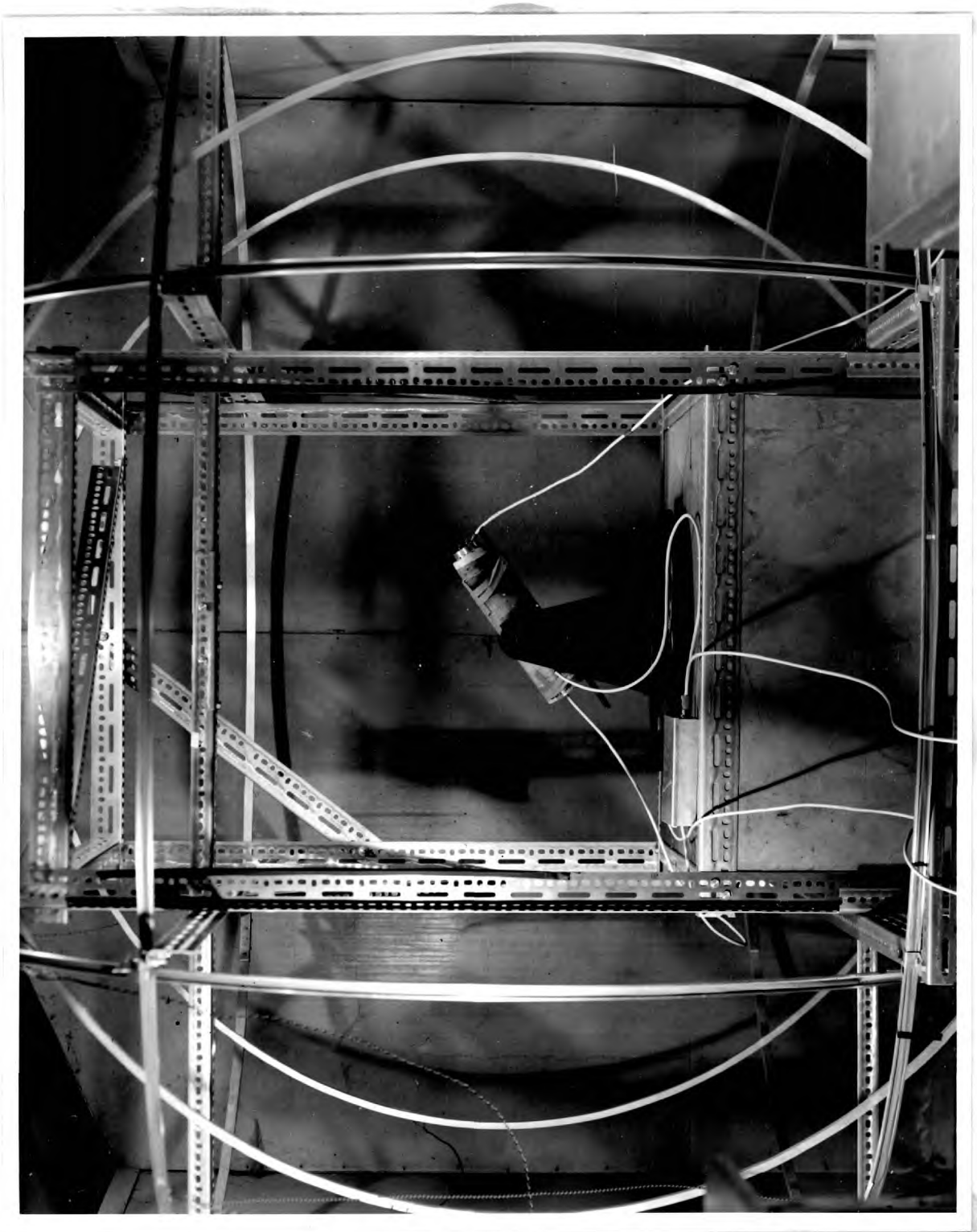

Fig. 3.10. Photograph of components of sensing head.

components, were firmly bonded. Expanded polystyrene was used to insulate the gas cell.

The optical components, shown black, consist of the filter and polariser at the lamp side of the gas cell and two Fresnel lenses. They were positively separated by rubber rings and held in place by the pressure of tufnol end pieces which were screwed to the polythene former.

The photocells are shown at the extreme left in an aluminium box, which has a circular hole cut in it to allow light to pass through. It serves the dual purpose of a radiofrequency shield and a rigid support.

The configuration permits satisfactory alignment of the optical axis with the H_1 coil axis, a condition which is necessary for accurate knowledge of the phase relations (Bloom 1962). Lamp and photocell mounting may be moved relative to the gas cell to adjust the focussing of the optical path.

A set of Orthogonal Helmholtz coils 7 feet in diameter was manufactured, and a stand which holds the gas cell at the coils' centre and which can be rotated about all axes was built. Fig. 3.11 shows the sensor and the preamplifier at the centre of the field coils. A heating coil of 40 gauge enamelled copper wire was wound round the gas cell and heating effected by passing five amperes through it. This arrangement worked satisfactorily, but was superseded by the more direct

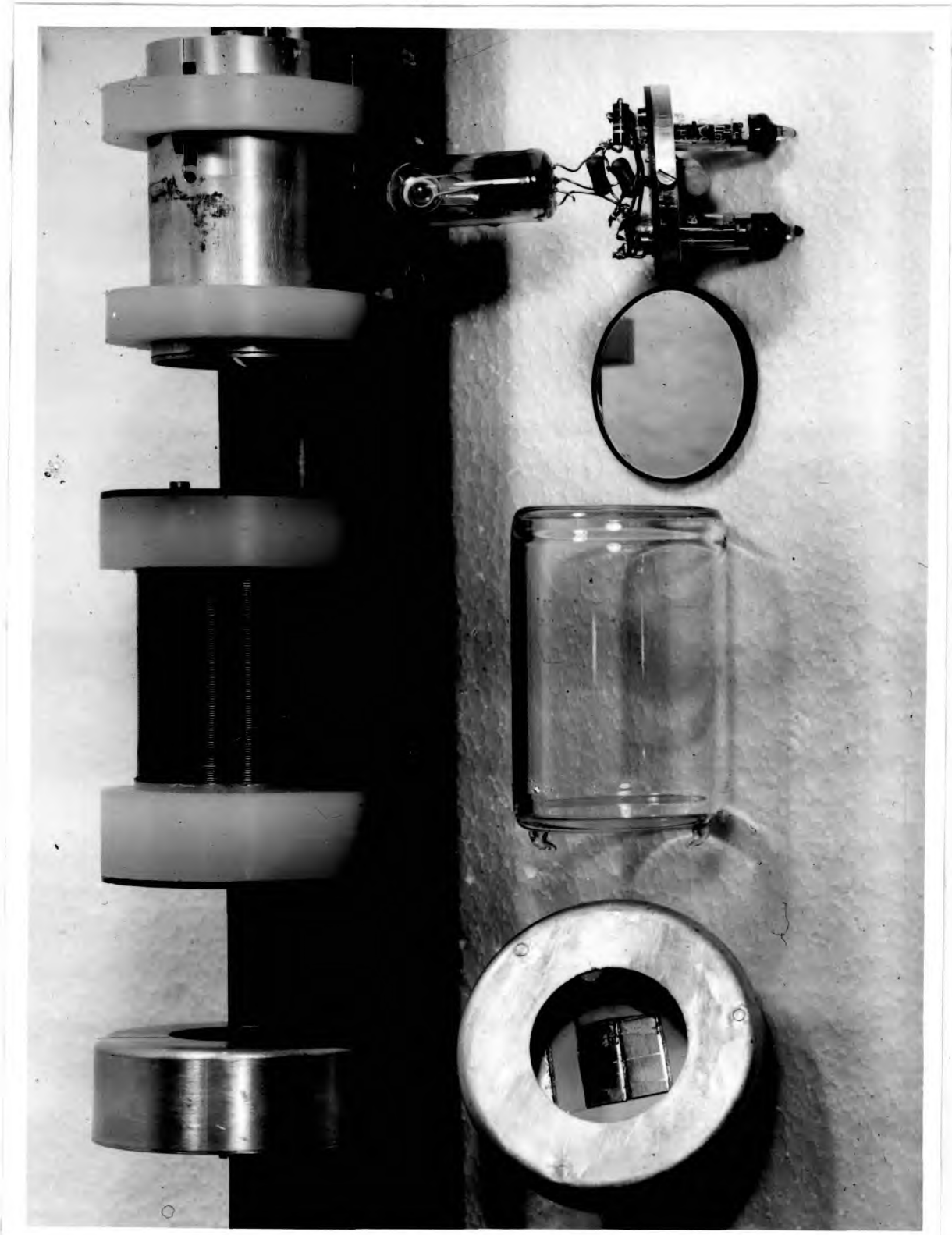

Fig. 3.11. Photograph of sensor in use in the Helmholts coil system.

and less cumbersome method of passing current through the H_1 coil itself. The current source is connected directly to the H_1 coil after the series resistor and capacitor which block its effect from the amplifier. This has the advantage of applying the heat as directly as possible to the gas cell itself within the thermal insulation sheath.

Improvements of this nature permitted investigations of the magnetometer to be carried out conveniently in low fields, prior to the construction of the high field instrument which has increased difficulties due to the photocell response and amplifier bandwidth.

It was possible to improve the signal-to-noise ratio in low fields to better than 20 to 1 and to operate from 50 Kc/s to about 300 c/s. The very low field operation was obscured by 50 c/s power fields and field gradients. At frequencies less than 1 Kc/s., amplitude modulation and frequency modulation of the magnetometer signal occurred at frequencies close to 50 c/s and 100 c/s. Initially this was taken to be a demonstration of the field due to the local power supply, but a similar effect can be presented by the interaction of the Rb^{87} component with the Rb^{85} signal in a field gradient. It is therefore not possible to state explicitly to what extent power field interferred with the magnetometer performance. Attempts to operate in fields less than 40γ were foiled by the 50 c/s power field, harmonics of which take over the

oscillation in all but the most favourable orientations.

General tests of the magnetometer showed it to behave in the expected way. The null zones were confirmed to exist along the field axis and perpendicular to it and self oscillation took place in only one hemisphere. It was possible to achieve operation in the other magnetic hemisphere by interchanging the connections at the H_1 coil. An electronic switch was built and tested which automatically chose the correct sense of the phase change for self-oscillation.

It was found possible to achieve self oscillation with the Rb^{87} component by overheating the gas cell. The best signal was of poorer quality than the Rb^{85} signal. The appearance of the Rb^{87} component on the normal signal due to Rb^{85} produces a frequency modulation and this is now used as the standard by which gas cell temperature is judged. Also, since excessive gain in the feedback amplifier produces the Rb^{87} component it is used as the criterion for optimum amplification.

Earth's Field Instrument

Design of an instrument to operate in the Earth's magnetic field, i.e. within the range 0.3 - 0.7 gauss, presents two main problems. The first is that of producing a transistor amplifier with 120 db gain over the range

100 Kc/s - 350 Kc/s and which is driven by a photocell matrix. The photocell impedance requires a series arrangement to reduce capacitive loss and this presents a large source resistance. In order to maintain the frequency response provided by the smaller capacitance a low value of amplifier input resistance is needed, with the resulting inefficiency of the mis-match.

The 90^{o} phase shift may be assigned to the photocells and thus amplifier and H_1 coil should produce no phase change over the working range.

Initial attempts to achieve the ideal conditions produced amplified signals with a very poor frequency response. The use of high frequency transistors made a considerable improvement and a typical signal of 0.2 volts p-p with a signal-to-noise ratio of 4 to 1 was possible. The use of a simple tuned amplifier to enhance the resolution and increase the amplitude of the signal permitted standard counting techniques to be used in the measurement of the frequency.

Investigations with this system showed that the magnetometer had a greater stability than the counting error, equivalent to 0.2 gamma, and was sensitive to field fluctuations of that order.

The second problem involved the intensity of the light beam. The lamp used up to this time had been designed for operation in the Ranger series of Lunar probes, launched

by N.A.S.A. in 1961, and it had been expected that the light output would be insufficient for high field applications.

The configuration of the lamp was that the bulb was held in place between the coils of the lamp oscillator by a small glass collar cemented to the tip of the bulb and to the tip of the valve. The assembly was enclosed by a glass tube and sealed. The intention was to provide a stable warm environment for the bulb, using the heat dissipated by the valve. Observation of the lamp performance showed that if it was heated by the hot air blower, the light output increased and produced a considerable improvement in signal quality. An attempt to stabilise this condition by enclosing the lamp-gas cell assembly in polystyrene lagging was partially successful. Improved signals were observed, and the thermal enclosure maintained the gas-cell temperature very well. However, continuous operation for several days produced signs of valve deterioration. The main symptoms of this are:

1. a reluctance on the part of the lamp to strike, i.e. to start the discharge on being switched on,
2. a tendency for the discharge to oscillate between the bright light of the rubidium and a dull light, thought to be a krypton discharge

In order to maintain a high bulb temperature without overheating the valve the lamp configuration was altered.

The bulb and its coils were enclosed in an evacuated jacket and the valve mounted on the reverse side of the card. This redesign resulted in considerable improvement in the lamp's qualities:-

1. The enhanced light output produced larger signals.
2. Striking is effected reliably and very quickly.
3. The light stability is very high.

The encouraging performance of the enclosed bulb lead to an investigation of the lamp oscillator. A version of the circuit used by Parson and Wiatr was modified for optimum performance. The configuration, in which two valves are operated in push-pull, presents more clearly defined operating qualities than the single valve oscillator and it was possible to acquire maximum magnetometer signal with a lower H.T. voltage. Several circuits have been designed and built for appraisal in respect of the various applications of the magnetometer and it is expected that a satellite instrument will incorporate a lamp consuming less than 2 watts total power and which can be fully operational within 30 seconds of being switched on by command. Fig. 3.12 shows the circuit for a two valve oscillator and a drawing of the configuration of the lamp. The bulb is held in place within its evacuated jacket by the tuning coils of the oscillator and their supports. Both jacket and valves are mounted on the insulated circuit card on which the circuit is built. The whole assembly

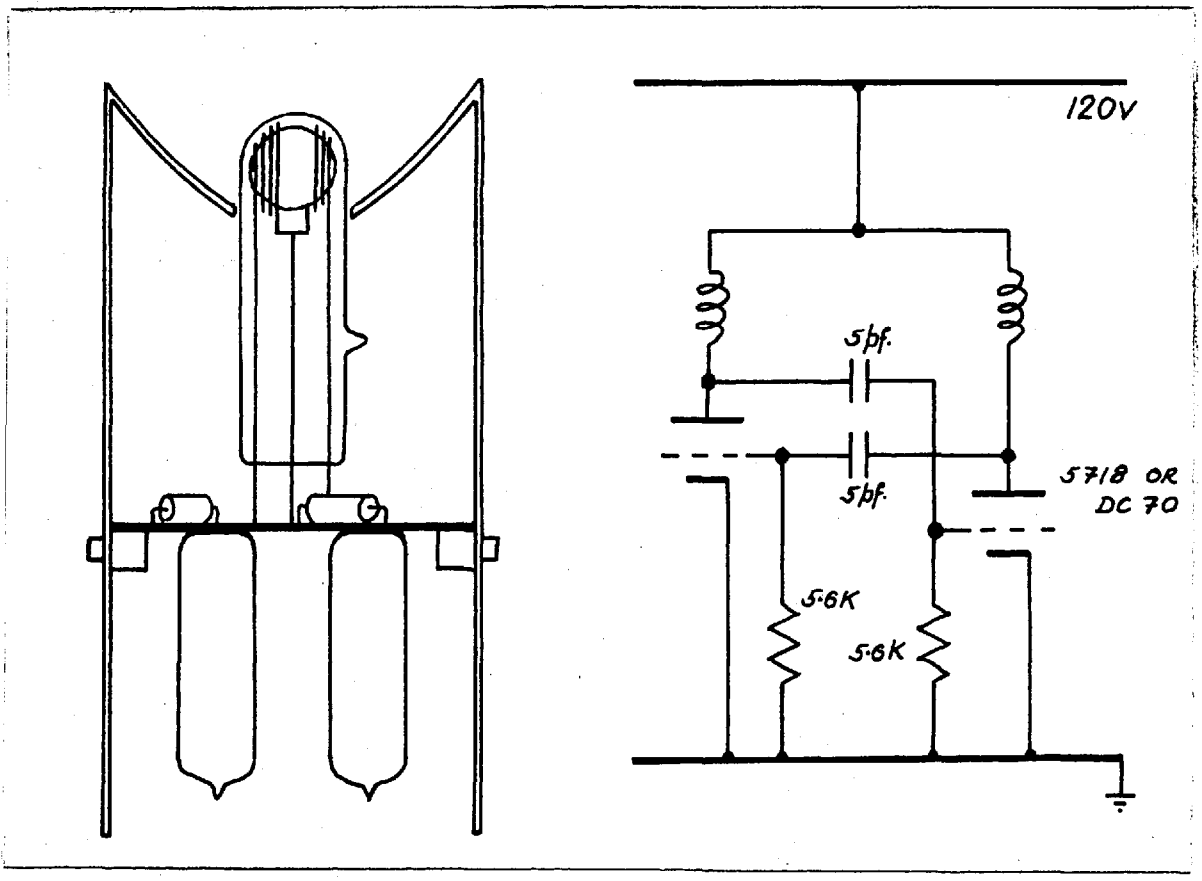

Fig. 3.12. Lamp circuit and assembly. The exciting coils are 4 turns 1 cm diameter 20 S.W.G. wire.

is contained in an aluminium case with a parabolic reflector attached. The drawing in Fig. 3.12 is approximately to scale.

Improvement in the signal quality due to the lamp led to a typical signal amplitude of 1 volt peak to peak and a signal-to-noise ratio of 10 to 1. Current and anticipated development of the rubidium vapour magnetometer is contained in Chapter 7, where the instrument and data it provided in field trials are evaluated and discussed.

NOTE

Fig. 3.2 shows the dependance of photocell output upon the load resistance which it is required to drive, and indicates a best match at 16 KΩ. According to the maximum power theorem this suggests 4 KΩ to be the internal resistance of a 1 cm x 1 cm photocell.

Consider the case of a single photocell connected across a load resistance 'z', shown in Fig. 3.13. If 'v' is the voltage produced by a photocell under a selected illumination then

$$i = \frac{v}{R+z}$$

where R is the internal resistance of the cell. The power transferred to z, is given by

$$i^2 z = \frac{v^2 z}{(R+z)^2}$$

If $z = kR$, then the power transferred to the load =

$$\frac{v^2}{R} \cdot \frac{k}{(1+k)^2} \qquad (1)$$

In the case of four cells in series, Fig. 3.14, each cell, given the same illumination, produces a voltage 'v'. Thus

$$i = \frac{4v}{4R+z}$$

and using the notation above the load power is

$$\frac{16v^2}{R} \quad \frac{k}{(4+k)^2} \qquad (2)$$

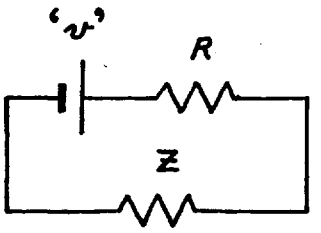

FIG. 3.13

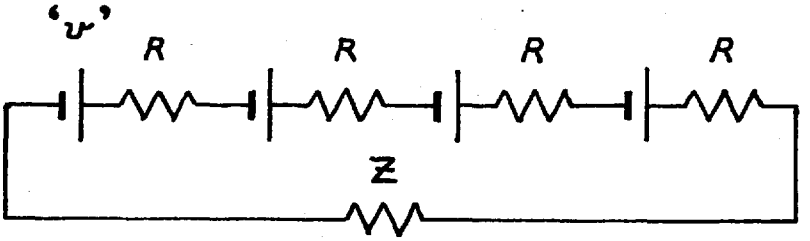

FIG. 3.14

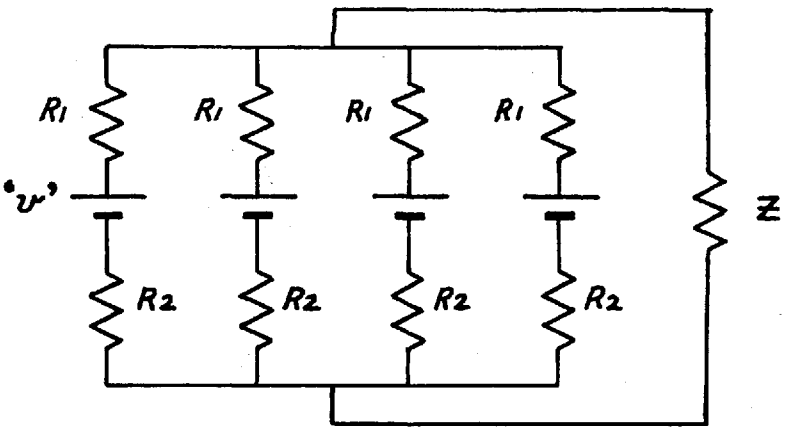

FIG. 3.15 A

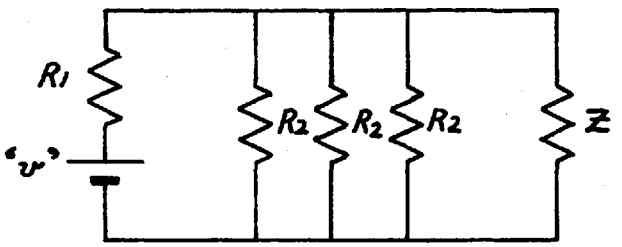

FIG. 3.15 B

For four cells connected in parallel it is necessary, for generality, to replace the internal resistance R, by R_1 and R_2 which represent forward and reverse resistances respectively. Fig. 3.15A shows the general circuit and Fig. 3.15B shows the current paths from any one cell. It is possible to specify the same illumination on each cell as before, and therefore the voltage 'v' produces a signal current

$$i = \frac{v}{R_1 + R^1}$$

where R^1 is given by

$$\frac{1}{R^1} = \frac{1}{z} + \frac{3}{R_2}$$

Thus $$i = \frac{v(R_2 + 3z)}{R_1R_2 + 3R_1z + R_2z}$$

The voltage across z is $(v - iR_1)$

$$= v \cdot \frac{z}{(R_1 + z + \frac{3R_1}{R_2} z)}$$

Thus Power in load $$= \frac{v^2}{R_1} \cdot \frac{k}{(1 + k + \frac{3R_1}{R_2} k)^2} \qquad (3)$$

Fig. 3.16 shows the fluctuations (2) and (3) plotted for values of k in the range $0 < k < 1\frac{1}{2}$. This illustrates that the series arrangement produces more power than the parallel connection. Even at $k = \frac{1}{4}$, which approximates to the practical value when the load represented is a common emitter transistor stage.

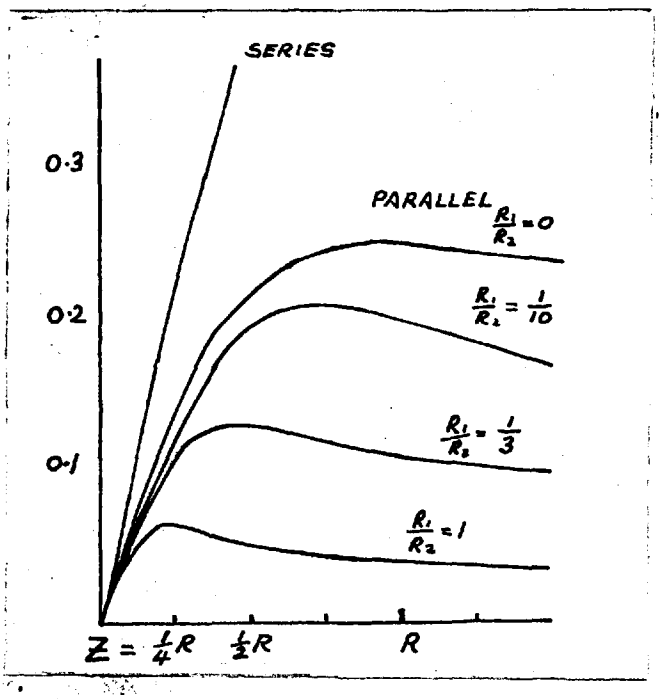

Fig. 3.16. Power transfer functions for series and parallel connected photocells.

The points inserted in Fig. 3.2 were calculated using equation (2) and show good agreement with experimental test.

CHAPTER 4

A DISCUSSION OF THE MAGNETOMETER

General Remarks

As previously discussed, the design of magnetometers using rubidium vapour separates into two sections largely due to the capacitive property of the photocells. At low electrical frequencies the photocells respond well to light modulation and produce an output which is not greatly phase distorted. At high frequencies their capacitance reduces their response to light modulation and produces a large phase change between input light modulation and output electrical signal. Thus ideally it is possible to produce the requisite conditions for self oscillation at high frequencies using a great deal of amplification and no added phase change, and at low frequencies using less amplification but inserting a 90° phase change.

It is possible to extend the range of each of these conditions by adjusting the variation of phase change with frequency and by taking advantage of the fact that, under certain conditions, self-oscillation can be maintained at frequencies differing from the resonance line peak, which corresponds to the 90° phase point. If the measurements of

magnetic field to be made do not require a high degree of precision as for example the absolute values of the field, without recourse to calibration, a broad resonance line width may be tolerated, and operation off the 90° point may be used to acquire a wide range of operation.

It has not been possible to measure the line width of the self-oscillator with great certainty. The method employed at low field strengths was applied in the Earth's field and indicated a maximum line width of 400c/s corresponding to 80 gammas. This represents an absolute accuracy of one part in a thousand.

The resonance line consists of the six lines corresponding to the individual transitions within the F level, adjacent lines differing in frequency in the Earth's field by 32 c/s and producing the main breadth of the unresolved line. The separation of these components is proportional to the square of the magnetic field (Parsons and Wiatr). The residual line widening due to light intensity and H_1 field strength is shown to be small as indicated by the measurement of the line width in low fields. In general then, the absolute accuracy of one part in one thousand should be regarded as an over estimate.

Low Field Magnetometer

The circuit for the preamplifier of a magnetometer to operate at low fields is shown in Fig. 4.1. The field range covered is from 50 gamma to 10,000 gamma, the lower figure being the lowest field in which a test was possible because of interference from the power fields. The photocell matrix is two 2 cm x 1 cm cells in parallel, producing a source impedance of 1 KΩ shunted by 0.1 μf. This presents a good match to the amplifier which has no special features other than the feedback in the emitter circuits of each stage. The 90° phase shift is acquired primarily from a small differentiating capacitor in series with the H_1 coil, and care is taken in the design to ensure that the phase change due to the amplifier and the photocells does not seriously affect the operating range of the instrument.

Phase Switching

The low field instrument using the preamplifier shown in Fig. 4.1 has been proposed for use in future Earth satellites. Since it is likely that such an instrument will assume all orientations possible with respect to the ambient field vector a more elaborate set of electronics was designed, incorporating a phase switch, which chooses the correct sense of the 90° phase condition to permit oscillation in either magnetic hemisphere.

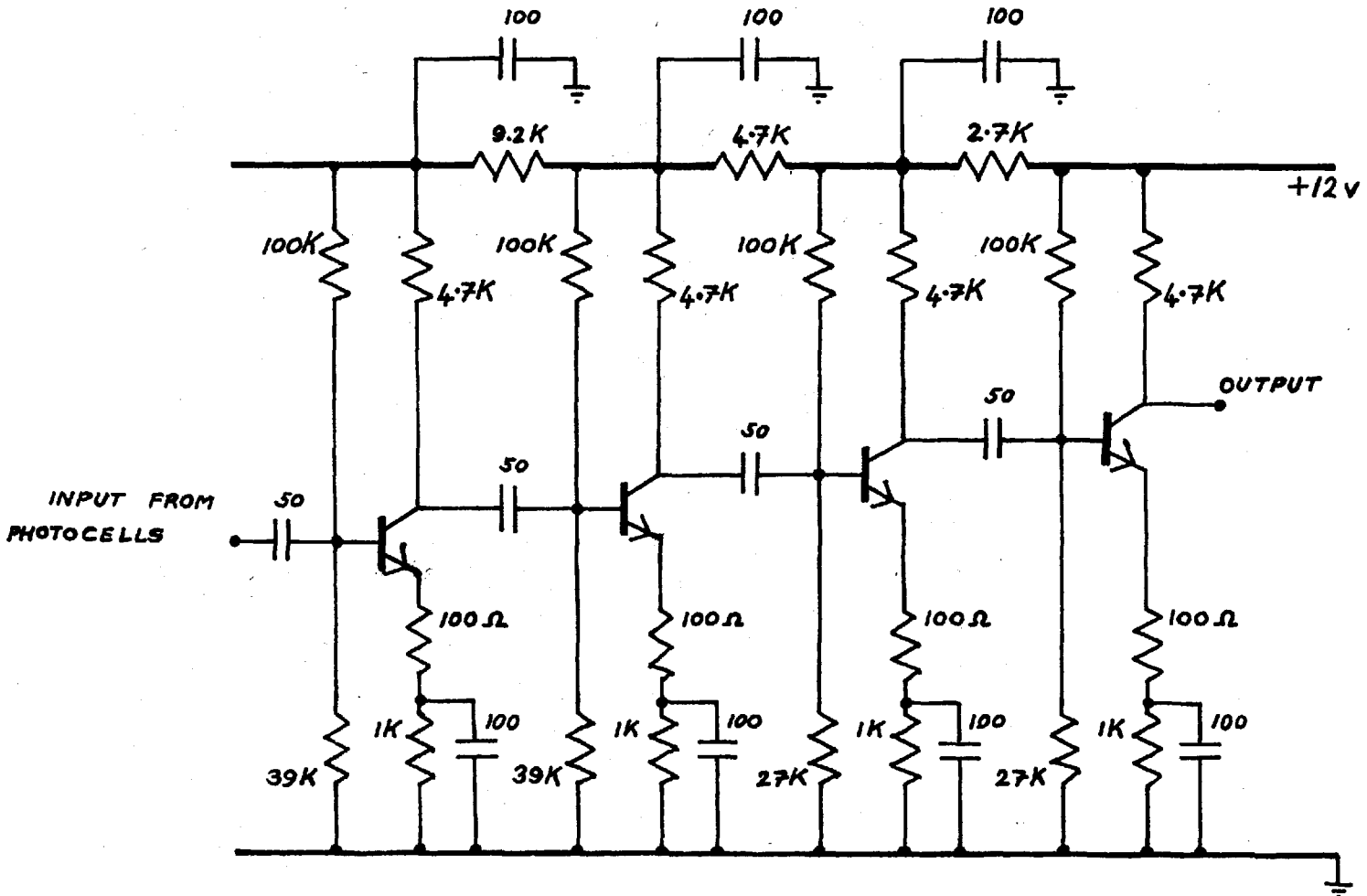

FIG. 4.1 LOW FIELD PREAMPLIFIER.
CAPACITOR VALUES IN MICROFARADS.

Fig. 4.2 shows the schematic diagram for the magnetometer incorporating phase switching, the prototype of which has been built and tested. The operation is standard practice with the exception of the unijunction U. and the Silicon Control Rectifier, S.C.R. Both of these components were suggested by Mr. Justin Shafford of N.A.S.A. and simplify to a very great extent the adjustment of the variables in the circuit.

The phase switch is inserted in the self-oscillating loop after the preamplifier. It consists of a phase splitting stage driven by the preamplifier, which produces an output in phase with its input, ϕ_o and an output 180° out of phase with its input, ϕ_{180}. These two signals are brought to opposite sides of a diode bridge which can be biassed in such a way as to short one of the signals to Earth, allowing the other to pass on to the H_1 coil, via an output amplifier which makes up the losses incurred in the phase splitting network. Fig. 4.3 shows the phase splitter and diode bridge circuit. Buffer stages, emitter follower stages with high input impedance and low output impedance, are inserted to prevent unwanted interaction within the circuit.

The biassing of the diode bridge is performed by a bistable multivibrator. Such a circuit is stable with either of its transistors conducting and the other cut off. The collectors of the multivibrator transistors are connected to

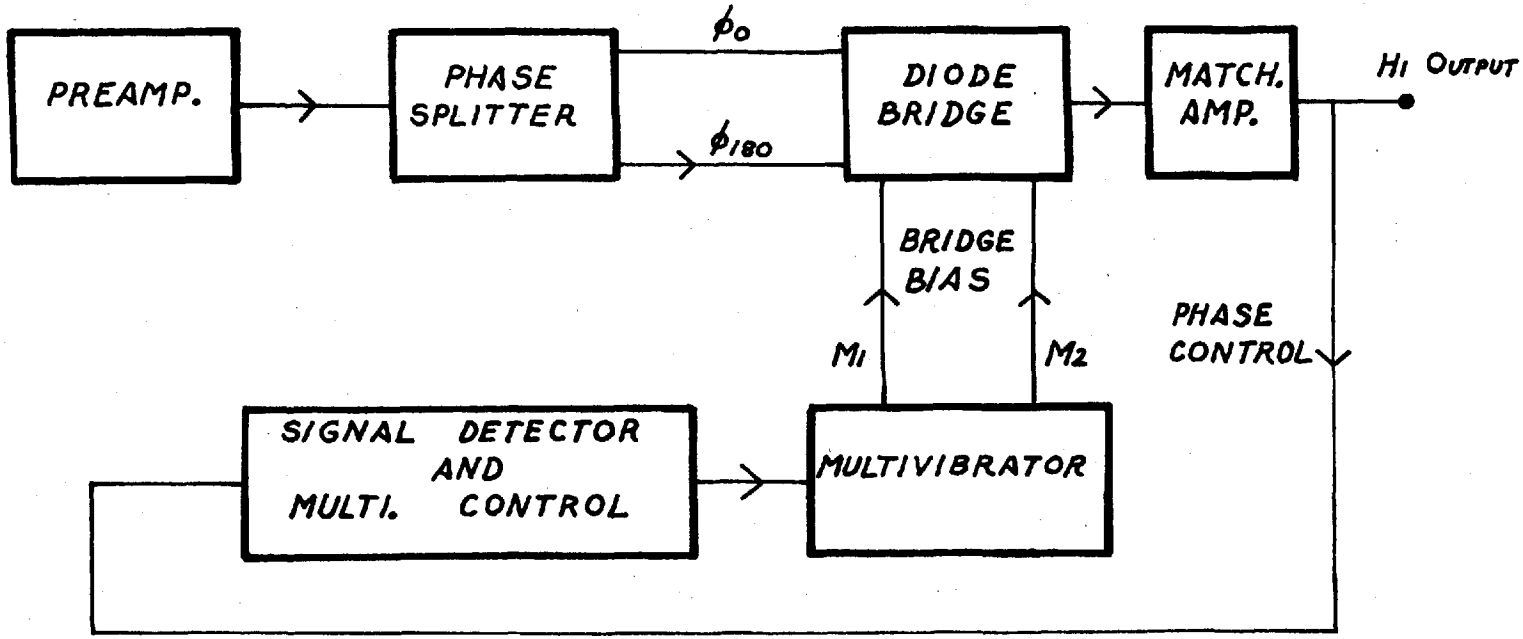

FIG. 4.2 PHASE SWITCH SCHEMATIC

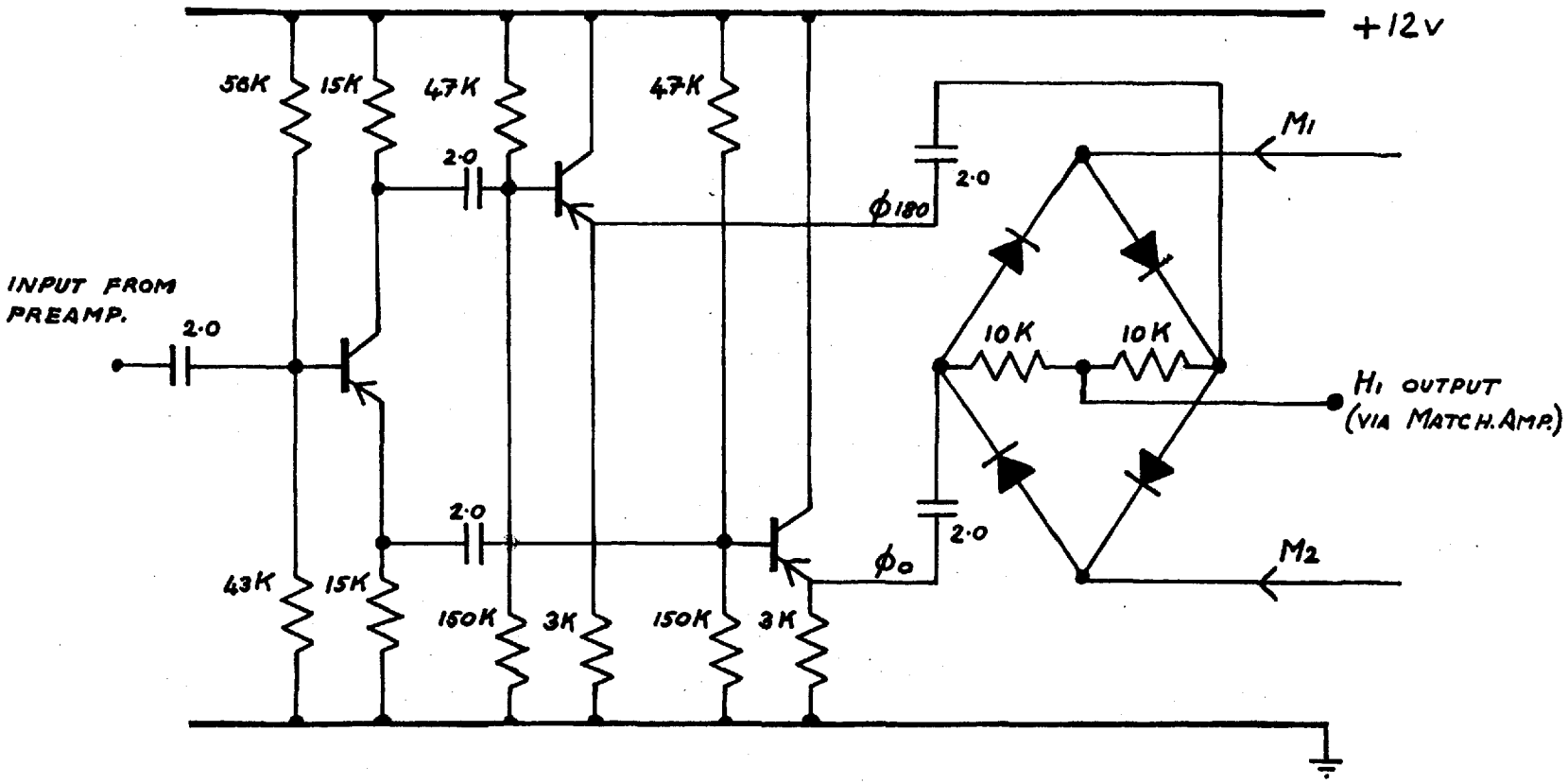

FIG. 4.3 PHASE SPLITTER AND DIODE BRIDGE.

opposite ends of the diode mesh so that in a stable state the end connected to the conducting transistor is at Earth potential, while that connected to the transistor which is cut off, is at the voltage of the power line. In this way the proper choice of the conduction direction in either side of the diode bridge allows one of the phases to be connected through the conducting transistor of the multivibrator to Earth, while the phase on the non-conducting side is unaffected.

The process by which the switch chooses the correct phase is one of sampling. The multivibrator is made to switch from one state to the other, alternately allowing either phase to reach the H_1 coil. The multivibrator drive is derived from the unijunction which acts in a similar way to a thyratron valve and produces a sawtooth wave form. This is differentiated by the 0.05μf capacitor and used to control the multivibrator. When the sensor enters an orientation favourable to self-oscillation, signal builds up very quickly in the appropriate phase condition. The signal level is detected and used to lock the multivibrator in the correct state.

Fig. 4.4 is the circuit for the multivibrator and its control elements. The build up of signal is detected by the silicon control rectifier, which conducts at a predetermined

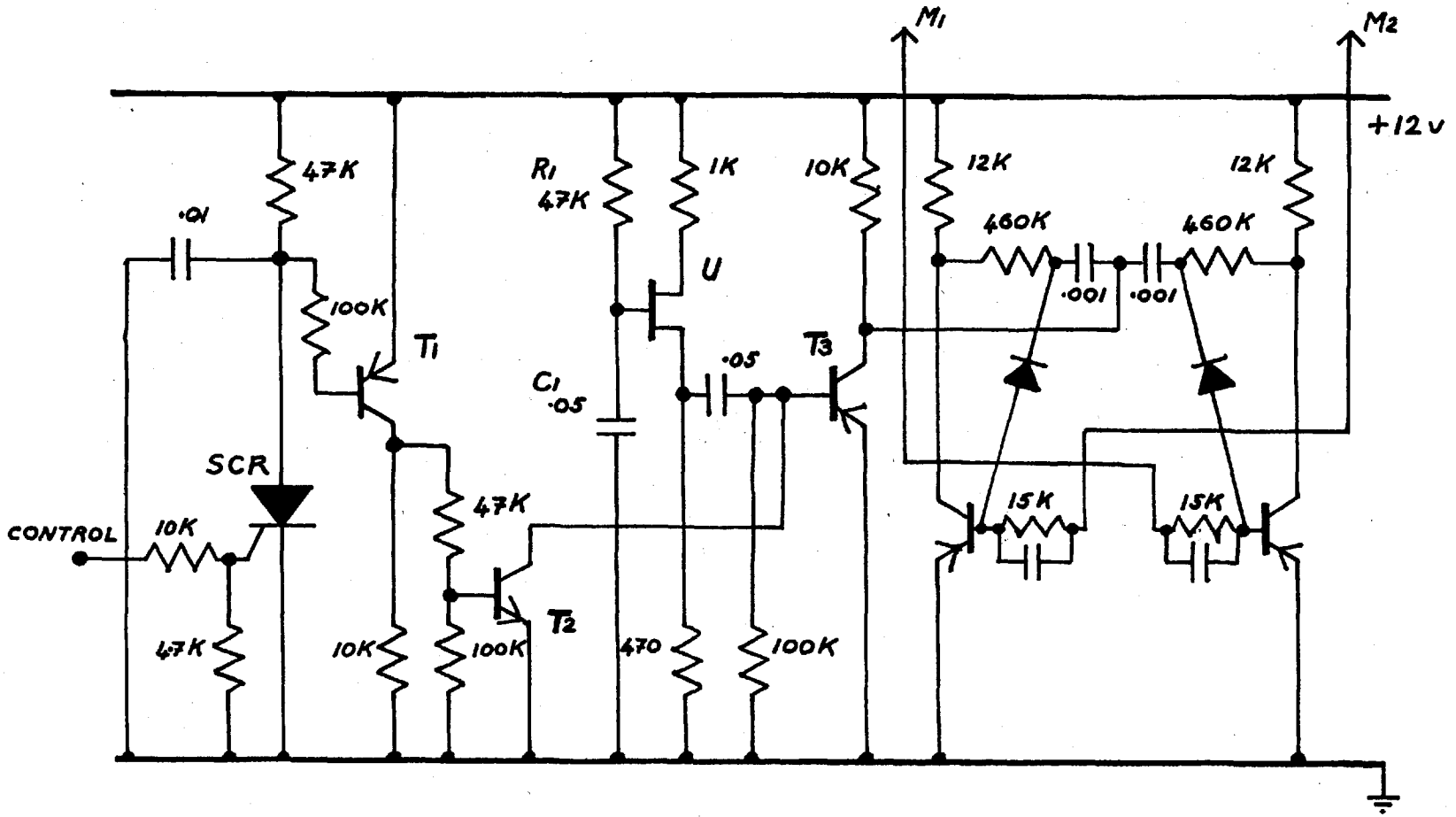

FIG. 4.4 PHASE SWITCH CONTROL AND MULIVIBRATOR CIRCUIT.

signal level and, through transistors T_1 and T_2, cuts off the transistor T_3, preventing the unijunction drive from reaching the multivibrator. The multivibrator remains locked on the chosen state until the signal deteriorates to below the level required to fire the silicon control rectifier, when the switch begins to sample the phases again.

The silicon control rectifier requires several cycles of signal to fire so that the rate of switching must be long enough for this to occur. The switching rate is controlled by the R_1C_1 time constant at the unijunction and it has been possible to achieve phase switching in the range of signal frequencies from 15 c/s to 500 Kc/s in bench tests.

It is also necessary to have the firing level of the silicon control rectifier sufficiently above the level of noise to prevent the switch locking itself within the noise level and therefore not searching for the correct phase. A convenient feature of the S.C.R. is that the level at which it ceases to conduct is lower than its firing level. This enables the switch to be designed in such a way that phase searching does not occur until the signal has completely disappeared.

The Earth's Field Magnetometer

The preamplifier circuit used for the Earth's field values is shown in Fig. 4.5, and operates over the range of fields from 0.05 gauss to 1 gauss, corresponding to the frequency range 25 Kc/s - 500 Kc/s.

The voltage gain in the range of frequencies greater than 100 Kc/s is $> 10^5$ and is constant over the range. Here the photocell matrix, which consists of four 1 cm x 1 cm cells in series, produces the 90° phase shift, and care is taken to keep stray phase shifts to negligible proportions. Phase shift due to the H_1 coil is minimised by a large series resistor which presents suitable output conditions to the amplifier, and permits a simple adjustment of the H_1 field current, without changing the amplifier gain; a facility which is necessary in optimising the feedback loop.

Since inductances and transformers were not to be used in the amplifier because of their possible magnetism, the amplifier phase characteristic was controlled by using small values of collector load. This reduced the output time constant due to output resistance and collector-to-emitter capacitance of the transistor, thereby improving the high frequency gain of the stage.

At frequencies below 100 Kc/s the amplification falls off and an associated phase change exists. This is used, in

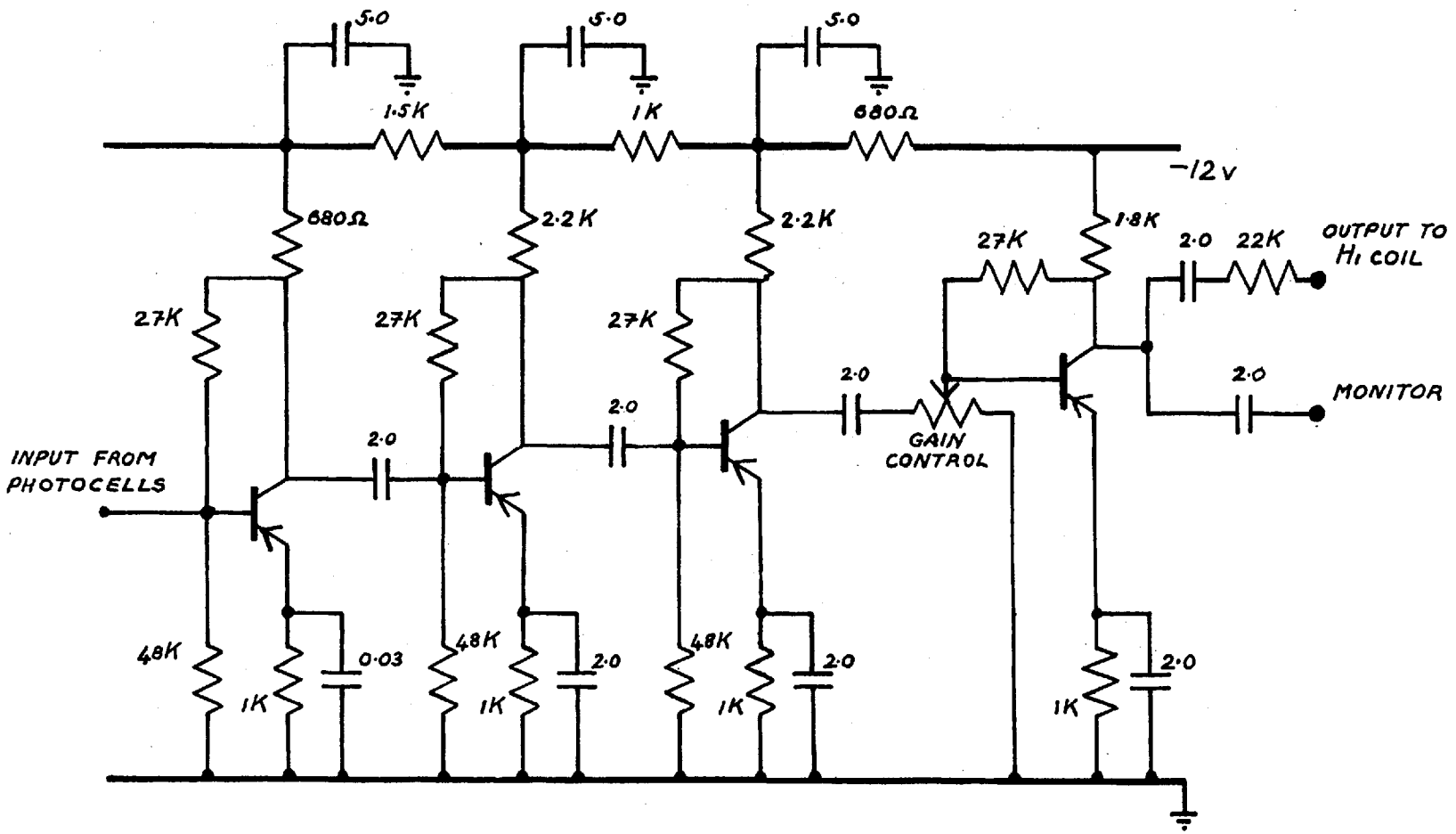

FIG. 4.5 EARTH'S FIELD PREAMPLIFIER
CAPACITOR VALUES IN MICROFARADS

conjunction with the enhanced photocell response and their intermediate phase shift, to extend the range of operation on the low field side.

A control is incorporated in the amplifier to adjust the level of amplification. This was used to study the signal quality under varying conditions of temperature, gradient and orientation and is a convenient method of adjusting to optimum signal conditions in the field.

Discussion of the Magnetometer

The properties of optically pumped self-oscillation were studied at low fields to take advantage of photocell response in order to optimise the design of a magnetometer. From the experience so gained the properties of the device as a magnetic field measuring instrument were then studies in the Earth's field. The operational testing of the magnetometer was carried out as a series of observations of micropulsations and is described in later chapters.

Orientation

Fig. 4.6 is a measured polar diagram of signal strength of the magnetometer and indicates the form of the polar and equatorial dead zones.

The variation of measured field with orientation, to be

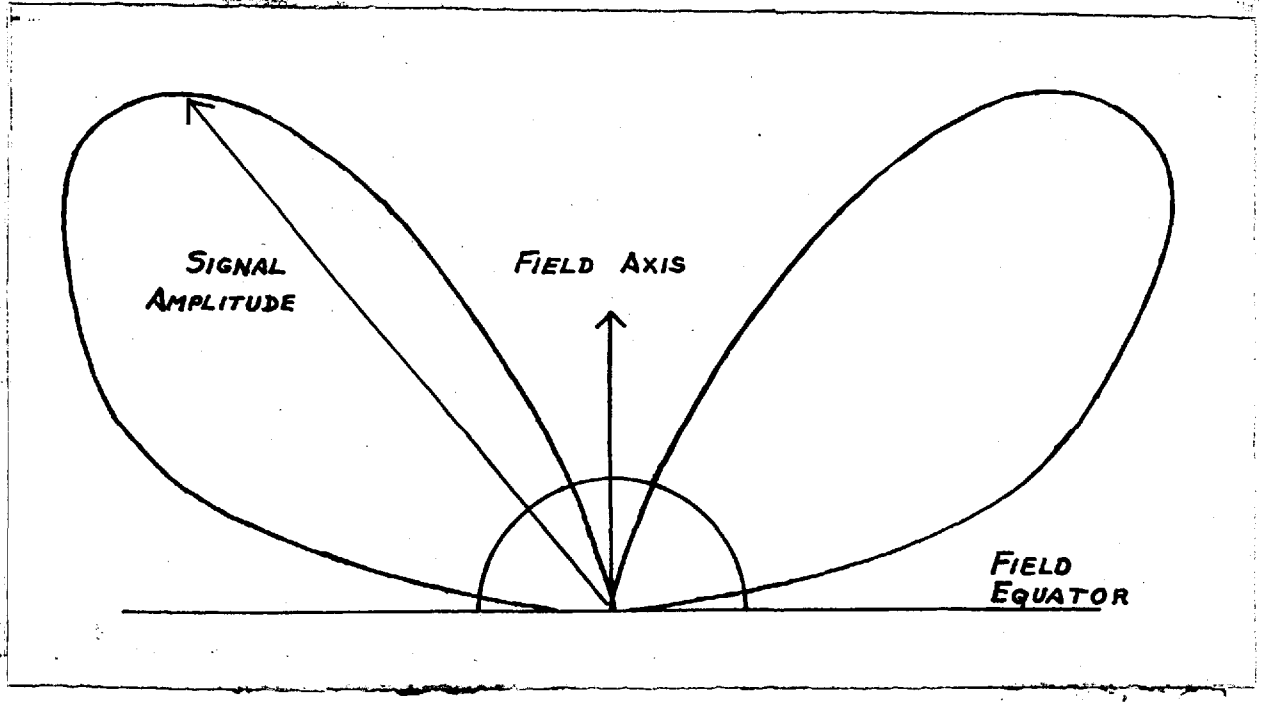

Fig. 4.6. Polar diagram for the self-oscillating magnetometer. The small circle represents the output noise level.

expected from the selective absorption of the individual lines, was measured. The measurement indicated that a variation of 3 γ existed between position where the magnetometer was inclined at 65° and 25° to the field direction. The greater value of measured field belonged to the 25° position. This variation is less than that quoted by other workers, some of whom mention a 10 γ variation (R. Morris private communication). Two sources of the disagreement are possible. The first is magnetism of components in the sensor assembly. The value used in the lamp is known to have magnetic elements in its construction, and the photocells may be deposited on a nickel base. Measurements with a valve

indicated that most of its magnetism is contained in the leads, which are largely removed in the construction of the lamp oscillator, and measurements, made by moving the active lamp relative to the gas cell, indicated that its effect in the usual operating condition was less than 1γ at the gas cell.

It is possible that the high light intensity used in this instrument produces a greater broadening of the individual line structure and reduces the orientation effect, compared with that observed by other workers who were perhaps operating with narrower line widths.

Temperature

Fig. 3.9 illustrates the thermal insulation of the sensing head. It is found that the lamp is fully operational within 30 seconds of being switched on in the normal range of ambient temperatures, 15°C to 45°C. The magnetometer produces stable signal conditions within the range of temperatures 25°C to 45°C. It is possible to operate within the range 20°C to 50°C using the gain control to adjust the feedback level and it is expected to obtain this working range automatically using AGC. Below 20°C there is insufficient signal from the rubidium 85 to produce oscillation and in the range 40°C to 50°C the rubidium 87 signal produces intermodulation which can be avoided by reduction of the

amplifier gain. Above 50°C the rubidium 85 signal is insufficient to maintain oscillation and the magnetometer operates on the Rb^{87} component. Fig. 4.7 shows photographs

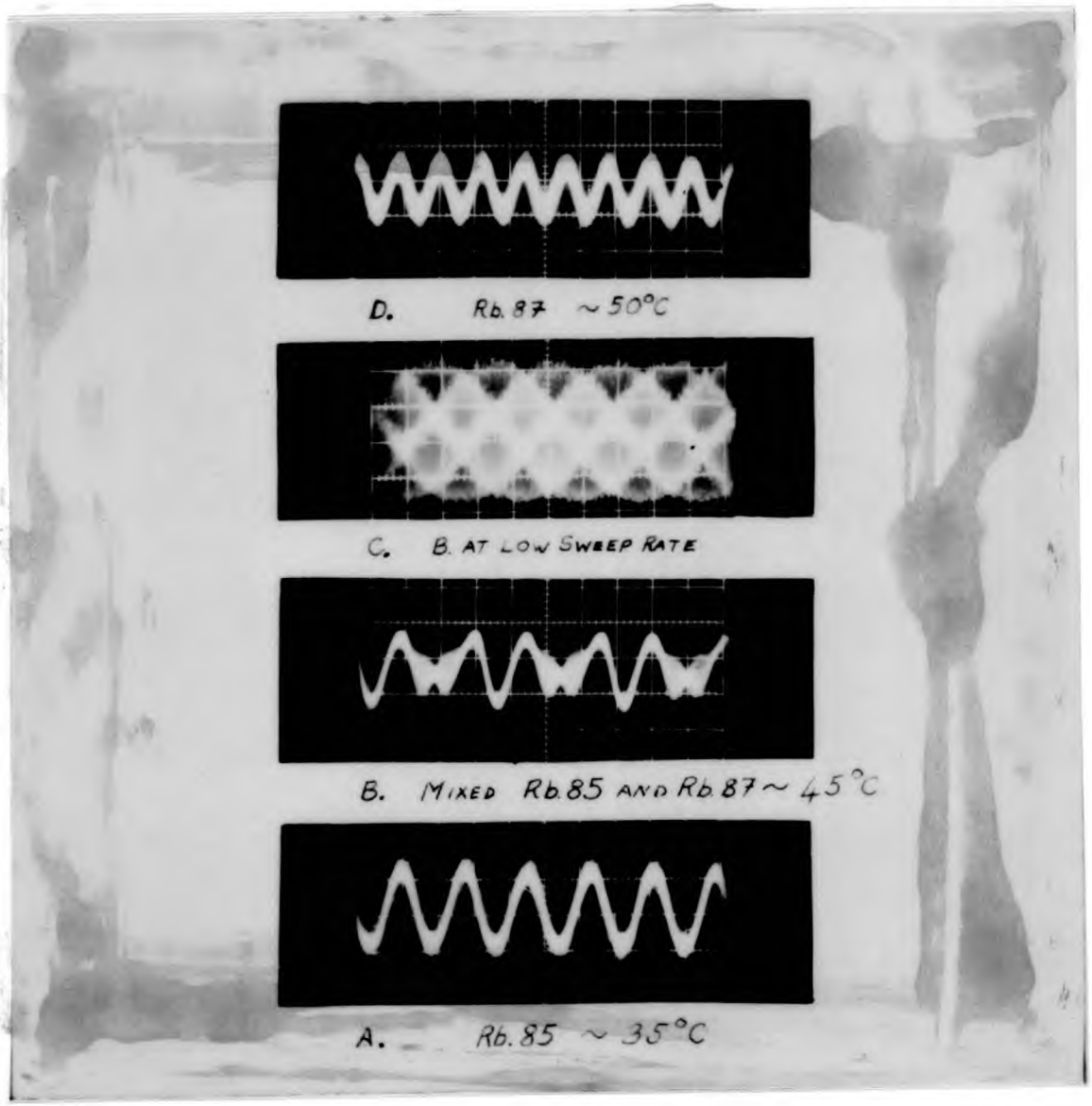

Fig. 4.7.
Illustrating the intermodulation of rubidium 85 by rubidium 87 at elevated temperatures, in Earth's field.
A) The rubidium 85 signal at 35°C, sweep rate $2\frac{1}{2}$ sec/cm.
B) Modulation of rubidium 85 signal by rubidium 87 signal at 45°C. C) same as B) photographed at a sweep rate of 1 msec/cm.
D) Rudibidum 87 signal at about 50°C.

of the magnetometer signal at various temperatures. These photographs correspond with the photographs lettered * similarly in Fig. 3.4.

Sensitivity

Bloom (1962) indicates a maximum sensitivity of 0.003γ for the self-oscillating magnetometer, limited by the photocell noise, and theoretical values of the time constants involved suggest a similar figure.

Measurements of the sensitivity of the operating magnetometer were restricted by the frequency counting apparatus, whose maximum resolution within a one second counting time was 0.05 gamma, and by the geomagnetic field noise. It was shown, by using a small calibrated magnet to produce field variations, that the magnetometer exhibited a resolution as high as the counting system permitted.

Further remarks about instrument resolution are contained in chapters 6 and 7, where the field system is discussed.

Frequency Response

The measurable frequency response of the self-oscillating magnetometer to field fluctuations is dependent on the time taken to make an actual measurement, when frequency is measured directly. Bloom indicates that the precession of

the rubidium atoms in the gas cell follows field transients faithfully and the practical frequency response of an instrument using the technique is limited by the bandwidth of the feedback loop. The discussion deals with field changes in the same direction as the field vector, and it is suggested that a transient at right angles to the H_o direction may quench the oscillation.

Fig. 4.8 shows the response of the magnetometer to field

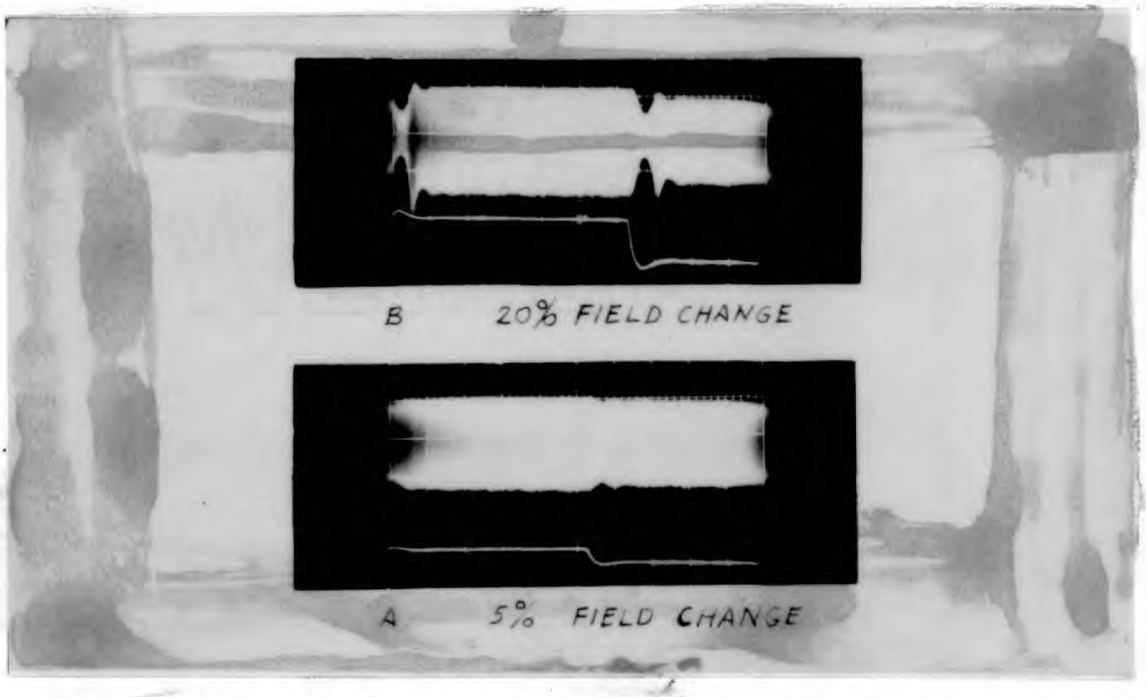

Fig. 4.8. Effect of a rapid transient on the magnetometer signal. The transient field is shown in the lower trace of each photograph, where the voltage across the vertically aligned coils is displayed. The sweep rate is 20 msec/cm.

transients, shown by the lower curve. It was not possible to show the frequency change during the transient. The amplitude modulation which takes place with large field change is taken to represent the response time of the feedback loop. This indicates a maximum response of 100 c/s (25% per second). However close inspection suggested that the frequency change was continuous during the transient, except in the case of the very large change. The significance of the ringing is probably a transient effect of the amplifier.

Field Gradients

Investigations of the effect of field gradient on the magnetometer signal were carried out using a small calibrated magnet. Signal amplitude was measured as a function of the distance of the magnet from the gas cell. Measurements were made with the magnet oriented along three orthogonal axes with the magnetometer in its optimum position in the Earth's field. Measurements were also made along the field axis, and in the plane perpendicular to it.

The conclusion drawn from the tests is that the self-oscillation is affected twice as much by a gradient across the field direction, as by the same gradient along the field direction. It was found that in the Earth's field, and in the gradient orientation which affected the signal most, a

10 gamma per cm. gradient reduced the signal by 10% of its gradient-free amplitude. Self-oscillation is completely destroyed by a gradient of 50 γ/cm. in the same condition.

Applications

The two forms of the magnetometer were designed and investigated under the auspices of the Royal Society Committee on Space Research. The high field version was considered suitable for rocket probes of the ionosphere and the low field instrument for Earth satellite and deep space probe applications.

Satellite observations fall into three categories and the applicability of the rubidium magnetometer is discussed for each case.

1. High altitude field mapping.

Observations of the strength and direction of the geomagnetic field at altitudes between 100 Km and 20,000 Km may be used to produce charts for use in describing the Earth's field by spherical harmonic analysis. The present harmonic analysis which uses values of Earth's field measured at ground level, shows a deviation ranging between 0.2% and 1.2% from values determined by Vanguard III at altitudes between 500 Km and 4,000 Km. It is expected that analysis

based upon measurements, made at altitudes which are sufficiently high to avoid the effect of local anomalies at the Earth's surface, will permit the determination of a reference field accurate to within 0.1%.

The absolute accuracy of the rubidium magnetometer has been shown to be 0.1%, which in a field of 10^4 gammas corresponds to a 10γ error of measurement. The inaccuracy of a vector measurement of such a field is largely dictated by the accuracy to which the reference coordinate system of the measuring instrument is known. An error of 3 minutes of arc in the reference coordinates may correspond to 10γ in the total field measurement. Such a precision of orientation presents a considerable engineering problem in the satellite system. Heppner et al (Cospar 1961) indicate that errors arising from the inaccuracy of locating the satellite in space in the flight of Vanguard III represented an equivalent field indeterminacy ranging between 20γ and 60γ at different locations.

Zmuda (1958) has shown, that, in the absence of external field sources, scalar field measurements may be used to calculate the coefficients in the harmonic analysis. This fact, together with the greater ease with which precision of measurement can be made using scalar field instruments indicates that the rubidium magnetometer may be preferred to

component field devices in this application. The wide operating range of field values of the self-oscillating system and the drift free character of its signal, are advantageous features of the instrument.

2. Rapid Variations

This category of measurements deals with the location in the exosphere of sources of the micropulsation activity which is measured at ground level. Observations of rapid fluctuations of field constitute a variation technique and the resolution is limited by the data handling capacity of the satellite telemetry system.

3. Low Fields

The observations in this category are:

a) measurements of the boundary of the magnetosphere, which is expected to be disturbed, and

b) measurements of the interplanetary magnetic field.

Detection of low field values ($\sim$100 gammas) is restricted by telemetry bandwidth, and in some cases auxiliary techniques are necessary to provide a known additional field to bring the signal frequency within the telemetry band. At these low frequencies the rubidium magnetometer has very little deviation from absolute accuracy, since the

phase change in the feedback loop may be precisely controlled at 90°, and the fine structure of the resonance line is effectively zero.

3. High field measurements

Rocket measurements are essentially confined to the examination of the ionosphere for current layers which are thought to be the source of geomagnetic field phenomena observed on the ground. The observations are made as the rocket passes through the current zones, and the variation of field strength is inspected for anomalous deviations which may be due to local currents. This is essentially a variation experiment, and the technical difficulties, associated with the rocket's flight characteristics, outweigh the problems associated with the magnetometer. The experiment would provide more detailed information if vector measurements were made. However the accurate orientation of the instrument and of the vehicle in flight is not possible.

Standard geomagnetic measurements on the Earth's surface are made by vector instruments, which measure component values. In order to obtain vector measurements from a scalar field instrument a system of biassing fields must be used, such as that described by Shapiro et al (1960) and used in the proton vector meagnetometer during the International Geophysical Year. The measurement of micropulsations is also

carried out in component field directions, and component information is necessary for the identification of mode and polarisation of the waves. However, it is expected that a sufficient fraction of micropulsation activity occurs in the total field direction and so can be detected. Thus the period of waves may be measured conveniently by the rubidium magnetometer, and an indication of relative amplitude may be available. It is therefore possible to take advantage of the high sensitivity, and broad frequency response of the rubidium magnetometer in synoptic observations of micropulsations. In field work where the instrument must be transported to several stations within a short time, the fact that useful measurements may be made which do not require accurate setting up of the sensor is an advantage.

Further discussion of the operation and effectiveness of the self-oscillating magnetometer in ground measurements of the geomagnetic field is contained in Chapter 7.

CHAPTER 5

A WORKING MODEL FOR THE ORIGIN OF MICROPULSATIONS

Introduction

In Chapter 1 the theoretical analysis which was discussed suggested a model from which it might be possible to arrive at the basic elements of micropulsation origin and propagation. In this chapter a simple model, based on this concept, is derived from the properties of the dipole field, and shown to satisfy the same general conditions as the mathematical treatment. Several inferences are drawn from the model, which may be used to suggest experimental investigations.

Geometry of the Dipole Field

In this section a dipole field is discussed using the two dimensional coordinate system shown in Fig. 5.1.

The magnetic potential Ω is described by

$$\Omega = - \frac{M \cos\theta}{T^2}$$

The total force at $P(r, \theta)$ is

$$F = \frac{M}{r^2} (1 + 3 \cos^2\theta)^{\frac{1}{2}} \qquad (1)$$

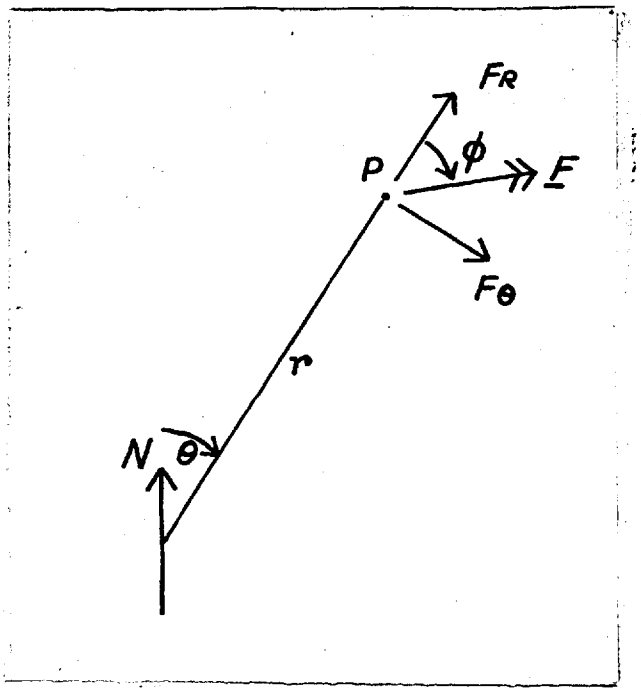

Fig. 5.1. Dipole coordinate system.

which makes an angle ϕ with the radial direction such that $\tan\phi = \frac{1}{2}\tan\theta$, a direction which is the tangent to the 'line' of force passing through P.

The equation of an equipotential line is

$$\Omega_i = \text{const.} = + \frac{M \cos\theta}{r^2}$$

and putting $+\frac{\Omega_i}{M} = D = \text{const.}$

becomes $D = \frac{\cos\theta}{r^2}$.

In the transformation $x = r\sin\theta$, $y = r\cos\theta$,

$$D = \frac{y}{(x^2 + y^2)^{3/2}}$$

$$\frac{dy}{dx} = \frac{3Dx\ (x^2 + y^2)^{\frac{1}{2}}}{1 - 3Dy(x^2 + y^2)^{\frac{1}{2}}}$$

$$= \frac{3Dr^2 \sin\theta}{1 - 3Dr^2 \cos\theta}$$

A line of force through a point is perpendicular to the equipotentials through the point, but does not have D = constant, and so

$$\left(\frac{dy}{dx}\right)_{\text{line of force}} = \frac{3\cos^2\theta - 1}{3\sin\theta\cos\theta}$$

Since $y = r\cos\theta$ $\quad dy = -r\sin\theta\, d\theta + dr\cos\theta$

$x = r\sin\theta$ $\quad dx = r\cos\theta\, d\theta + dr\sin\theta$

Therefore

$$\frac{-r\sin\theta\, d\theta + dr\cos\theta}{r\cos\theta\, d\theta + dr\sin\theta} = \frac{3\cos^2\theta - 1}{3\sin\theta\cos\theta}$$

ie. $$2r\cos\theta\, d\theta = \sin\theta\, dr$$

$$\frac{dr}{r} = \frac{2d(\sin\theta)}{\sin\theta}$$

Integrating

$$\log r = 2\log(\sin\theta) + k$$

i.e. $$r = C\sin^2\theta \qquad (2)$$

This is the equation of a line of force and since $r = C$ at $\theta = 90$, C is the equatorial radius of the line.

Substituting r from (2) in (1), the variation of field strength along a line of force is given by

$$F = \frac{M}{C^3}\ \frac{(1 + 3\cos^2\theta)^{\frac{1}{2}}}{\sin^6\theta} \qquad (3)$$

The length of a line of force is calculated by $dl^2 = (r\, d\theta)^2 + (dr)^2$ and $r = C \sin^2\theta$

$$dr = 2C \sin\theta \cos\theta \, d\theta$$

whence

$$dl^2 = C^2 \sin^4\theta \, (d\theta)^2 + 4C^2 \sin^2\theta \cos^2\theta \, (d\theta)^2$$

$$dl = \pm C \sin\theta \left[\sin^2\theta + 4\cos^2\theta\right]^{\frac{1}{2}} d\theta$$

$$= MC \, (1 + 3\cos^2\theta)^{\frac{1}{2}} \, d(\cos\theta).$$

Hence

$$e = \int_{\theta_1}^{\theta_2} + C(1 + 3\cos^2\theta)^{\frac{1}{2}} \, d(\cos\theta)$$

$$L = \frac{\sqrt{3}}{2} C \left[\frac{2}{\sqrt{3}} + \frac{1}{3} \log\left(\sqrt{3} + 2\right)\right]$$

$$L \doteq 1.4\, C$$

Thus $2L \doteq 2.8C$ is the total length of a line of force whose equatorial radius is given by C.

Fig. 5.2 illustrates the geometrical disposition of some representative lines of force for the Earth, and the magnitude of their field strength on the magnetic equatorial plane. Fig. 5.3 shows the calculated variation of field strength (eqn. 5.3) along a line of force. The point of interest is that within $\pm 35^\circ$ of the dipole equator the strength of the field is sensibly constant, and bounded on either side by high and rapidly increasing field strengths. The length of this constant section is given by $\int_{55^\circ}^{125^\circ} C \, (1 + 3\cos^2\theta)^{\frac{1}{2}} \, d(\cos\theta)$, and is approximately

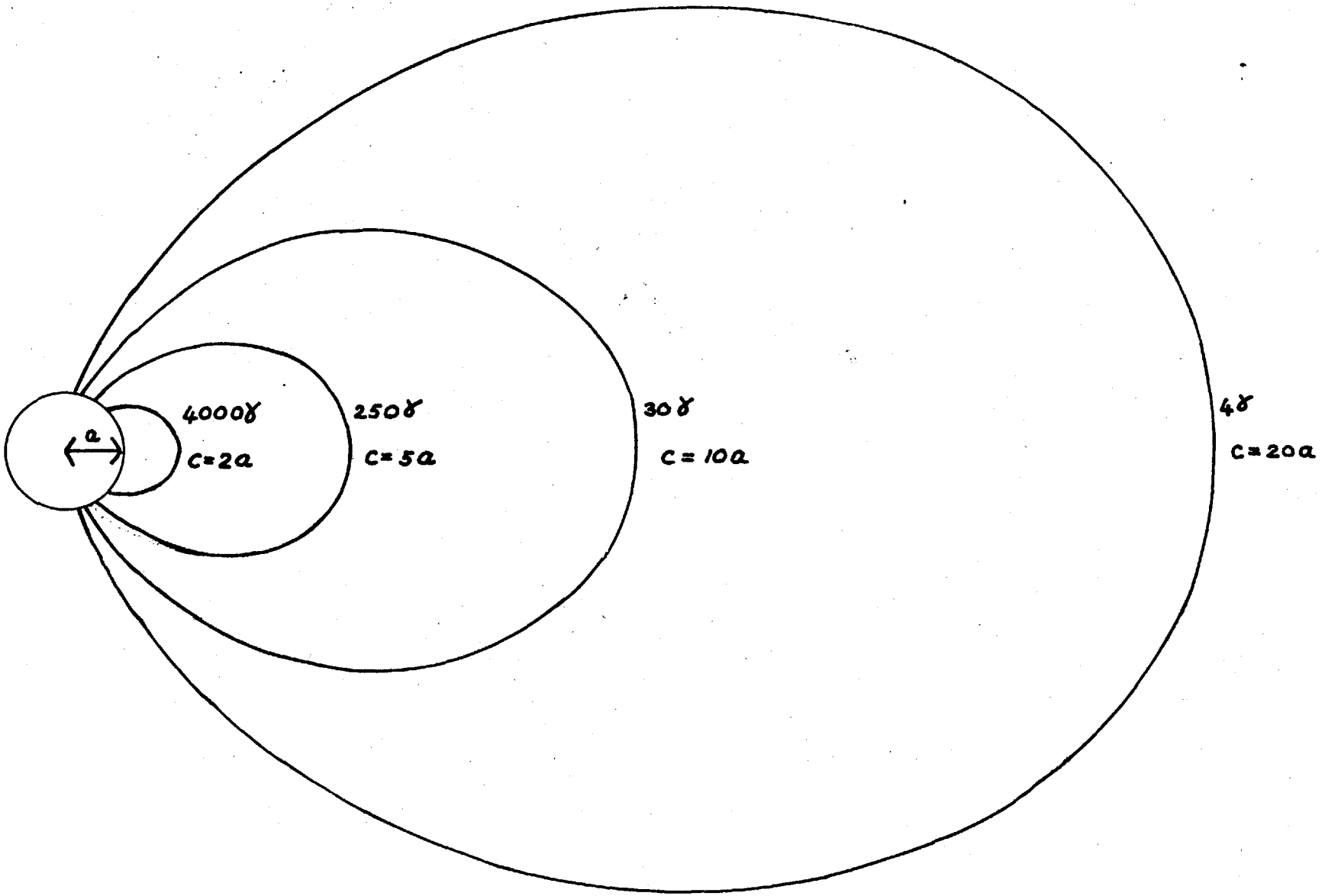

FIG. 5.2 THE LINES OF FORCE OF A DIPOLE.

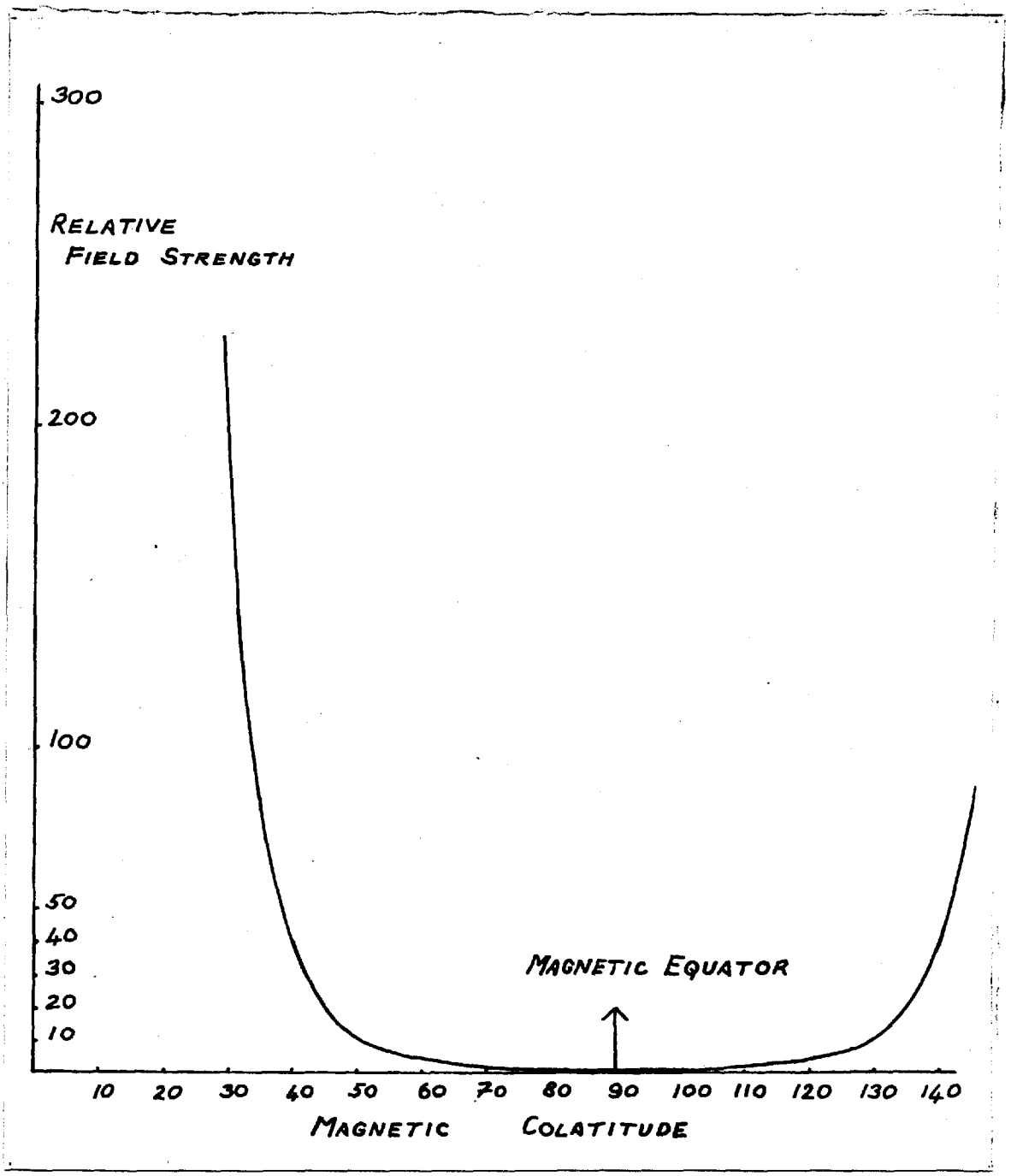

Fig. 5.3. Variation of field strength along a line of force, as a function of magnetic colatitude.

equal to C, the equatorial radius of the line in question.

Maxwell (A Treatise on Electricity and Magnetism. § 642) shows that the stresses in a medium due to a magnetic field of strength F consist, in the simple case of an unmagnetised medium, of a hydrostatic pressure $F^2/8\pi$ perpendicular to the force direction, and a longitudinal tension $\mu F^2/4\pi$ along the force direction. The pressure will be seen to play an important part in determining the interaction between energetic particles emanating from the sun and the Earth's field.

The tension, associated with a line of force, suggests that a situation exists which is analogous to the case of a stretched string, and that if the limits of the constant field section of a line of force are taken to be fixed, vibration may occur*. The period of vibrations of such a system is given by $T = 2l\sqrt{\frac{m}{P}}$, where l is the length of the resonant section, m is the mass density and P represents the tension. If the magnetic tension is substituted in this equation the periods of the vibrations may be calculated, provided some inertial property can be assigned to the motion. This is discussed in more detail later.

*The 'vibrating string' model, which is discussed in some detail in this chapter is based on the analogy between the oscillation of an elastic string and a line of force, suggested by Alfven, Cosmical Electrodynamics, Oxford Univ. Press, New York, 1950. A similar model has recently been used by Sugiura and Wilson (Journal of Geophys. Res. Vol. 69, No.7, 1964) to explain perturbations of lines of magnetic force at conjugate points.

The boundary conditions used to define the vibrating action of the lines of force of a dipole field are presented by the rapidly increasing tension and pressure associated by the force function (eqn. 5.3) outside the central section. Here the string analogy is perhaps better replaced by one representing the line of force as a spring. In this case the magnetic stresses are represented by the stiffness of the spring, and the boundary region is where the stiffness increases rapidly, with a corresponding decrease in flexibility.

The inference is that the dipole field of the Earth has a cavity, wedge shaped in the meridian plane, all round its equatorial plane and defined by the almost constant field strength of the central section, and that conditions exist which indicate that a resonant behaviour may be expected.

Interaction between the solar stream and the maghetosphere.

The model which describes the Earth's situation with respect to the solar system in shown in Fig. 5.4 in which the scale is half that in Fig. 5.2 and the same lines of force are represented. A stream of particles emitted by the sun flows past the Earth. The direction of the particle stream, the so called Solar Wind, is radial from the sun and it consists for the most part of protons and electrons.

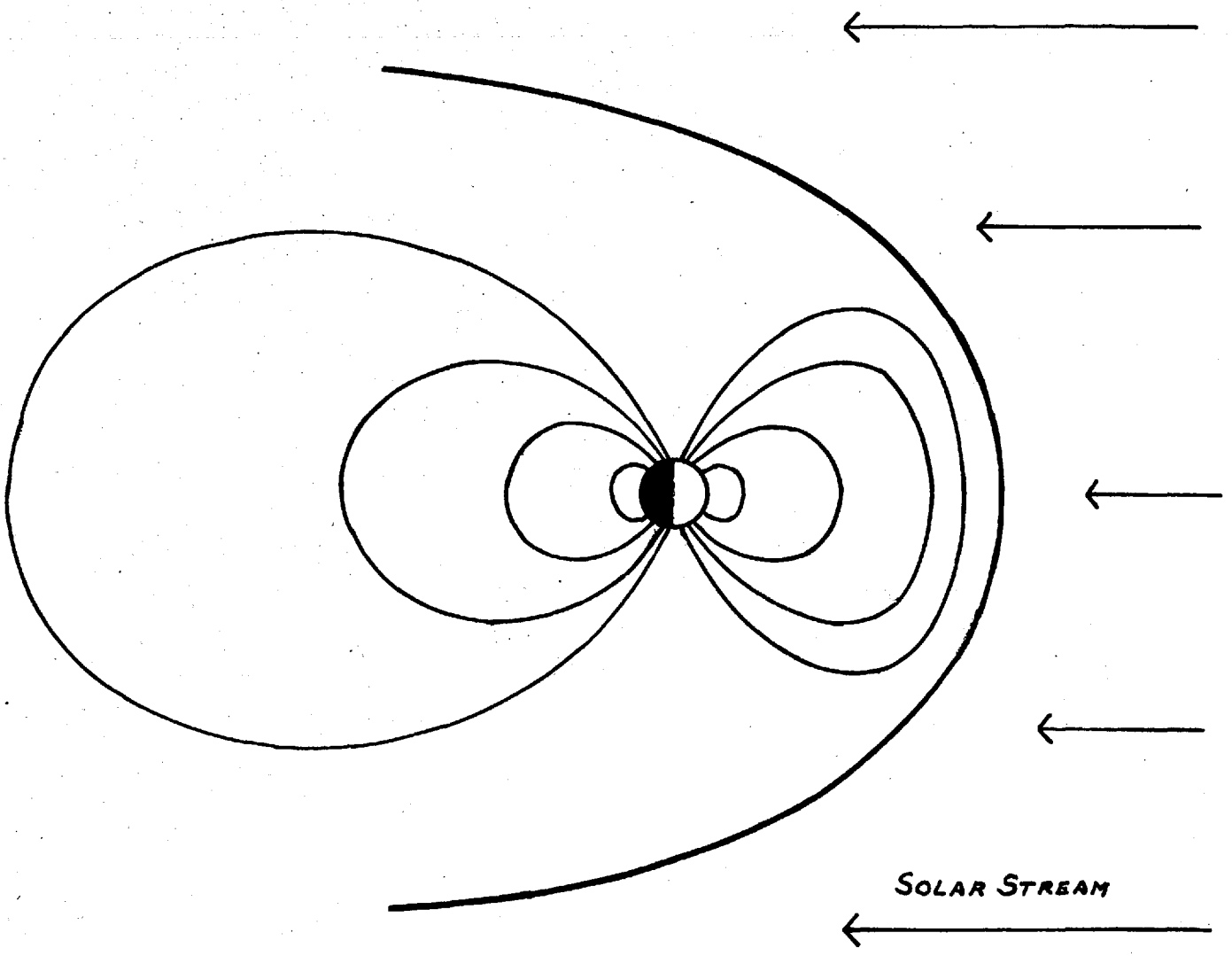

FIG. 5.4 DEFORMATION OF THE DIPOLE FIELD WITHIN A CAVITY (RADIUS = 10 a) BY THE SOLAR STREAM. [SCALE = $\frac{1}{2}$ FIG. 5.2]

It is assumed to be homogeneous and electrically neutral, assumptions which in general are required to explain why it does not dissipate by the action of electrostatic repulsion. The solar stream may be regarded as the important vehicle for the transmission of solar activity to the environment of the Earth.

The primary action of the solar wind on the magnetosphere is to deform the shape of the dipole field. The conditions occurring at the boundary between solar wind and magnetosphere are not easily arrived at uniquely, but some general conclusions may be drawn which are adequate for present purposes. Firstly, since the solar wind consists of large numbers of free electric charges, it may be regarded as a good conductor of electricity. Consequently the geomagnetic field lines at the boundary must be parallel to the boundary, and may not project into the conducting medium. Secondly, the pressure of the impinging plasma stream must be equalled by the outward magnetic pressure of the dipole, which is in effect the definition of the boundary between 'Earth' and 'Space'.

These two conditions imply a narrow boundary zone and a compression of the outermost lines of the dipole field on the side of the Earth facing the Solar Stream of particles.

On the night side of the Earth, the boundary is less clearly defined because the equations, involving the

hydromechanics of fluids and their electromagnetic interaction with the Earth's field, are too cumbersome to solve directly. Solutions have suggested an extension of the magnetosphere on the night side, although, since the dipole extends to infinity in the absence of a conducting medium, the significance of the extension is not clear. The tear drop model described is closely analogous to a compressible sphere which in a fluid stream, is compressed at the side of impact of the fluid, by the impinging fluid pressure, and extended at the rear by the vacuum it creates in the fluid. By analogy, it may be expected that the wave patterns found in the simple case will have their equivalent in the regions of solar wind near the Earth. It has been suggested that vortices in the 'wake' formed in the solar wind by the Earth may be a possible source of some disturbances.

Bearing in mind the dipole characteristics displayed in Figs. 5.2 and 5.3 the conjectured form of the deformed dipole field of the magnetosphere may be represented as in Fig. 5.5 which is drawn in the equatorial plane and illustrates the positions of the lines of force, or meridians, under the action of a constant solar wind. Here the solar wind is taken to be an infinite uniform stream and the field lines belong to one group which in the undisturbed state would have the same radius as those shown by the dotted continuations. It is clear that the section of a line of force within $\pm 35^{o}$ of the equator

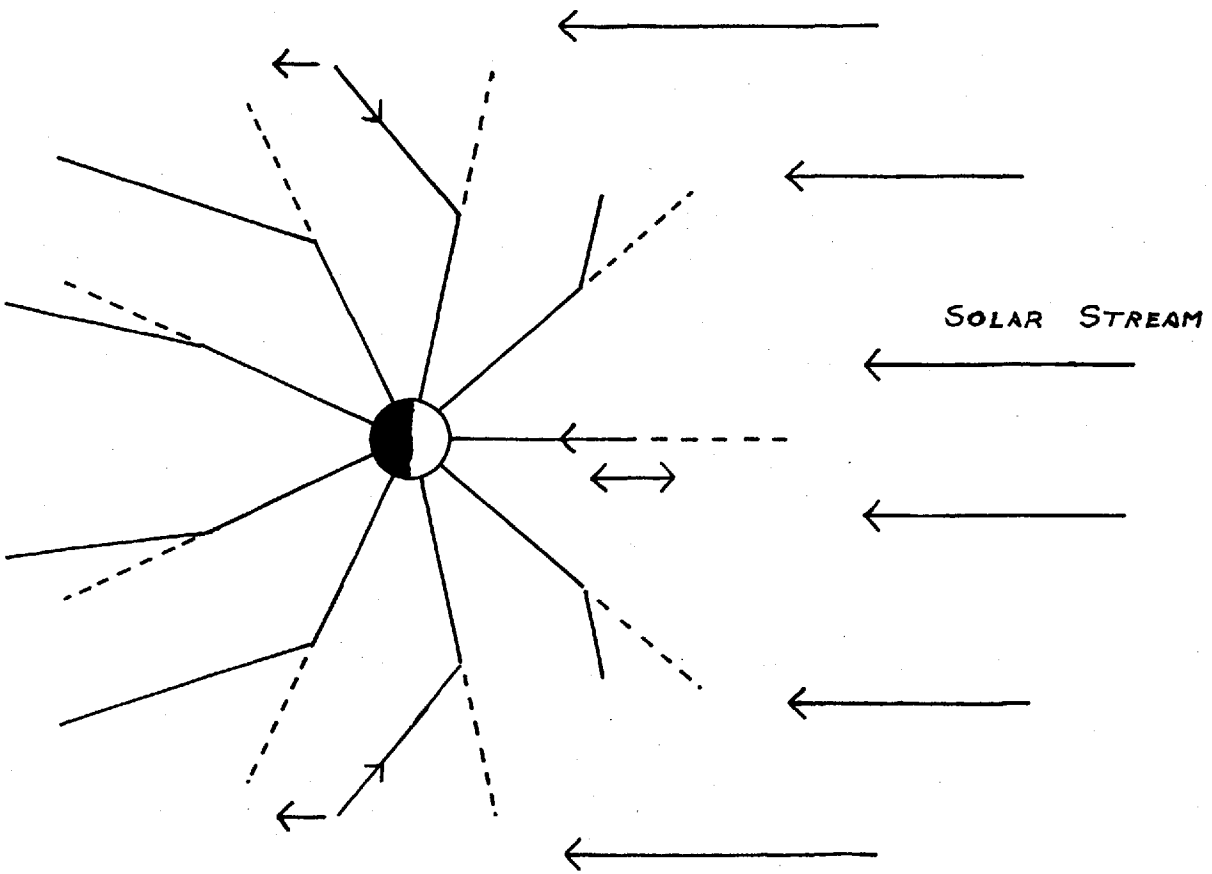

FIG. 5.5 ILLUSTRATING THE DEFORMATION OF THE MERIDIAN PLANES BY THE ACTION OF THE SOLAR STREAM.

is more strongly deformed by particle pressure, due to its uniformly weak field strength and its geometrical position.

If resonant behaviour may be attributed to a line of force, it can be excited by any small irregularities in the solar wind stream. Small changes in the conductivity or velocity of the particle flux will excite resonant vibration in a manner analogous to the wind blowing on telegraph wires. The precise form of the exciting mechanism and its interaction with the lines of force cannot be discussed with any confidence, however it is not unreasonable to assume that some interaction does exist which is capable of exciting the vibration. If the central section of a line of force is taken to be the active section, several conclusions may be drawn from the model.

If it is assumed that small disturbances of the plasma stream are normal to the plasma front, the initial displacement of the line of force lies in the direction of the velocity vector of the stream. If this direction is called 'Noon' then the diurnal variation of the resonant behaviour may be related to it. In Fig. 5.5 suppose the Earth to be rotating in a counter clockwise direction. At noon the resonant interaction produces linearly polarised vibrations in the magnetic meridian, which, if transmitted to the Earth's surface along a line of force, would appear as pulsations in the meridian plane and perpendicular to the total force

direction.

At sunrise, the top of Fig. 5.5, the disturbance produced would be perpendicular to the meridian in an undeformed dipole field, and would produce linearly polarised pulsations in the E-W horizontal plane. Similarly, at sunset the pulsations would be in the E-W plane. In the case where deformation of the line exists, the restoring force is not co-planor with the disturbance. This produces eliptically polarised vibrations of the line, which at sunrise are counter clockwise in Fig. 5.5 and at sunset are clockwise. The characteristic pulsation activity at the ground is, in these cases, eliptically polarised in the plane perpendicular to the field direction, in opposite senses on either side of the noon meridian. Thus in the course of a day the plane of polarisation of pulsations might be expected to rotate round the field direction from the horizontal in the morning, through vertical at noon, back to horizontal in the evening, and the sense of its polarisation reverses at noon.

Period of the modes

If a line of force may be regarded as a stretched string, the frequency of modes is given by $\nu = \frac{n v'}{2l}$, where n is the order of the mode, v' is the corresponding wave velocity and l is the length of the vibrating section. It can be shown that the wave velocity for propagation of a magnetic

disturbance along a line of force is

$$v = \frac{F}{2}\sqrt{\frac{\mu}{\pi\rho}}$$

where F is the field strength,

μ is the permeability, and

ρ is mass density of exosphere particles.

For the resonant section, with n = 1

$$J = \frac{F}{4l}\sqrt{\frac{\mu}{\pi\rho}}$$

Also, since $T = C \sin^2\theta$ for a line of force, and t = a for a spherical Earth, $C = a/\cos^2\lambda$ describes the point where a line of force with equatorial radius C meets the Earth's surface, with λ, the geomagnetic latitude, equal to $90^\circ - \theta$

Hence T_λ, the period of fundament resonance of a line of force, referred to the magnetic latitude on the Earth's surface where the line intersects the Earth is given by

$$T_\lambda = \frac{1}{J} = \frac{4l}{F}\sqrt{\frac{\pi\rho}{\mu}}$$

Considering the central section of a line, with l = C

$$T_\lambda = 4C\sqrt{\frac{\pi\rho}{\mu}} \cdot \frac{1}{F}$$

Using equation (3) $T = 4C\sqrt{\frac{\pi\rho}{\mu}} \cdot \frac{C^3}{M}\left[\frac{\sin^6\theta}{(1+3\cos^2\theta)^{\frac{1}{2}}}\right]$

$$= \frac{4a^4}{M}\sqrt{\frac{\pi\rho}{\mu}} \cdot \frac{1}{\cos^6\lambda}\left[\frac{\sin^6\theta}{(1+3\cos^2\theta)^{\frac{1}{2}}}\right]$$

In fact the substitution for F is more correctly replaced by an integration of the form $\int F.dl$. However within the

vibrating section considered it is sufficient to take $F = \frac{M}{C3}$, i.e. the equatorial value. The term in square brackets is included in the calculation to indicate that a variation does exist within the section. The simplified form of this equation $T_\lambda \propto \frac{1}{\cos^8\lambda}$ is the same as that derived by Dungey in his discussion of the resonant modes of oscillation of the magnetosphere, and used by other authors as the basic equation describing the behaviour of micropulsation periods with latitude.

The $\frac{1}{\cos^8\lambda}$ law indicates that $T_\lambda \to \infty$ when λ approaches 90°, i.e. at the poles. It is clear that a cut-off period must exist in the real situation, corresponding to the finite outermost line of force. This also suggests that a polar 'dead zone' may exist, lines of force within which do not connect directly with their couhterparts at the opposite pole.

The equation for the wave velocity in the above shows that, although a magnetic line of force in free space has no mass, and thus, if displaced from its equilibrium position by some means, would return to it on release at 'infinite' speed, and with no resultant oscillation, the interaction between a line of force and any electrically charged particles in its vicinity, is such that the inertial properties, which requires finite force to produce finite acceleration, is present in the displacement of magnetic lines. Thus ρ, the density of

charged particles, replaces m, the string density, in the velocity formula.

It is not intended to deal with the particle content of the exosphere in a detailed way. However, the general structure of the particle distribution has a strong bearing on the form of the latitude dependence of period and on the boundaries of the resonant cavity.

A particle, travelling across a line of force, experiences an acceleration toward the line of force due to the interaction between the magnetic field and the component of its velocity perpendicular to the field direction. In the exosphere this leads to a trapping of particles by the geomagnetic field lines where the particles spiral along the lines until their parallel velocity is reversed, at the so-called mirror points, by the increase in field strength as the poles are approached. In the propagation equation the wave velocity is inversely proportional to the square root of the particle density, so that the mirror points represent the extremities of a low velocity zone created by the density of trapped particles. It is clear that the location of the mirror points, although dependent on several factors, is associated closely with the high field region at the ends of the vibrating section discussed. In this way an enhancement of the reflecting properties of the high velocity region outside the central section may be imagined. Such a dependence

of the Alfven velocity upon particle density is used by Kato to derive a resonant cavity at low altitude, using the very high particle density of the upper ionosphere.

A second important respect in which the particle density distribution affects this discussion is where its magnitude produces a deviation of $T\lambda$ from the $\frac{1}{\cos^8\lambda}$ law. Fig. 1.2B shows a model for the density distribution with altitude, and it is clear that where lines of magnetic force traverse regions of high particle density, viz. those interacting the Earth at low latitudes, the fundamental period of oscillation is increased because of the greater inertial property of the gas. At the same time, consideration of a magnetosphere which is constrained to be inside a cavity in a conducting medium, suggests that the high latitude periods given by the $\sec^8\lambda$ law may be reduced, a greater reduction occurring at greater latitude. When the dipole geometry is considered it seems likely that the greatest effect of the compression will exist in the vibrating section of the outermost lines, resulting in a flattening of the $\sec^8\lambda$ curve at high latitudes. Fig. 5.6 shows the sort of modification in the simple theory, of the effect of confining the dipole field to within 10 E.R. which is illustrated in Fig. 5.3, and of the low altitude particle density.

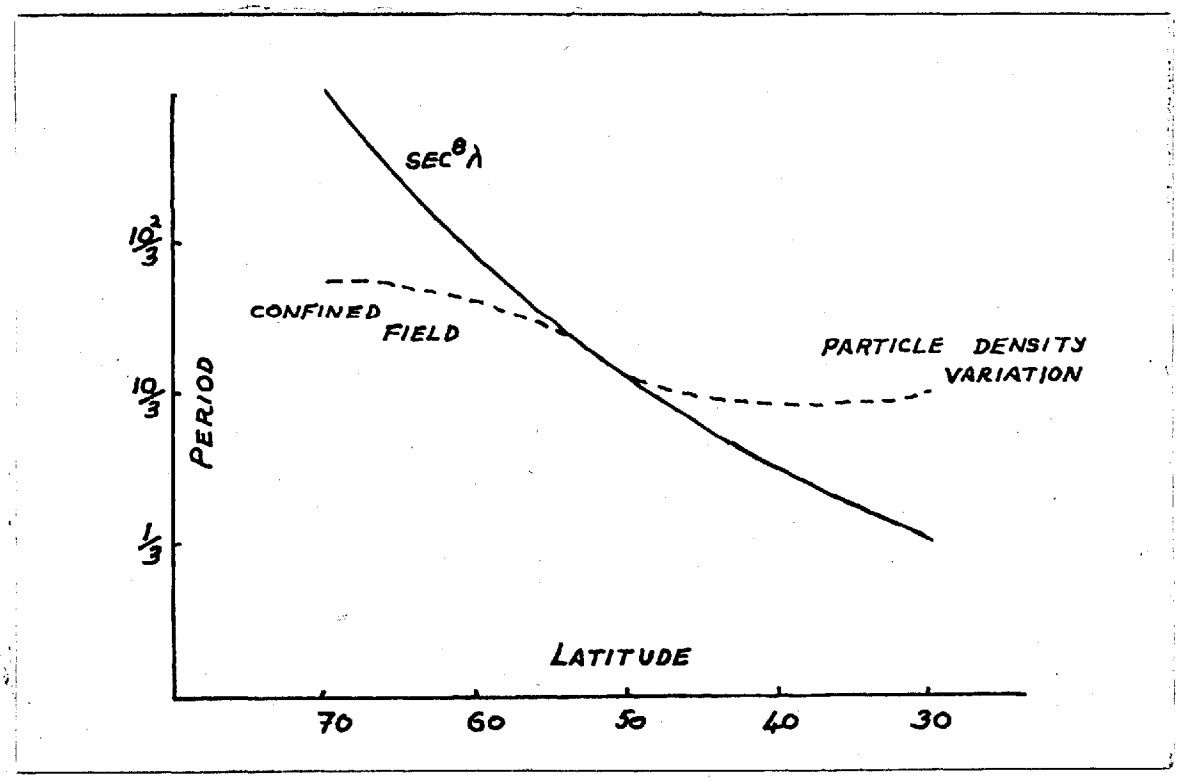

Fig. 5.6. Illustrating the $\sec^{8}\lambda$ law and its modifications due to the pressure of the solar wind and variation of particle density in the exosphere.

Modes of propagation

It is not clear what the interaction process causing small disturbances of the magnetic field may be. If the boundary is very clearly defined, and it may be assumed that few concentrations of particles cross into the magnetosphere, then the inference drawn previously holds, at least for the noon meridian. At sunrise and sunset it is likely that a proportion of the disturbance is along the particle stream vector, but if an intense burst of fast particles of one

electrical sign passes in the solar stream at these regions, the electromagnetic interaction upon a line of force is likely to be normal to the stream vector. If the magnetosphere boundary is circular in its equatorial section, it is possible to argue that the polarisation of vibration should be in the meridian, everywhere on the day side of the Earth.

Considering again the noon meridian, if particle bursts can cross the boundary, with sufficient energy not to be trapped by the outermost lines of force, then the disturbance on the field line is perpendicular to their velocity vector, and may in consequence produce an E-W polarisation.

The magnetic field disturbances so far discussed have been perpendicular to the field direction, and it has been assumed that transmission takes place along the lines of force. It has also been assumed that no interaction occurs between adjacent lines of force.

The displacement of a line of force in its meridian plane from its equilibrium position implies that in the displaced position the force value has been changed by an amount, say ΔF, in the field direction. ΔF corresponds to the difference in force between the line's equilibrium value and the value of the line, in equilibrium through the displaced position. Thus, it occurs that where previous

remarks have dealt with oscillations occurring in the meridian plane it is more correct to think of the disturbance vector as lying in the direction of the field line. This corresponds to the poloidal mode described by Dungey, and transmission takes place isotropically.

In the case where a line is displaced to a position on its own shell during oscillation, it is clear that no such longitudinal vibration exists. This represents the torsional mode.

It is possible that oscillations taking place in the meridian plane may give rise to a component which has its disturbance perpendicular to the field line and is transmitted along the field line as indicated earlier in this chapter.

Thus, both modes of vibration may be inferred from the dipole field geometry without specifying very different conditions for their origin, and an interaction between them may be expected. Watanabe indicates an interaction between modes and this seems a reasonable condition to exist in fact. Also a complete lack of interaction between lines of force specified so far is not realistic, and it would seem reasonable to expect that considerable volumes of the exosphere are involved in any oscillation, particularly in the case of Pc activity which lasts for long periods of time.

Such volume oscillation may be indicated by the line width of the observed pulsations.

Conclusions

Several features of micropulsation occurrence may be inferred from a model of the exosphere based on the dipole field geometry, using simplifications which, in general, are no more sweeping than those required by the more specific mathematical treatment.

1. Transverse waves may exist, which display a clearly defined polarisation content. However, the mode of excitation cannot be specified and may lead to different polarisation features.

2. An oscillation where the disturbance vector is in the meridian plane may exist.

3. A latitude dependence of period is associated with the geometry of the situation.

4. Diurnal variation of the polarisation and mode of occurrence may be expected of both types of oscillation. Exact measurements of these variations may allow conclusions to be drawn about the excitation process of the vibration.

Several reservations are necessary in an intuitive analysis such as this, in view of the apparent discrepancies with the mathematical treatment of the obvious lack of experimental verification.

The model does not indicate a specific difference between the transverse and isotropic modes. In fact the difference is due to the behaviour of exosphere particles. Thus, in the case of transverse waves the boundary conditions may be specified, since propagation is along a line of force. In the isotropic mode, which has been thought to be excited by the same mechanism as the transverse, the propagation is, in the simplest case, at right angles to the field line and the final resonant cavity is not specified in an intuitive way. It is possible that secondary resonances may be available, cf. Kato, where standing wave patterns are formed in a selective way from disturbances travelling down from high altitude. The boundary conditions within such cavities may affect the polarisation properties inferred from the simple model, in the formation of standing wave patterns.

The only divergence from the mathematical treatment is the stated possible existence of a transverse mode with its disturbance in the meridian plane, and the suggestion that this may be the source of elliptical polarisation in observed events. The direction of rotation of polarisation of such an event observed at conjugate points in the north and south hemispheres would be opposite. Such events have been observed. However, Piddington has indicated that such polarisation phenomena can be explained because of the anisotropy of the

conductivity of the exosphere.

The events discussed have been related in a more or less direct way to the incidence of solar plasma on the magnetosphere. The same modes of resonance are available on the night side of the Earth, but their excitation cannot be specified. However, observations of the occurrence throughout the night of specific events may allow some conclusions to be drawn as to the position of their source in the magnetosphere, since their occurrence is limited.

One further point is relevant to the discussion of night time events. Since the dark side of the Earth does not suffer the confining influence of the impinging plasma stream the modifications of the latitude dependence of period due to this cause do not apply, and it is to be expected that a greater variation of period will occur in the case of P_ts than in the case of Pc's.

The direction of the plasma stream vector does not coincide with the optical direction of solar radiation, because of the rotation of the sun about its axis and the motion of the Earth within its orbit. This, together with the fact that the geomagnetic dipole is eccentric, may indicate that a reference time scale, related directly to those phenomena might be more appropriate than local time.

The polarisation modes to be expected cannot be specified

in a precise way because of the unknown manner in which excitation may occur. Experiment must therefore be directed toward identifying the mode of occurrence and its polarisation properties. From observations of this nature it may be possible to indicate the exciting mechanism of exosphere oscillations.

The most important reservation about the analysis contained in this chapter concerns the two diemensional analysis, and the interaction of neighbouring lines of force, via the medium in which they exist. The two dimensional analysis corresponds to the mode with m = 0 in Dungey's work. It is not intended to consider any change in the order of mode or symmetry which may be dependent on a coupling of adjacent lines of force. However, since it is unreasonable to assume that each line of force may oscillate independently it is necessary to take account of the possible effects upon the conclusions which have been drawn so far. It has been indicated that large volumes of the exosphere may be involved on any given oscillation event.

Consider an event which is stimulated by a precise impulse delivered to a chosen line of force and which is transmitted to the ground along the lines of force. If interaction exists it produces a widening of the region of occurrence of the event on the ground in two essential ways. The first is where the

interaction takes place between adjacent lines on the same shell, and produces a broadened range of longitude over which the event may be detected. The second is where the interaction causes lines of force at lower altitude to be excited, and produces a widened range of period and of latitude over which the event may be observed. Measurements of the range of occurrence in latitude and longitude of events which may be thought to originate from a very distinct event, may indicate the degree of interaction which does take place. Further, the time taken for the interaction to be transmitted between adjacent lines may be represented by a variation of time duration of occurrence on the ground, or of a time constant of the detected event, over the range of occurrence.

In the case where many excitation events occur in a short time, in a random way, which corresponds to the case of Pc activity, considerable volumes of the exosphere may oscillate. The large volume oscillation may be sustained by individual stimuli occurring at widely separated locations and with quite different characteristics. Therefore it is to be expected that the general level of activity may contain all polarisations occurring in a random manner, and the broadening of the resonance will result in a broad line width of the observed pulsations. Further the distinct latitude dependence of micropulsation period may be hidden within the range of

occurrence of the pulsations caused by a large scale volume oscillation of the exosphere. The degree to which such interaction effects occur can be determined to some extent by experiment, and is highly significant in the interpretation of measured events.

Finally, it must be stated that since the excitation processes envisaged in this section have been derived from the solar wind, and since the variation of field strength within the vibrating section is rapid with altitude the resonant actions discussed should occur at high altitude, and therefore represent high latitude events. It is not possible to indicate the range of latitude within which the assumptions used are valid because of the vagueness of these assumptions. However, Dungey's analysis of the same type of phenomenon was limited to geomagnetic latitudes greater than 40° and it seems reasonable to place the same general lower limit to the latitude range covered by this discussion.

CHAPTER 6

THE FIELD TEST

Introduction

The field test to which the instrument was subjected was designed to enable an accurate appraisal to be made of the Rubidium Vapour magnetometer and its associated monitoring system. At the same time it was intended to act as a source of experimental information on micro-pulsations leading to the design of future investigations both on the ground and using satellites.

From the review of present knowledge and the consensus of theoretical opinion it seemed possible to attempt to establish the dependence of pulsation period on latitude of their occurrence. To this end a traverse approximately along a line of longitude was made. Four observations were visited in middle and high latitudes where the change of period is expected to be most noticeable. Only one magnet-ometer system was available for the work, so that coincident measurements were not possible. It was thought that pulsat-ions at each station might display sufficiently distinct period features that a generalisation based on recordings taken at different times would be satisfactory. The four

locations are shown in Fig. 6.1, the geography of North-West Europe. They are Kiruna (magnetic latitude 65.3°N), Lerwick (62.5°N), Eskdalemuir (58.4°N) and Hartland (54.6°N). Recordings were made for about seven days at each station.

The equipment used in the field work is listed in Table 6.1. The total weight of the apparatus is 120 lbs and mains power consumption is less than 100 watts.

TABLE 6.1

A. Lamp power supply	115 volts	15 ma
	6 volts	300 ma
B. Amplifier power supply	12 volts	10 ma
C. Decoder power supply	10 volts	0.75 ma
D. Frequency Counter		
E. Decoder		
F. Potentiometer recorders	6" per hour 30" per hour	

A domestic fan heater was taken on the field work to ensure adequate heating facility, and an oscilloscope, in most cases borrowed from the observatory, was used in the initial setting up procedure to monitor signal quality.

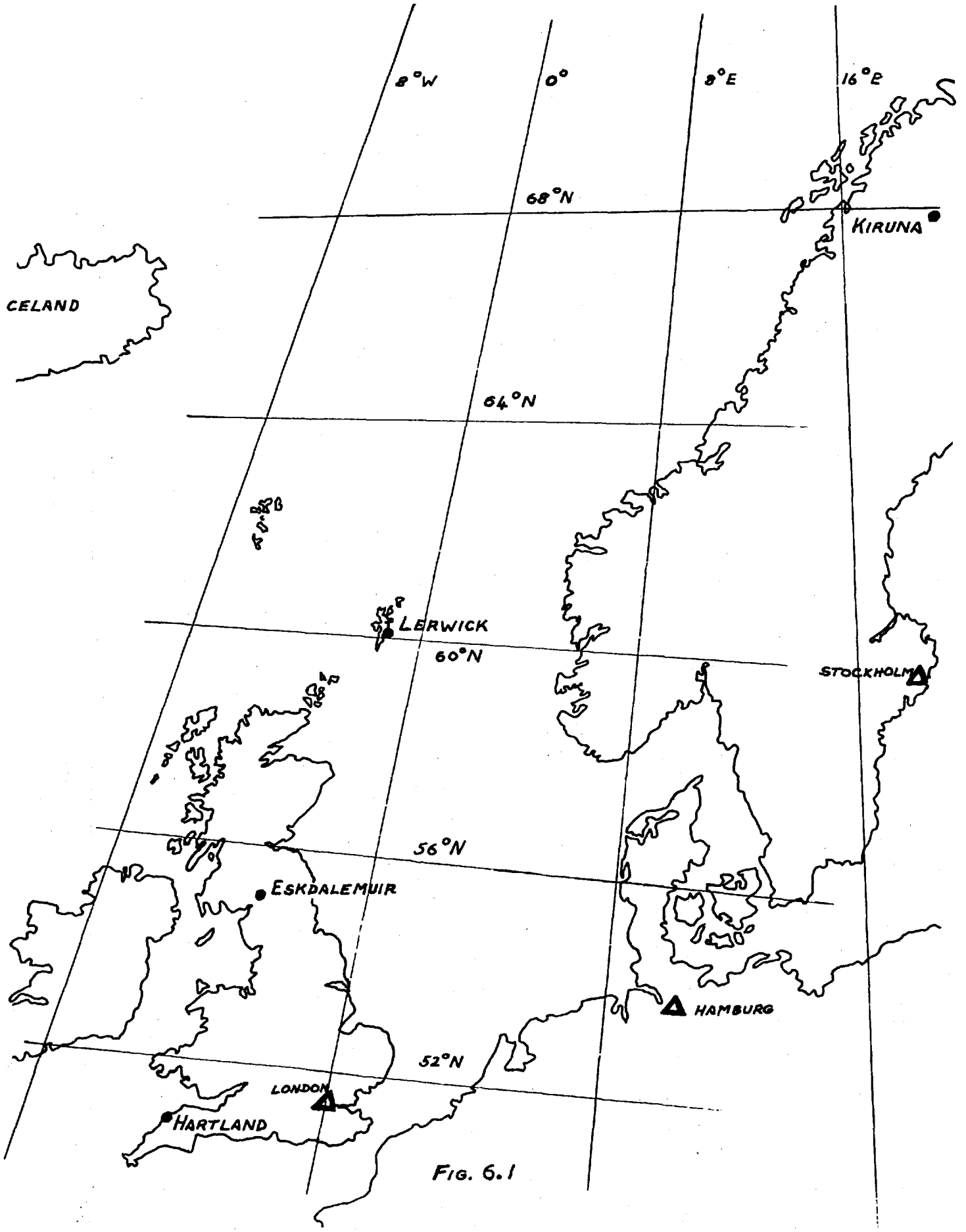
8°W
0°
8°E
16°E
68°N
KIRUNA
CELAND
64°N
LERWICK
60°N
STOCKHOLM
56°N
ESKDALEMUIR
HAMBURG
52°N
LONDON
HARTLAND

FIG. 6.1

Frequency measuring system

In order to attain the highest possible sensitivity, and to take advantage of the digital form in which the magnetic field measurement is presented by the self-oscillating magnetometer, a frequency counting technique was employed. It can be argued that since the present application is to small variations of field value, the frequency counting system is used in a very inefficient way. However, its directness and the facility with which measurements and tests, other than those of micropulsations, can be made, recommend frequency counting at the outset.

An alternative method, that of using a frequency discriminator to demodulate the magnetometer signal was tried. This method introduced some of the difficulties common in other types of highly sensitive magnetometers, but not inherent to the self oscillator. The discriminator output is liable to drift due to variations of input signal amplitude, temperature and supply voltage, and it was clearly not possible to improve the magnetometer signal to noise ratio sufficiently to acquire the resolution with a discriminator of which the self oscillator is capable.

It was considered to beat the magnetometer signal with a standard local oscillator to produce an audio frequency output which could then be applied to a frequency discriminator. The

resultant situation is not greatly different from the simple case and a certain degree of limitation would be imposed by the limited final bandwidth.

It is possible to construct a very compact recording magnetometer using a frequency discriminator and such an instrument may well have applications where variations of field need only be measured with a resolution of 1 gamma.

The counting system, which is illustrated schematically in Fig. 6.2 was designed with the Venner frequency counter

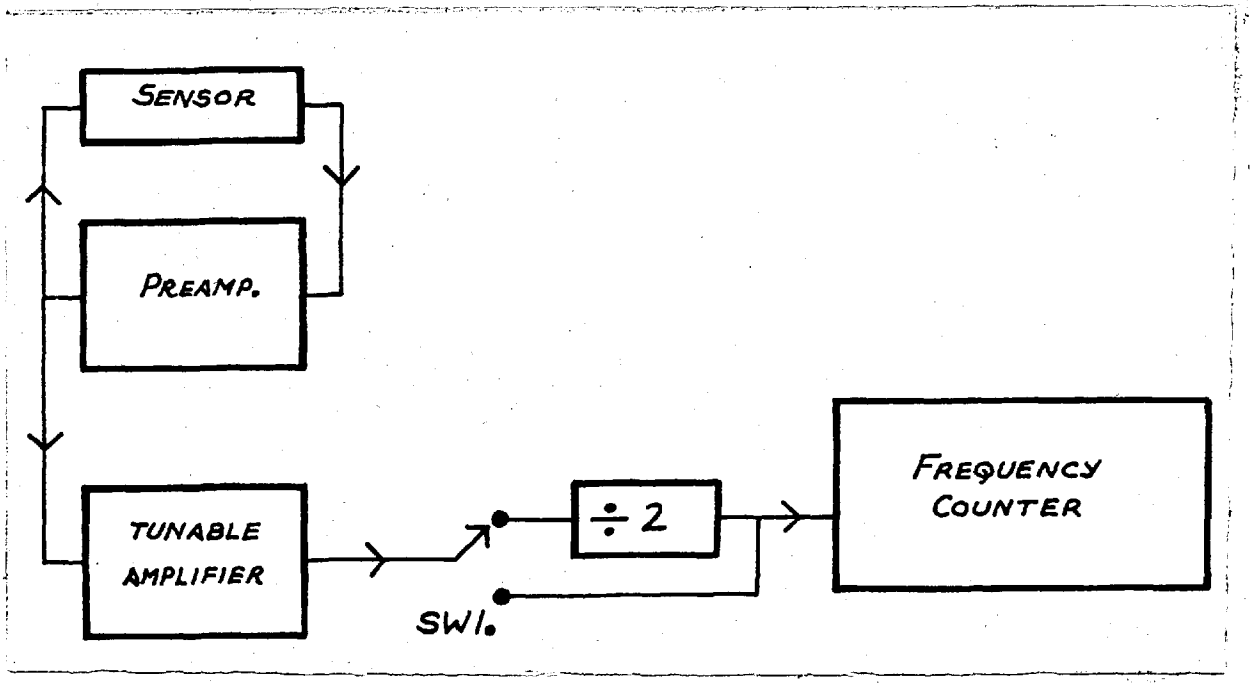

Fig. 6.2. Schematic diagram of the frequency counting system.

(TS 3336) as the basic element. The system originally included automatic recording of the data, in binary form

on punched tape. This is the most direct way of recording information received by telemetry from a rocket born magnetometer, in a form suitable for machine analysis.

The magnetometer consists of the sensor and Earth's field preamplifier described previously (Fig. 4.5), with the addition of a tuned amplifier, which has a bandwidth of 20 Kc/s (shown in Fig. 6.3) whose purpose is to amplify the

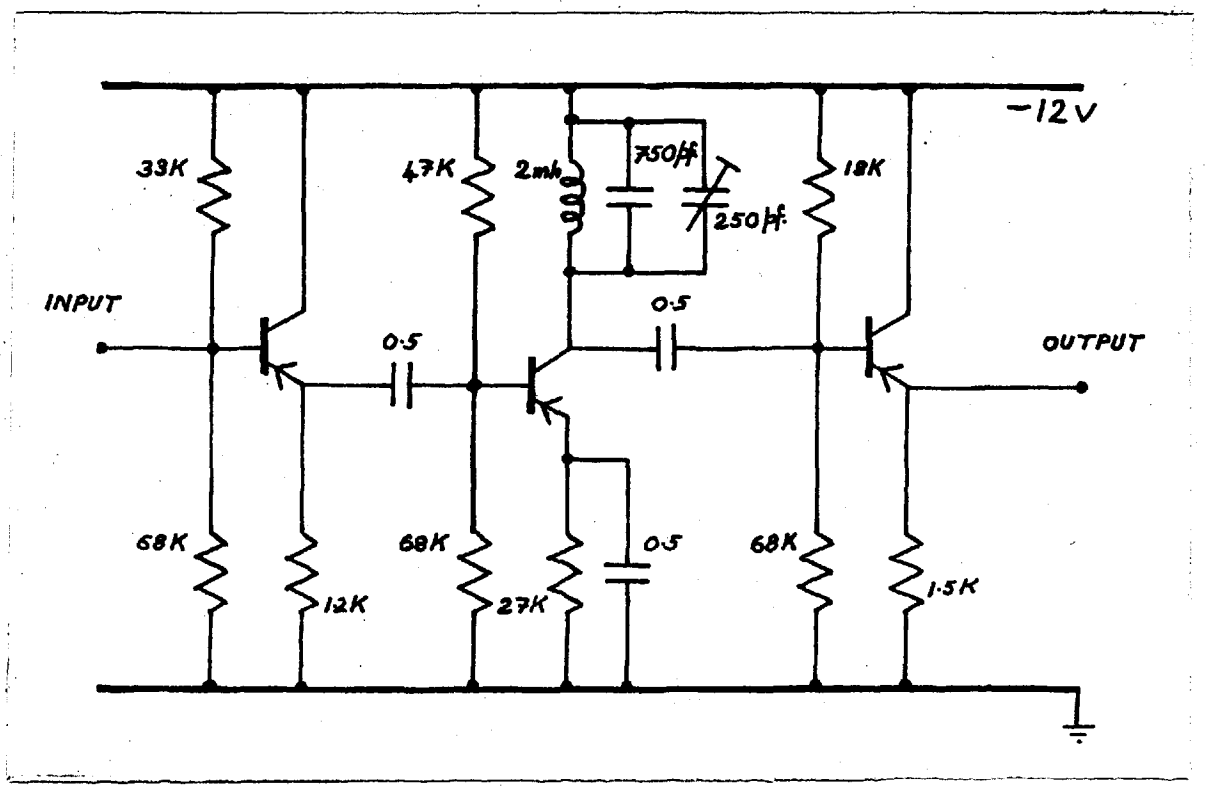

Fig. 6.3.Tuned amplifier circuit.

signal and improve the signal-to-noise ratio. The biassing of the last stage of the tuned amplifier is such that the

transistor is overdriven at the peaks of the signal wave, resulting in a clipped output whose amplitude does not vary with small variations of the input signal amplitude. This procedure ensures that the triggering of the counter is affected as little as possible by small variations in the quality of the magnetometer signal. Using the tuned amplifier it is possible to produce sensible frequency measurements from less than a one to one signal-to-noise ratio from the magnetometer.

Two facilities are available in the counter. The direct measurement of frequency is carried out by counting the number of magnetometer cycles occurring during a selected time interval, which is accurately set in the counter by counting a specified number of pulses from a standard oscillator. The reference standard of the Venner counter is a 1 Mc/s oven controlled crystal oscillator whose stability is better than one part in a million. The direct frequency measurement by this method results in an uncertainty of $\pm$ 1 count in the magnetometer signal measured, which for Rb^{85} operating in a typical Earth's field signal of 200 Kc/s produces a resolution of 1 in $2 \times 10^5 \times T$. T is the time in seconds over which a measurement is made. For a one second counting time this represents a sensitivity of 0.2 gamma, and for ten seconds 0.02 gamma.

In order to improve the resolution without resorting to long counting times, and the corresponding loss of high frequency information, the counting procedure is inverted. The second facility in the Venner counter allows a fixed number of magnetometer cycles to be counted. This number is selected absolutely and used to define a time interval in which pulses from the standard oscillator are counted. Thus the measured quantity is the time required for the chosen number of signal pulses to pass, and is limited to $\pm$ 1 μsec. due to the uncertainty in counting the standard. The signal-to-hoise ratio of the magnetometer signal is sufficiently high for the uncertainty due to noise to be less than 1 μsec. The resulting accuracy of measurement is 1 in 10^6 x T. Using the same values as before, the resolution with a 1 second counting time is 0.05 gamma.

It is clear that in both methods of counting the resolution attainable is directly proportional to the time over which a measurement is made. The measured quantity is thus the average value over the counting time, and a continuous record of field measurements consists of a series of discrete field values separated in time by the time taken to make a count. In Fourier analysis it requires three points to specify a sine wave uniquely, and in the analysis of continuous trains sampled as above it is not possible to

resolve fluctuations whose periods are less than twice the sampling rate. Since the field work was to be carried out without machine analysis in the first instance, it was decided to let experimental test be the criterion in arriving at the compromise between resolution in field strength and resolution in time. A small magnet was rotated by an electric motor to produce suitable fluctuations of field at the sensor and it was found that a period five times as long as the sampling rate could be distinguished clearly. Periods less than this value can be detected, but their recorded quality depends very much on the precise value of the period and its phase with respect to the sampling process.

The sampling time includes the 'display time' of the counter. This is the time during which the counter holds the counted number and resets itself for the next count. The minimum display time in the counter used is approximately one second, so that the maximum sampling rate is limited to a great extent by this.

Typical Pc periods observed by Lock and Stevens (private communication) at Christchurch, Hants., have periods of the order of 40 seconds and reported periods by other authors have similar values. Taking this into account, it was possible to use a one second counting time to produce a resolution of 0.05 gamma, and a short period response of 10 seconds. Since reported amplitudes of micropulsations indicated component

values of the order of 1 gamma, this resolution was thought adequate.

The 'divide by two' unit ($\div 2$) shown in Fig. 6.2, and the switch SW1, was inserted into the counting circuit because the times over which a frequency count can be made, and the number of cycles over which a period count can be made, can only be changed by factors of ten in the counter. Thus frequency may be measured for 0.1 sec., 1.0 sec., 10 secs etc. and period measured over 10^4 cycles, 10^5 cycles etc. It was therefore a considerable improvement to the range of counting times to be able to divide the magnetometer frequency by two, making it typically 100 Kc/s in the Earth's field. Thus a 10^5 cycles period measurement produces a counting time of 1 second with the 'divide by two' switched in, and of $\frac{1}{2}$ second in the normal case.

Note: The electronic arrangement of the divide by two facility was found, by the manufacturers, to be more conveniently made by doubling the number of cycles used to gate the counter, and this is what was done in practice. For clarity it is more easily described in a literal way.

Table 6.2 shows a table of the resolution and the counting time of the Venner counter using the two methods of frequency measurement and the 'divide by two' modification.

The 'Function' column indicates the type of count used and its length. The 'Full Scale Deflection' column shows the scale value of the recording system which monitors the 'tens and units' digits of the counter display.

TABLE 6.2

Function	Divide by 2	Sampling time	Full Scale Deflection	Resolution in gammas
10 secs	Normal	11 secs	2	0.02
	÷2	21 "	1	0.01
1 sec	Normal	2 "	20	0.2
	÷2	3	10	0.1
0.1 sec	Normal	1.1 "	200	2.0
	÷2	1.2 "	100	1.0
10^4 cycles	Normal	1.05 sec	100	1.0
	÷2	1.1 "	50	0.5
10^5 cycles	Normal	1.5 "	10	0.1
	÷2	2.0	5	0.05
10^6 cycles	Normal	6 secs	1	.01
	÷2	11 "	0.5	.005

Recording System

At the end of the counting period, the counter displays a number corresponding to the number of cycles of magnetometer signal occurring in the chosen time or the number of micro-seconds taken to pass the chosen number of signal cycles. In the Earth's field and using a counting period of one second

the number displayed has six digits.

Since geomagnetic variations have a long time constant, and micropulsation amplitudes are reported to be of the order of one gamma to ten gammas it is sufficient to monitor only the two least significant digits of the displayed count (i.e. the 'tens' and 'units'). In this way instrument sensitivity is retained at the recording stage, since full scale deflection is one hundred times the smallest measurable variable. In the example used previously, where a one second period is made in the Earth's field using the divide by two facility, the corresponding full scale deflection is 5 gamma.

The monitoring arrangement is illustrated schematically in Fig. 6.4, where, for simplicity, the output signals are shown directly associated with the displayed count. The switch SW2 is a provision to enable recording to be carried out at one tenth of the best sensitivity by monitoring the 'hundreds' and 'tens' of the count. This facility extends the range of values shown in Table 6.2.

The counter output for each digit consists of four pins, 1,2, 4, 2^{*}, each of which during the display period may have a voltage -8v or -2.5v corresponding to a YES or NO condition. The decimal digit represented is the sum of the designated values which are active (the YES or -8v condition). Thus for example a 'five' is represented by -8v on the 1 and 4 pins,

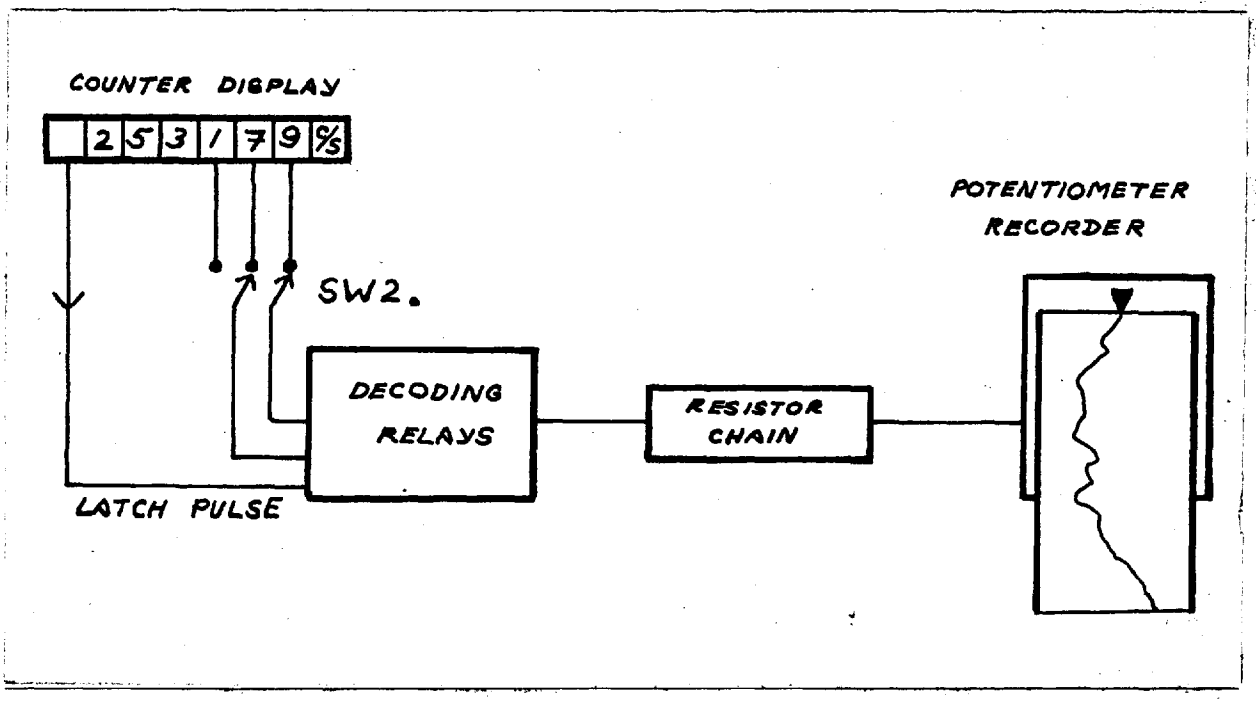

Fig. 6.4. Schematic diagram of the monitoring system.

the 2 and 2^{*} pins being at -2.5 v. The pins correspond to the outputs of the binary units used in the counting process.

To present an output form suitable for analogue recording on a paper chart, it is necessary to decode the coded binary readout into serial decimal form. This is done by an array of relays and a chain of resistors, which produce a voltage staircase to correspond with the decimal numbers.

The schematic diagram of relay closures used to convert the four line 'binary coded decimal' output to decimal digits is shown in Fig. 6.5. The numbers by the relay contacts represent the binary outputs and the decimal values appear

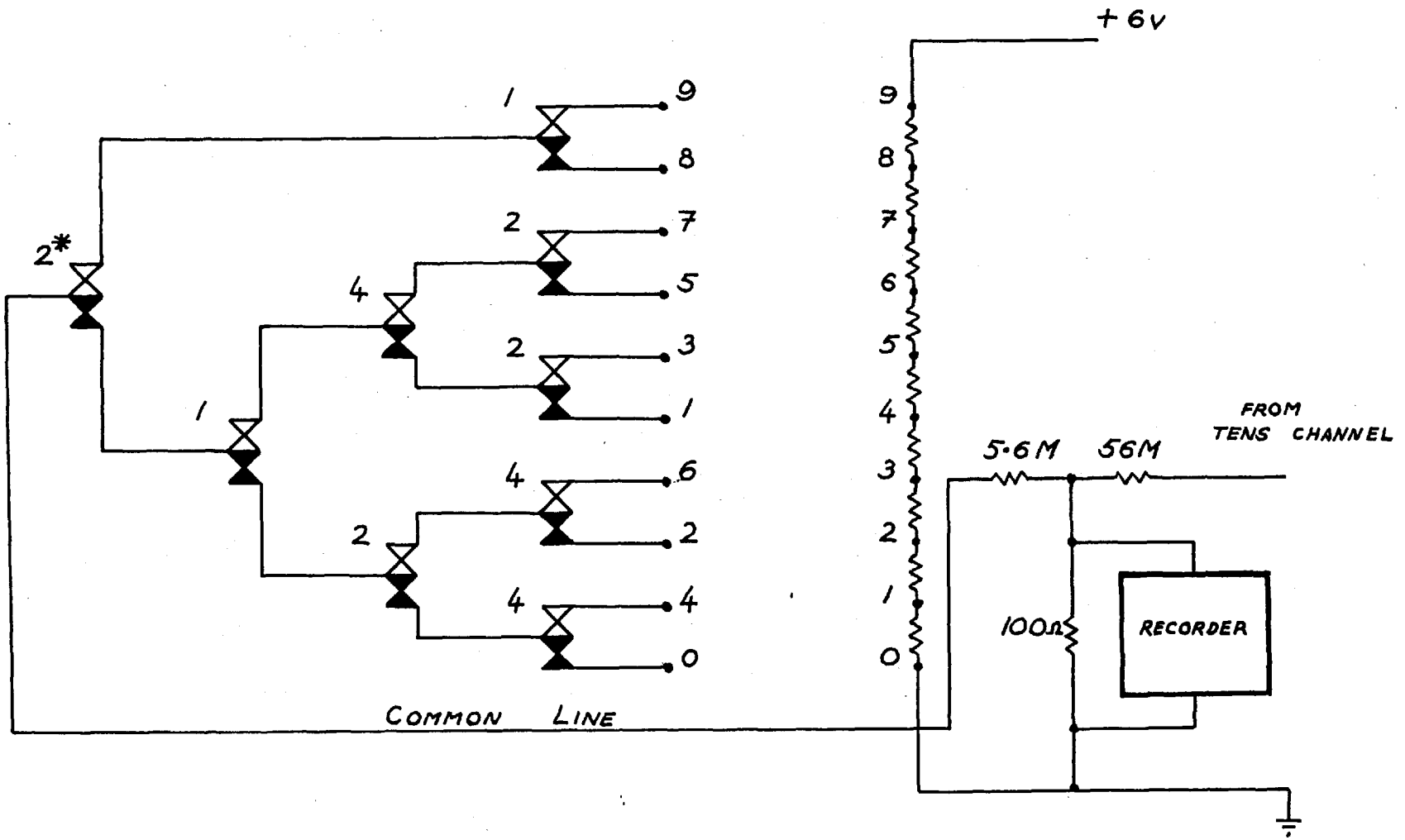

FIG. 6.5 RELAY MATRIX AND RESISTOR CHAIN.

on the right of the diagram. Unshaded contacts are in the position of being open when the corresponding relay is unenergised. Shaded contacts represent the closed side of the change over. Thus, for example, when the 1 and 4 relays are energised, pin 'five' of the decimal system is connected through the relay '2', which is closed to 'five' when it is unenergised, through relays '4' and '1', and via relay '2*' to the common line. In this way the decimal digits are built up. The arrangement of the relay change-overs is such that when any two or more relays are energised the sum of their values only is connected to common. If this were not taken care of all the decimal digits comprising the sum would be connected to common. For example, in the previous case the decimal 'one' is blocked from the common line by the '4' relay, and the decimal 'four' is blocked by the operation of the binary 1 in the selection matrix.

The manner in which the final output is arranged is shown in Fig. 6.5. A series of equal resistors is connected as a potentiometer, with a stable voltage connected across it. The voltages at the resistors are then in the ratio 0, 1, ...9. The corresponding points of the relay matrix are connected here and the closure of selected relays connects the common line to the appropriate voltage, in this way producing a staircase of equal voltage steps corresponding to the decimal digit represented. The common line is connected via a voltage

divider and potentiometer recorder to Earth as shown. The voltage divider serves two functions other than matching the output to the recorder. By arranging the two channels corresponding to the 'tens' and 'units' digits to have voltage dividers differing in ratio by a factor of ten, it is possible to use identical decoding channels for each digit. Also to ensure that the recorder circuit does not load the resistor chain in any way it is necessary to have a large resistor in the recorder circuit. Such loading would result in non-linearity of scale. The voltage used in the divider chain may be supplied by the counter or a dry battery, and a potentiometer is used to permit convenient adjustment of the full scale deflection of the system.

The counter outputs are not sufficiently powerful to drive the relays and driver stages are included, one for each binary pin. Fig. 6.6 illustrates the use of the Venner TS 34 stage in this application. The TS 34 conducts through the relay when the -8.5 v level is applied to its input. The 39 resistor is used to obtain the correct bias, and the Zener diode to maintain the bias when the stage is not conducting.

Because the counter outputs are directly connected to the counting units, it is necessary to isolate the relays from the counter during the count phase. If this were not done the relays would attempt to follow the counter as it sums pulses

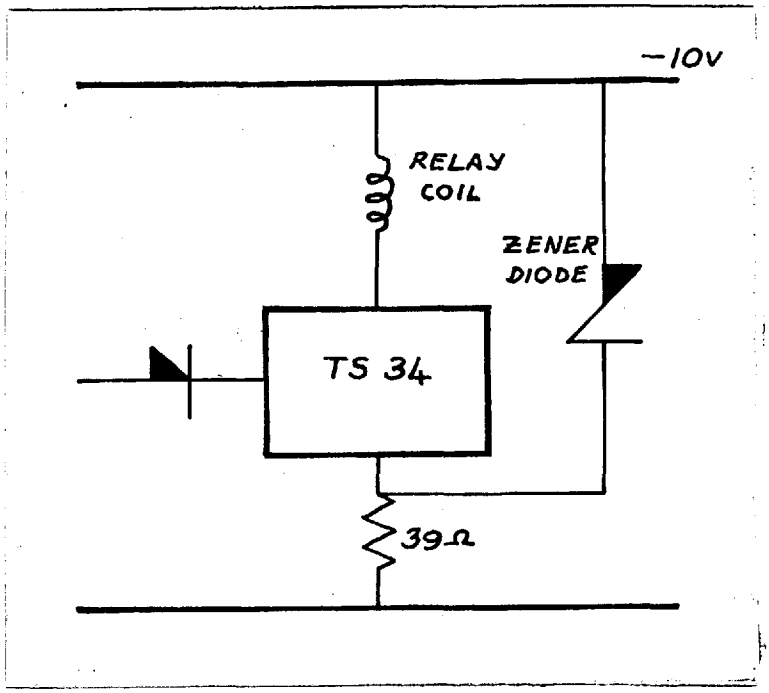

Fig. 6.6. Relay drive using the TS 34 stage.

in the counting process, to the detriment of the recorded signal. The method by which reliable read out is achieved makes use of the display time of the counter, when all the counting units are held at their appropriate values. The relays are isolated from the counter outputs except for a for a short interval during the display time when they are commanded to interrogate the counter.

The sampling process requires a latching arrangement on the relays in order to hold them in their appropriate 'sampled' states during the rest of the counting cycle. Fig. 6.7 shows the driver circuit with the addition of latched sampling. The change over A is operated by the latching relay and the

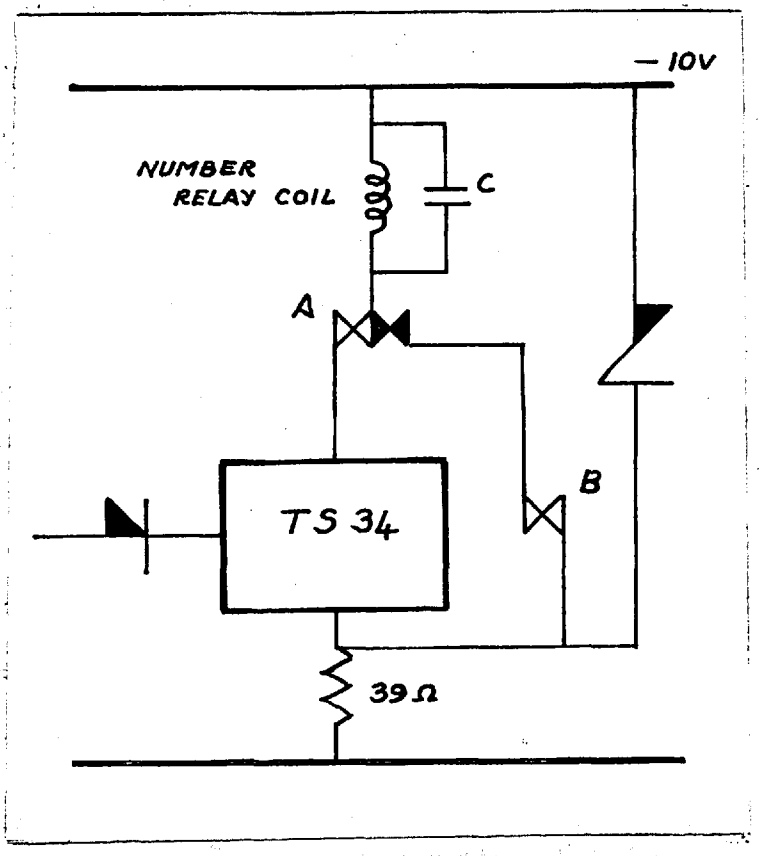

Fig. 6.7. Relay drive incorporating latching.

contact B, normally open, is operated by the number relay. A command pulse energises the latching relay, changing over the contacts A, and thus connecting the number relay to the TS 34. If the TS 34 is conducting, the number relay is energised closing the contacts B. At the end of the command pulse contacts B change back, disconnecting the number relay from TS 34. The capacitance C, discharges through the number relay coil, maintaining the relay in the energised state long enough for the change-over of the contacts A to be effected. If this condition is satisfied at the end of the command pulse the number relay is then energised directly from the

-10 volt line and holds itself there until the next command connects it to the TS 34. If the TS 34 is not conducting the contacts B open, and at the end of the sampling command the number relay remains unenergised.

The command signal is derived from a pulse generated by the counter at the end of the count period. Since the counter pulse has a duration too short to achieve reliable operation of the relays, it is used to trigger a flip-flop circuit, shown in Fig. 6.8. The flip-flop is a circuit which has one

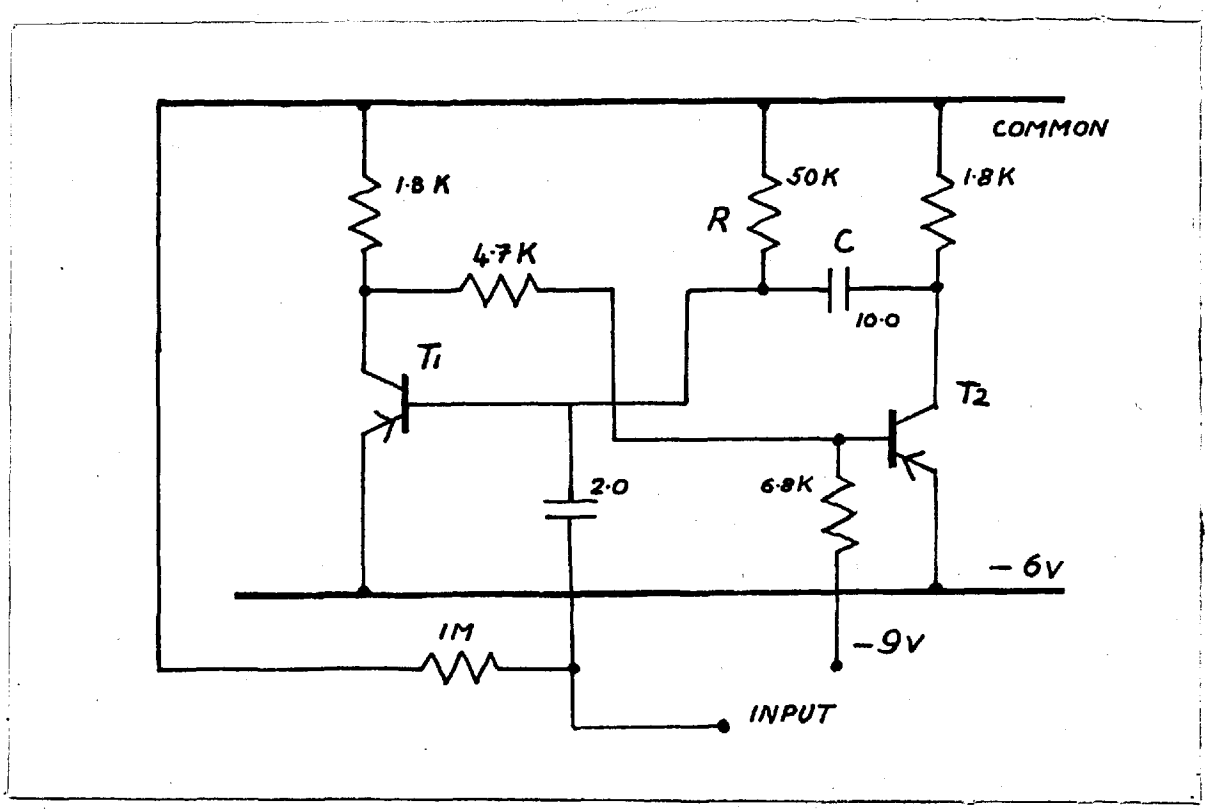

Fig. 6.8. The flip-flop circuit.

stable state, with T_1 conducting and T_2 cut off. The counter pulse ($-8\frac{1}{2}$ v) instantaneously lowers the voltage at the base of T_1, cutting the transistor off. The rise in T_1's collector voltage raises the base voltage of T_2, causing the transistor to conduct and so lowering its collector voltage. This state lasts until the capacitor C has reversed its charge sufficiently to raise the base of T_1 to make the transistor conduct, cutting T_2 off. The time constant RC determines the duration of the process. In the circuit used, the command pulse length is 0.5 seconds.

Fig. 6.9 is a schematic diagram of the decoding system. The flip-flop output has insufficient power to drive the latching relay and therefore is made to activate a TS 34 stage (Fig. 6.6), which drives the relay. Since a latching change-over is required by the driving circuit of each binary digit, relays using four sets of change-over contacts are used. Thus one latching relay is needed per decimal channel, and the command pulse is used to activate two driver stages, one for each channel. The four change-overs on each relay are enough to supply the decoding capacity, together with the extra contact required in the latching circuit. The latching contact, B is Fig. 6.7, is not shown in Fig. 6.9.

The current used by the relays and their drivers ranges between 0.3 and 0.7 amperes in normal operation, and is

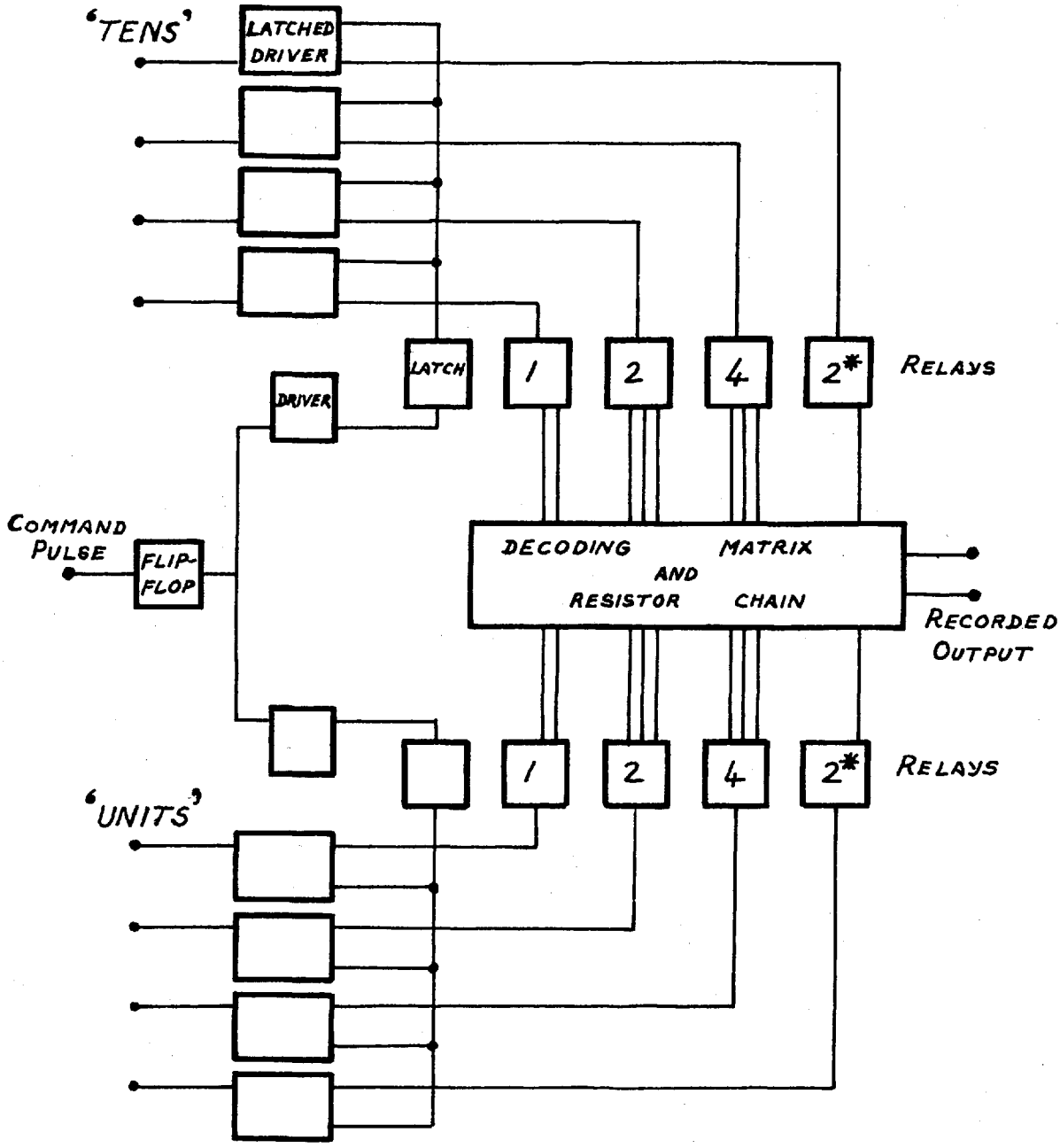

FIG. 6.9 SCHEMATIC DIAGRAM OF THE DECODING SYSTEM.

supplied by a lead-acid battery, or a suitable power supply.

Instrument Performance

The operation of the counting and recording system was tested at Silwood Park by making continuous measurements of the Earth's magnetic field there. It was not possible to identify any micropulsation events because of the 'noise' in the geomagnetic field due, presumably, to the electric rail system around Greater London. The amplitude of the random fluctuations at Silwood is of the order of 10 gammas, with time constants within the range of micropulsation periods. This field variation is responsible for much of the difficulty encountered in making observations of resonance line width at low fields and of the orientation effect. Recordings made at night showed a cessation of the magnetic noise at approximately midnight and a gradual build-up beginning about 0500 hours. The instrument performed satisfactorily under the test conditions, where the laboratory was kept warm, and attention was available when required.

One of the features resulting from mohitoring the last two digits of the count is that the recorded field value is always on scale. For example if the last three digits change from 599 to 601 the recorder pen changes position from 99 to 01. Thus in theory there should be no loss of information due to large field changes. In practice the advantage of the

feature is often reduced by having micropulsations occurring on an average field value close to 00 or 99. The resulting record may present some difficulty in the analysis. Figs.6.10 and 6.11 show examples of the 0 - 99 shift.

The field observations were carried out successfully at all of the stations visited. Recordings were made at chart speeds of 6" per hour, 3" per hour 1" per minute and ½" per minute. It was found that for general observations 6" per hour was a satisfactory speed, and it was used in the analysis that follows.

Under normally quiet conditions it was possible to operate the instrument using a sensitivity of 5 gammas full scale, although at Kiruna the very large amplitude field fluctuations which occur in association with the auroral current system necessitated the use of a full scale sensitivity of 20 gammas. Both the large scale activity, and the reduction of sensitivity resulted in a loss of micropulsation information.

The counting and decoding system functioned in a satisfactory way. It was found that unreliable gating of the frequency counter could occur if the room temperature rose above 30°C. Because of this a housing was constructed around the sensor so that its ambient temperature could be kept high while the room temperature was allowed to remain at normal values ($\sim$ 20°C). Because of the problems of

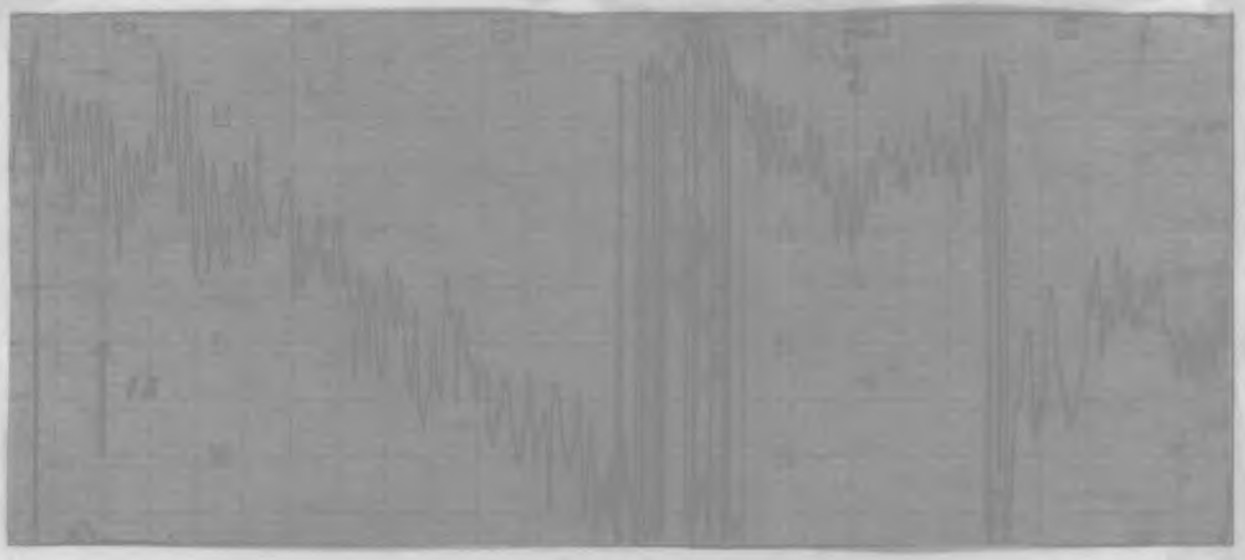

FIG 6.10 A

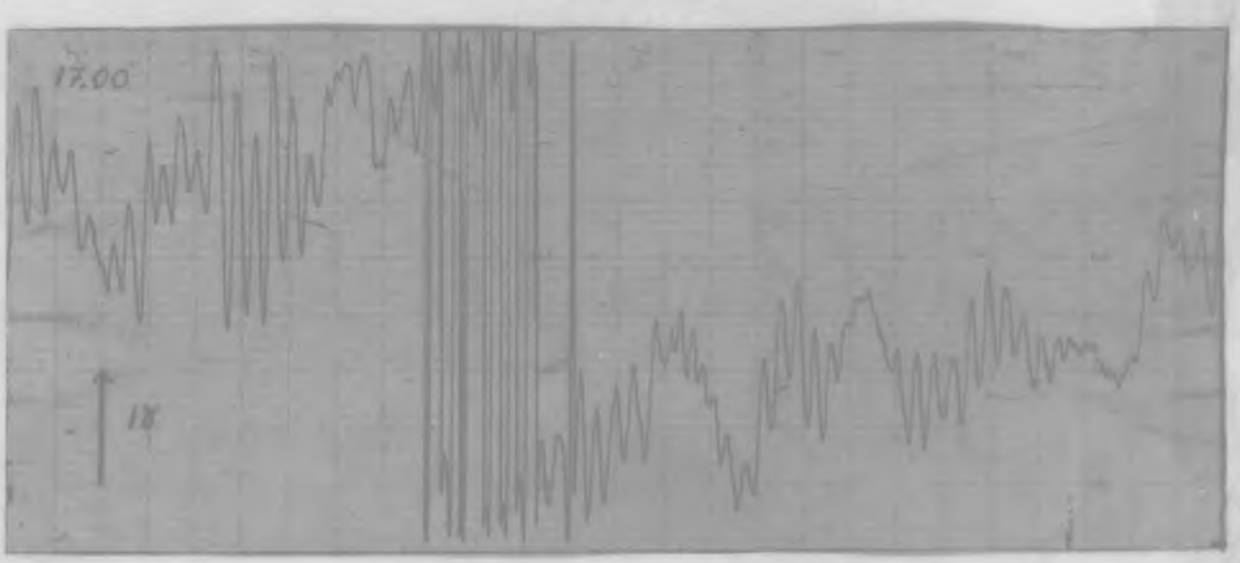

FIG 6.10 B

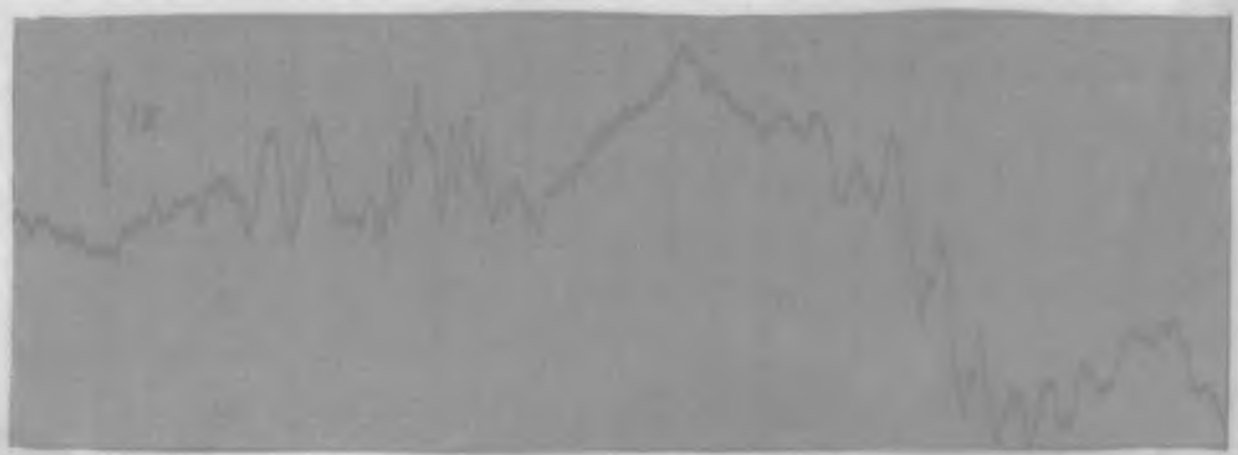

FIG 6.10 C

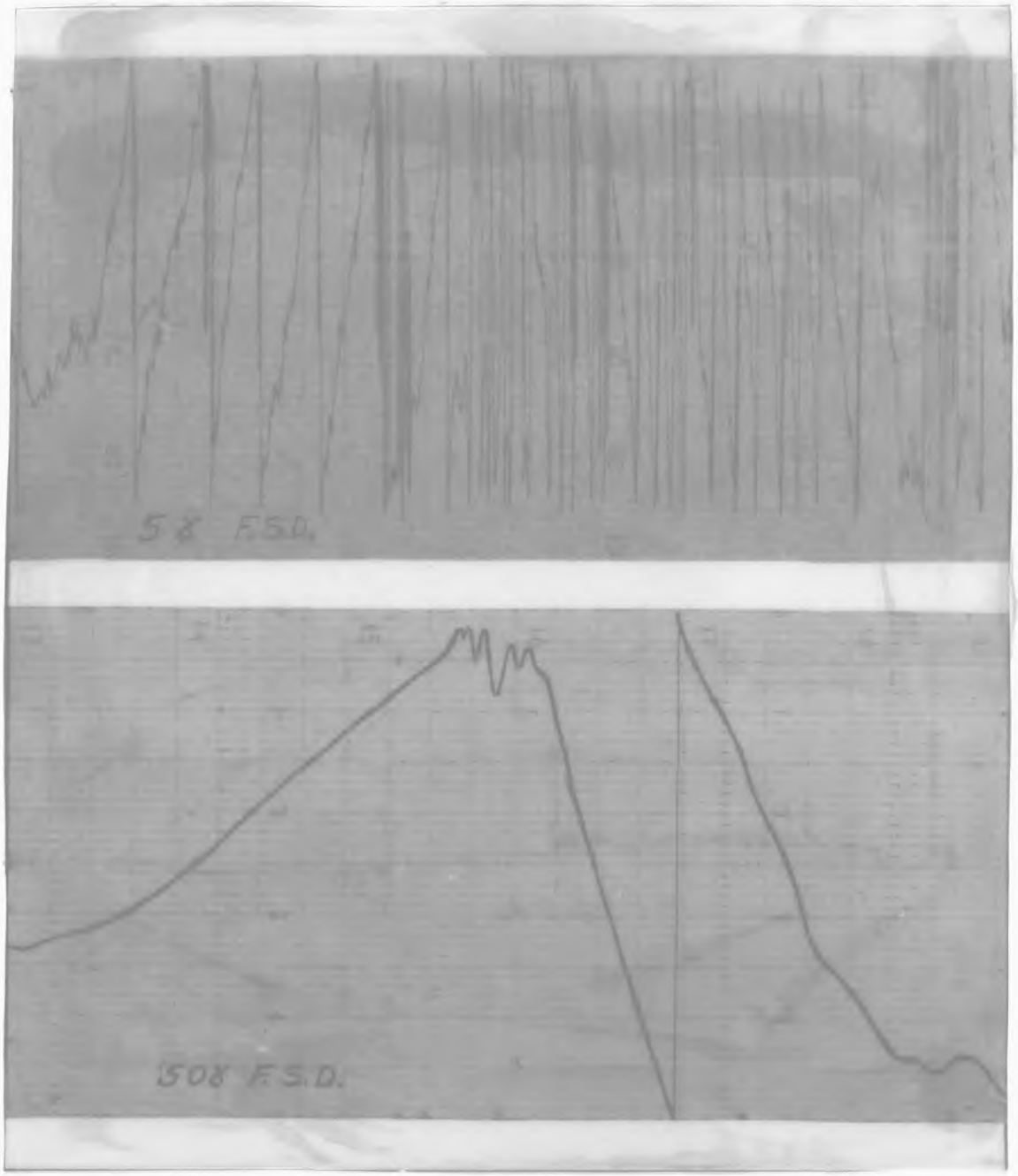

Fig. 6.11. A section of record, reconstructed from the original.

supplying heat to the housing, and interference when the fan heater used was closer than six feet to the sensor the final arrangement consisted of a housing with a long tunnel, constructed from polystyrene sheets. It was possible to stabilise the temperature inside the housing under varying conditions of room temperature by adjustment of openings in its construction. The polystyrene served a double purpose as shock insulation in the packing cases used in the transportation of the equipment.

It was found that proximity of the sensor to the electronic equipment resulted in interference which took the form of spurious counts. Part of this was attributed to the magnetism produced by the decoding relays. It was therefore necessary to maintain a distance of over ten feet between the sensor and the main electronic units.

It was demonstrated to be possible to operate the recorders remotely from the rest of the equipment, allowing such tasks as the changing of charts to be carried out in the main observatory office, while operating the equipment in a distant building. At Lerwick the distance between the magnetometer and the recorders was 300 yards. This was of considerable advantage where an immediate examination of the magnetic field activity was required.

Timing pulses were added to the recorded sighal by short circuiting the recorder input by a relay closure

available from the observatory chronometer. Timing pulses were taken at five minute intervals, and it was found that a three second closure was sufficient for the purpose. The significance of the technique lies in the ability to acquire reliable and accurate time correllation between recordings of events at two or more stations. For phase measurements of periods in the region of 30 seconds, the 1 second accuracy available is sufficient to detect a 10° phase change.

At Lerwick an attempt was made to measure the component of micropulsation activity in the horizontal plane. To do this the vertical field was backed off using a set of Helmholtz coils. Current was supplied to the coils by a battery and controlled by a rheostat. The records showed a slow increase of field opposite in sign to the diurnal variation at that time, and a high noise level. Pulsations were observed, but doubts as to the stability of the battery current, and the effects of gradients due to the coils exist. It was known that the batteries used were run down. The conclusion drawn from the test was that the technique was feasible for measurements of component activity, and if successful would provide a sighificant increase in the effectiveness of the rubidium magnetometer as a detector of micropulsations. Further remarks about the biassed field operation of the instrument are contained in Chapter 7.

The difficulties resulting from the large amplitude fluctuations observed at Kiruna indicate that the unfiltered recording of magnetic fields is not a suitable method of detecting micropulsations of low amplitude in auroral regions. A simple RC filter would eliminate enough of the longer period events to allow the small Pc's to be detected consistently. However, such a device would result in a variation of the magnetometer system response with micropulsation period, because the large events have time constants not greatly differing from those of Pc's. Since true response over a very broad range of periods is one of the advantageous features of the rubidium magnetometer, loss of long period information is to be avoided. At the other latitudes visited loss of information due to field activity was negligible.

Fig. 6.10 shows sections of record. In A, Pc activity occurred in the forenoon and in B, similar activity occurred in the late afternoon. On both records the full scale deflection is 5 gamma and the chart speed 6" per hour.

Fig. 6.10C shows a section of record taken at Hartland in which activity, occurring at 01.00 displays a marked irregularity both of period and of form. The broadening of the trace is due to a $\pm$ 1 count variation, initially thought to be due to the magnetism of the relays, although it may have been low level pulsation activity at periods $\sim$ 5 secs.

Fig. 6.11 shows a section of record taken at Kiruna during a period of large scale activity. The effectiveness of the 0 - 99 shift is clearly demonstrated, as is the loss of information inourred during such activity. The scale value is 5 gamma and the chart speed is 6" per hour. The lower record shows a reconstruction drawn from the original.

Footnote: Later work showed that the magnetism of the relays could have been responsible for such trace broadening. However it has since been shown that 50 c/s magnetic fields can produce a similar effect on the counted field, by frequency modulations of the magnetometer signal. The occurrence of this type of effect has been correllated directly with the time of the use of external lighting at one of the Observatories.

CHAPTER 7

ANALYSIS OF MICROPULSATION DATA AND CONCLUSIONS

General Remarks

In the measurement of pulsations the object of the field study was to provide a working knowledge of the nature and occurrence of the phenomena within the latitude range conveniently available. It was hoped that the traverse of stations, which are close to the same longitude, would provide results sufficiently typical of each latitude that a comparative study could be made on that basis. Specifically, the latitude dependence of micropulsation period was to be examined, and it was thought possible that an indication might be found of events appearing in one region which do not appear elsewhere. The basis of this test is Kato's conclusion that toroidal waves, being generated at the magnetosphere boundary occur only at high latitudes, and that Pc events occurring in middle latitudes are due to a poloidal mode of excitation. The toroidal mode, distinguished by $E = 0$ in Dungey's analysis, has its magnetic variation in the East-West plane, while the poloidal mode has its variation in the plane of the magnetic meridian.

For a dip angle i, referred to the horizontal Earth's surface, the variations in total field magnitude due to the contributions of variations δH and δZ are respectively,

$$\Delta F_h = \delta H \cos i$$

and

$$\Delta F_z = \delta Z \sin i$$

For the latitudes at which observations were made $i \approx 70^\circ$ so that

$$\Delta F_h = 0.35\ \delta H$$

$$\Delta F_z = 0.95\ \delta Z$$

Fluctuations in the plane normal to the field direction are related by the formula

$$(F^1)^2 = F^2 + \delta D^2$$

where D represents the small variation normal to F.

i.e.
$$F^1 = F\left(1 + \left(\frac{\delta D}{F}\right)^2\right)^{\frac{1}{2}}$$

$$= F\left(1 + \tfrac{1}{2}\left(\frac{\delta D}{F}\right)^2 + \ldots\ldots\right)$$

and $\Delta F = F^1 - F$ is the variation in field magnitude due to D, and is given by

$$\Delta F = \tfrac{1}{2}\frac{\delta D^2}{F}$$

Thus a peak amplitude of a pulsation in the plane perpendicular to F of 10 gammas produces a variation in the total field of 10^{-3} gammas, an entirely negligible amount.

Thus it is clear that measurements using the rubidium magnetometer indicate pulsation activity in the meridian

plane only, and then largely the vertical component in high latitudes.

General Analysis

A general analysis was carried out in an attempt to arrive at a statistical distribution of the frequency spectrum throughout the day, at each station. The method employed was to measure the periods of pulsations occurring during each hourly interval and plot these as a function of time of day.

Some features of the method should be noted:

1. No account is taken of the amplitude of pulsations.
2. No account is taken of continuity or coherance of wave trains within each hourly interval. For this reason continous activity with a variable period content is often included as two, or three, discrete period points.
3. The overall error of period measurement is of the order of 1/5 of the period.
4. The period range 10 - 250 seconds is covered.

Remarks concerning the records at individual stations are given below.

a. Kiruna: Here large scale activity resulted in the loss of a considerable amount of low amplitude information, particularly in the evening and night time. The measurements

made at Kiruna are plotted against G.M.T. which is used throughout this discussion. A correction of 1½ hours should be added to the plotted time scale to adjust the results to a local time reference.

b. Eskdalemuir: Here records were obtained which contained a considerable amount of activity at periods less than 30 seconds. The form of the activity suggests in places that it is in fact spurious, due to inadequate functioning of the magnetometer system. That it occurred mainly at night suggests that the thermal environment was at fault causing the sensor temperature to fall below the limit required for consistent operation. However, much of the activity was regular in pattern, and periods of this order had been observed at the other stations, or suggested by fluctuations of very low level comparable with the ± 1 count resolution of the system. For these reasons it has been included in the analysis.

The general form of the analysis does not include any determination of energy content. It shows the periods available for pulsation activity during the course of the day.

The main features of the analysis are displayed in Fig 7.1 where the chart of the collected data is shown. The change in frequency content between day and night is

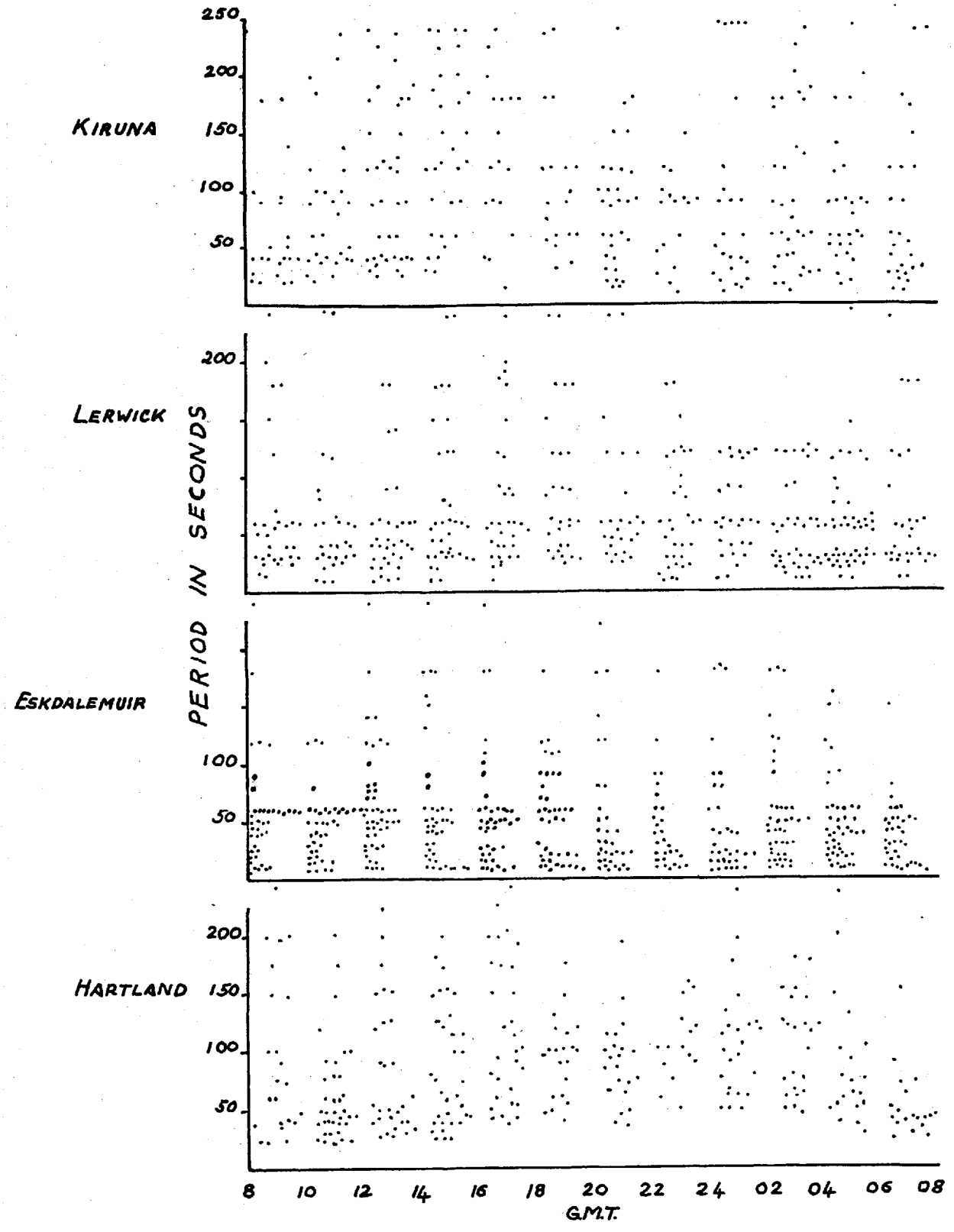
KIRUNA
LERWICK
ESKDALEMUIR
HARTLAND
PERIOD IN SECONDS
250
200
150
100
50
200
100
50
200
150
100
50
8
10
12
14
16
18
20
22
24
02
04
06
08
G.M.T.

FIG. 7.1

shown by all stations. The comparative lack of points during the hours 16.00 to 02.00, particularly in the period range 30 - 60 seconds corresponds to the time when Pc activity is not apparent.

Fig. 7.2 shows the spectral content for each station, taken from Fig. 7.1. A shows the frequency spectrum covering the whole day and the histograms have been normalised approximately. B and C show the histograms for the day and night intervals, corresponding to the times shown, and are taken from A. The results from Hartland and Kiruna show clearly the difference in period content between what may be called the day and night phenomena, and the same trend is identifiable at Lerwick. The Eskdalemuir record shows the trend clearly if periods less than 30 seconds are neglected.

The period interval used in the compilation of the histograms of Fig. 7.2 was 25 seconds. This was chosen on the basis of the error in measurement of periods at about mid range of the spectrum shown, and also because of the indeterminate way in which a value was assigned to continuous trainswhose period changed during the course of an hourly interval. Whereever possible an average value was assigned to such a case. However in some instances it was necessary to plot two points for the hour if clearly defined periods resulted from the variation.

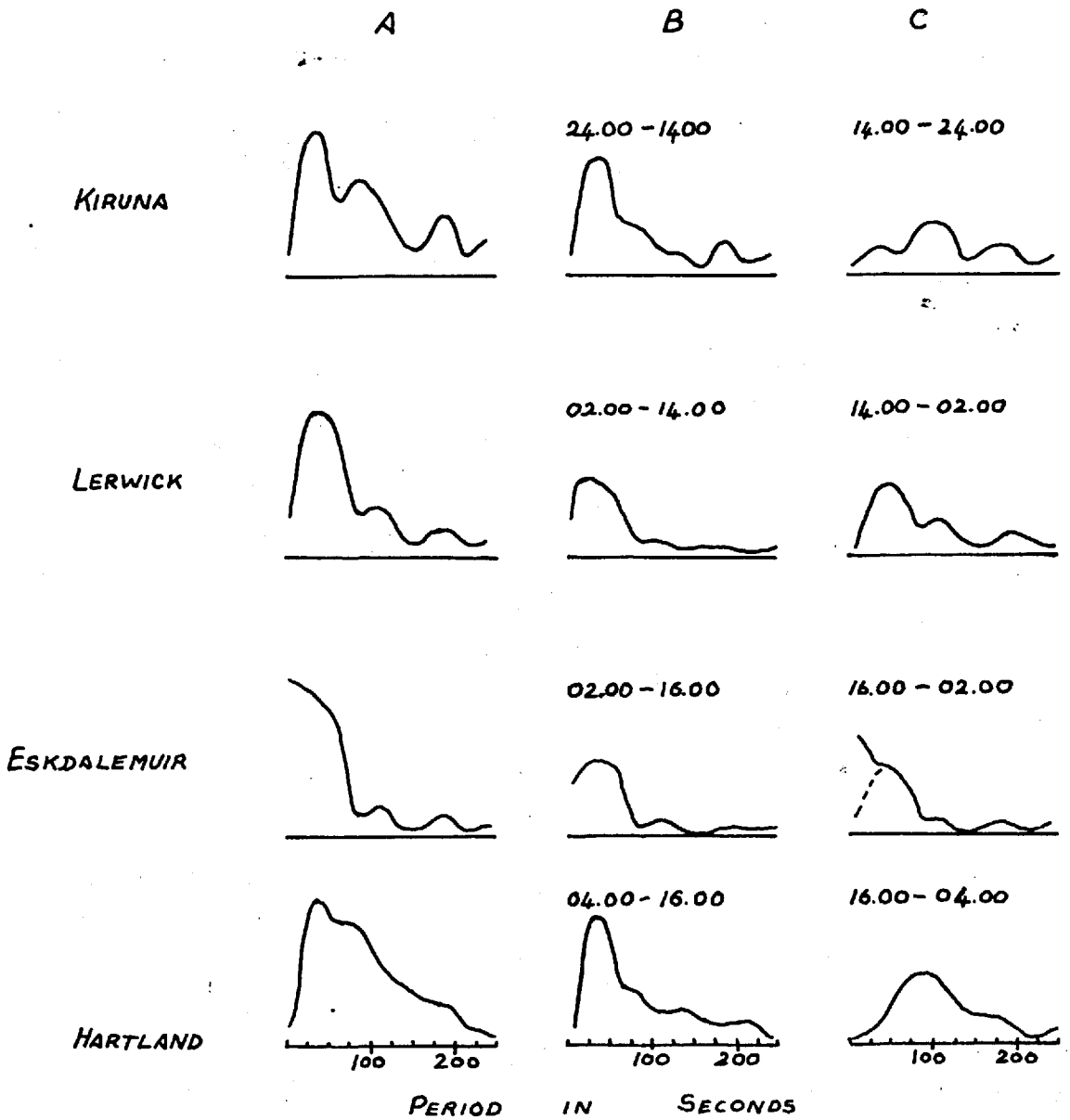

FIG 7.2 FREQUENCY SPECTRA FROM FIG. 7.1.

A) TOTAL DAILY OCCURRENCE

B) DAYTIME OCCURRENCE } TIMES SHOWN

C) NIGHT TIME OCCURRENCE }

A feature of the spectral content which is indicated by the histograms of Fig. 7.2. is the harmonic content of activity, displayed at Lerwick and Kiruna at periods of approximately 120 and 180 seconds. The harmonic relationship appears to be exhibited particularly well by Pc's and is shown in most of the records used to illustrate this discussion. In Fig. 7.2 the higher terms at approximately 30 secs, 45 secs, 60 secs and 90 secs, which are obvious on examination of records, are not resolved in the histograms.

The trend has been confirmed by Dr. M.J. Usher, who carried out a detailed spectral analysis of the Hartland records, taking into account the number of waves of each period. The resultant spectrum shows clear peaks at 40 secs., 65 secs., and 90 secs. The maximum at 65 seconds may be due to the intermodulation between waves at 40 seconds and 90 seconds., although this is not definitely indicated.

Fig. 7.3 shows the diurnal variation of Pc activity. The values were arrived at by assigning to each hour a number 0, 1, 2 to correspond to the degree of continuity of the events. 0 corresponds to the lack of any activity of a continuous nature, 1 to detectable activity up to 0.5 gammas peak to peak amplitude, and 2 to continuous pulsations of large amplitude ($>$ 0.5 gammas) lasting, with good coherence throughout the hour. No account was taken of period and no precise definition of Pc was adhered to. Because of this

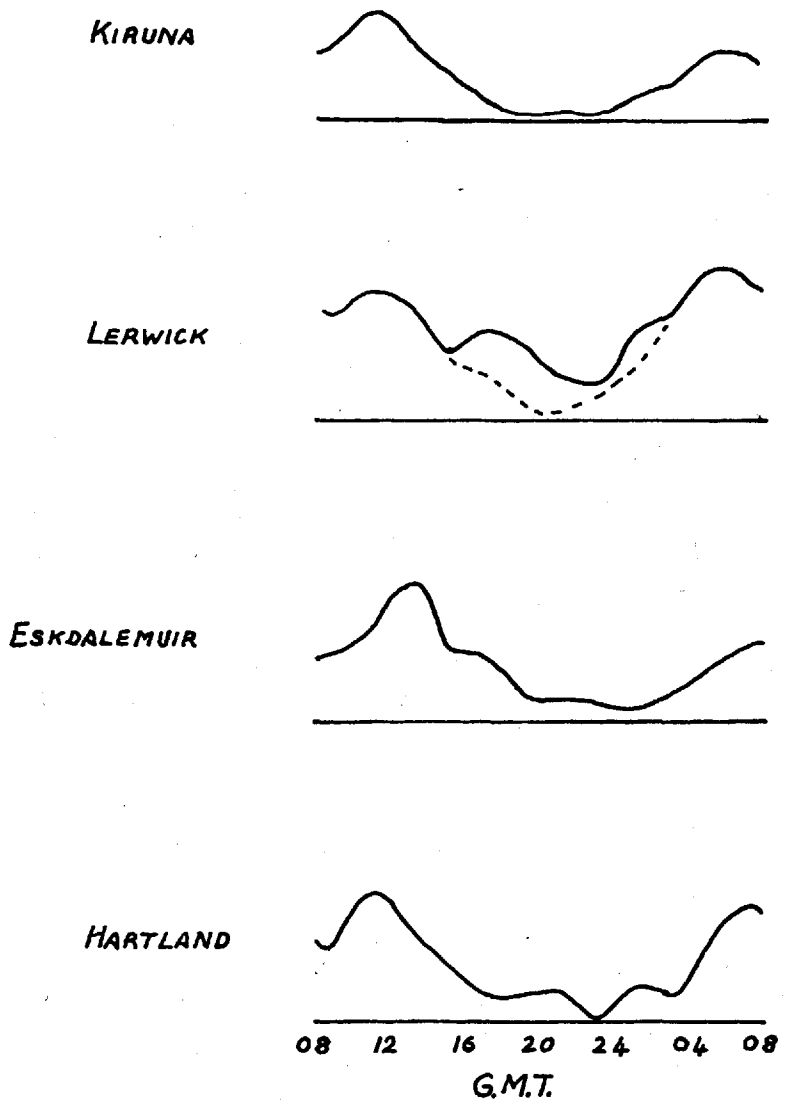

FIG. 7.3 THE DAILY OCCURRENCE OF CONTINUOUS ACTIVITY.

last condition the Lerwick graph does not show a distinct minimum at night. Evening and night pulsations at Lerwick often lasted for times greater than 30 minutes and showed a tendency to recur within short intervals. For this reason many night time events were classified with the value 1, where a specific definition of Pc might have excluded them. The dotted line in the Lerwick graph illustrates the effect of neglecting events of this nature.

Figs. 7.1 and 7.3 illustrate the broad time range of the occurrence of Pc activity throughout the day.

Fig. 7.4 shows histograms representing the selectivity of Pc activity. The information was obtained by measuring the distance between adjacent peaks in a single continuous train of waves, neglecting any waves or pulses which showed obvious deformity. The accuracy of measuring the period of individual waves is $\pm$ 3 seconds and it is possible to estimate the frequency occurrence within a second. There is no apparent change in line width over the range of latitudes investigated. The periods of the events shown in Fig. 7.4 have no significance, since good sections of Pc activity were chosen in a purely arbitrary way.

The width of the line at half maximum is about $\frac{1}{4}$ of the period of the line peak. A close scrutiny of many continuous pulsations, however, shows that good quality events with

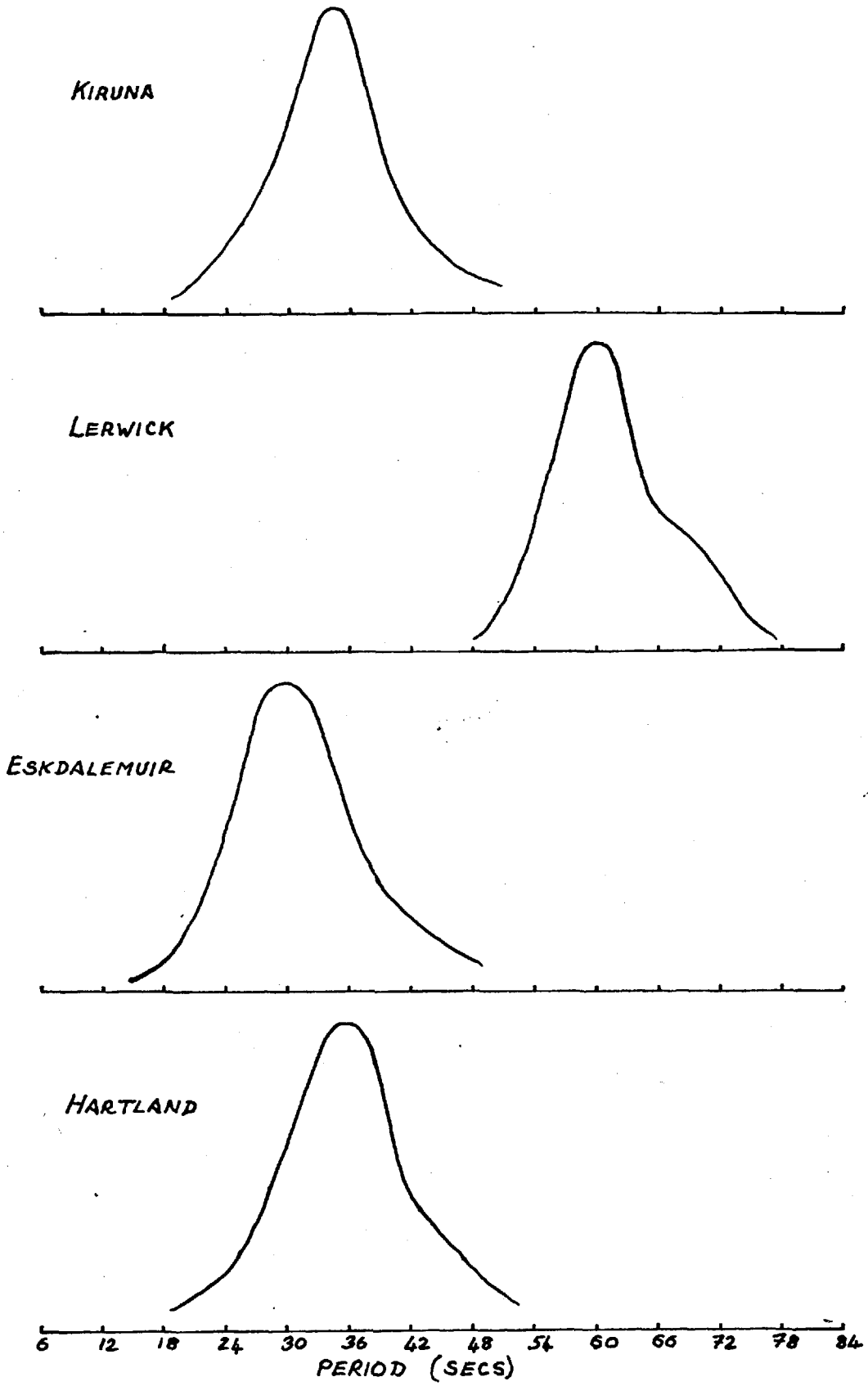

FIG. 7.4 LINE WIDTH OF Pc ACTIVITY

large signal-to-noise resolution and apparent continuity, in fact exhibit a great degree of incoherence. It seems likely that many randomly occurring wave trains are intermixed.

Consider two waves $A_1 \cos\theta$ and $A_2 \cos(\theta+\phi)$ superposed to give

$$A = A_1 \cos\theta + A_2 \cos(\theta+\phi)$$

$$\frac{dA}{d\theta} = A_1 \sin\theta + A_2 \sin(\theta+\phi)$$

$$= A_1 \sin\theta + A_2 \sin\theta\cos\phi + A_2 \cos\theta \sin\phi$$

i.e. $$\frac{dA}{d\theta} = \sin\theta\,(A_1 + A_2 \cos\phi) + A_2 \cos\theta \sin\phi$$

which may be written

$$\frac{dA}{d\theta} = R \sin(\theta+\psi)$$

where $R \cos\psi = (A_1 + A_2 \cos\phi)$

$R \sin\psi = A_2 \sin\phi$

wave peaks are defined by $\frac{dA}{d\theta} = 0$

i.e. neglecting $R = 0$ which is a trivial case,

$$\sin(\theta+\psi) = 0$$

i.e. $$\theta + \tan^{-1} \frac{A_2 \sin\phi}{A_1 + A_2 \cos\phi} = N\pi$$

or $$\theta = N\pi - \tan^{-1} \frac{A_2 \sin\phi}{A_1 + A_2 \cos\phi}$$

$\Delta\theta$, which is the distance between adjacent peaks, is

controlled by the inverse tangent function. Thus if A_1, A_2 or ϕ vary during a long train of waves $\Delta\theta$ is altered. This is the case with incoherent pulsations and it is possible, therefore, that the interference of incoherent wave trains is responsible for broadening the resonance width of Pc's detected and analysed in the above manner. Fig. 7.5 shows sections of record where the incoherence of pulsation activity is displayed.

It was possible, while at Kiruna, to compare the rubidium magnetometer records with those obtained from the micropulsation variometer at the observatory. This instrument, which was designed and built by Dr. Hans Voelker, of the Geophysical Institute of the University of Göttingen measures magnetic variations in the three component direction H, Z and D, using an induction device. The sensitivity is $\sim$ 4 mm/γ and the frequency response is essentially flat between 10 seconds and 100 seconds period. The incoherence which was obvious in the rubidium magnetometer, was not shown distinctly on the component records, and may have been due to the lower resolution of the optical recording system, and the filtering of the signal. The component records show that variations in amplitude and period occur irregularly in each component, and that variations in phase exist between components. Such variations are thought to be sufficient to account for the incoherence observed in

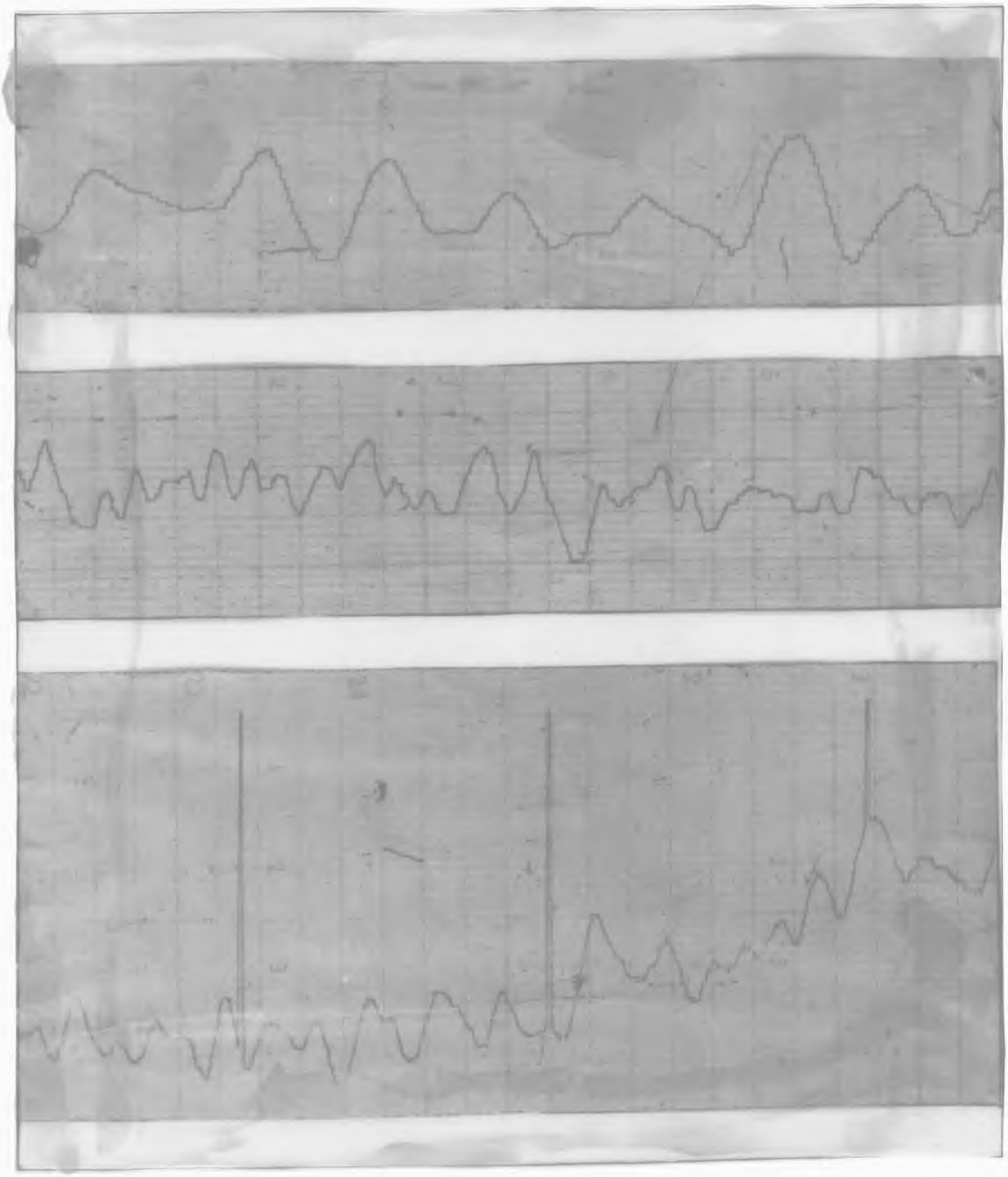

Fig. 7.5 Records illustrating incoherence in trains of Pc activity.

the total field measurements made by the rubidium magnetometer. The variometer showed that H and D are usually disturbed to the same degree, while Z exhibits pulsation activity only during extremely disturbed times. The last point confirms Dungey's remarks, where the Earth's surface is taken to be a good conductor.

Mixing of frequencies occurs in several forms. Fig. 7.6 shows two consecutive sections of record occurring between 0400 and 0500, showing several distinct frequencies. The horizontal time scale advances from left to right, and is 6" per hour. The two clear components of period 35 seconds and 70 seconds at 05.15 and 05.25 illustrate the harmonic structure in one form.

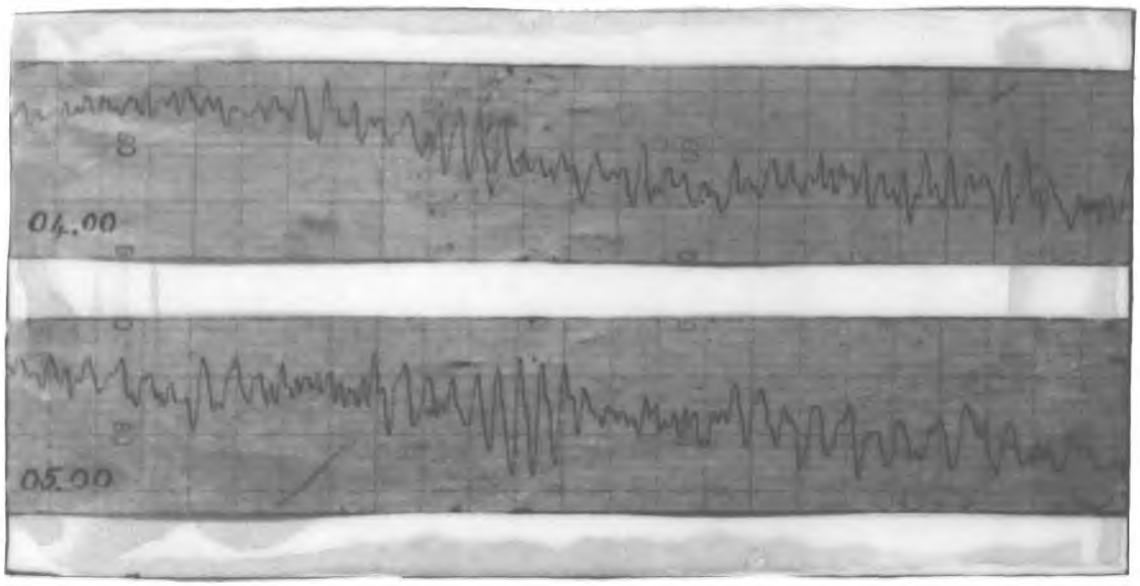

Fig. 7.6. Two consecutive sections of record showing the intermixing of pulsation periods at 30 seconds, 60 seconds and 90 seconds.

Figs. 6.10A and B show records of pulsations where highly resolved Pc's are intermodulated in one case, Fig. 6.10A, with a shorter period fluctuation and in the other Fig. 6.10B with a long period event.

Fig. 7.7 shows two sections of the same record covering the times 05.45 - 06.45 and 07.30 - 08.30 and illustrates two parts of a continuous train of Pc activity which changes its predominant period from 30 seconds at 06.00 to 60 seconds at 08.00. Intermodulation of the two frequencies occur in the later section. The intervening section of record is not shown, because the pulsations occurred at the region where the 0 - 99 shift operates, and spoiled the recording. The activity shown in the latter part of the first section continued until the beginning of the second.

Fig. 7.8 shows three consecutive hours of record taken from 22.45 to 01.45 at Lerwick. The sections show pulsations of 120 second period associated with long period field fluctuations. The length of the long pulsation varies between 20 minutes and 30 minutes. The association between the two fluctuations is further characterised by an amplitude modulation of the shorter period waves at a frequency which corresponds to that of the long period train. With only two exceptions the bursts of short period events occur on the leading limb of the long wave, which represents increasing field strength.

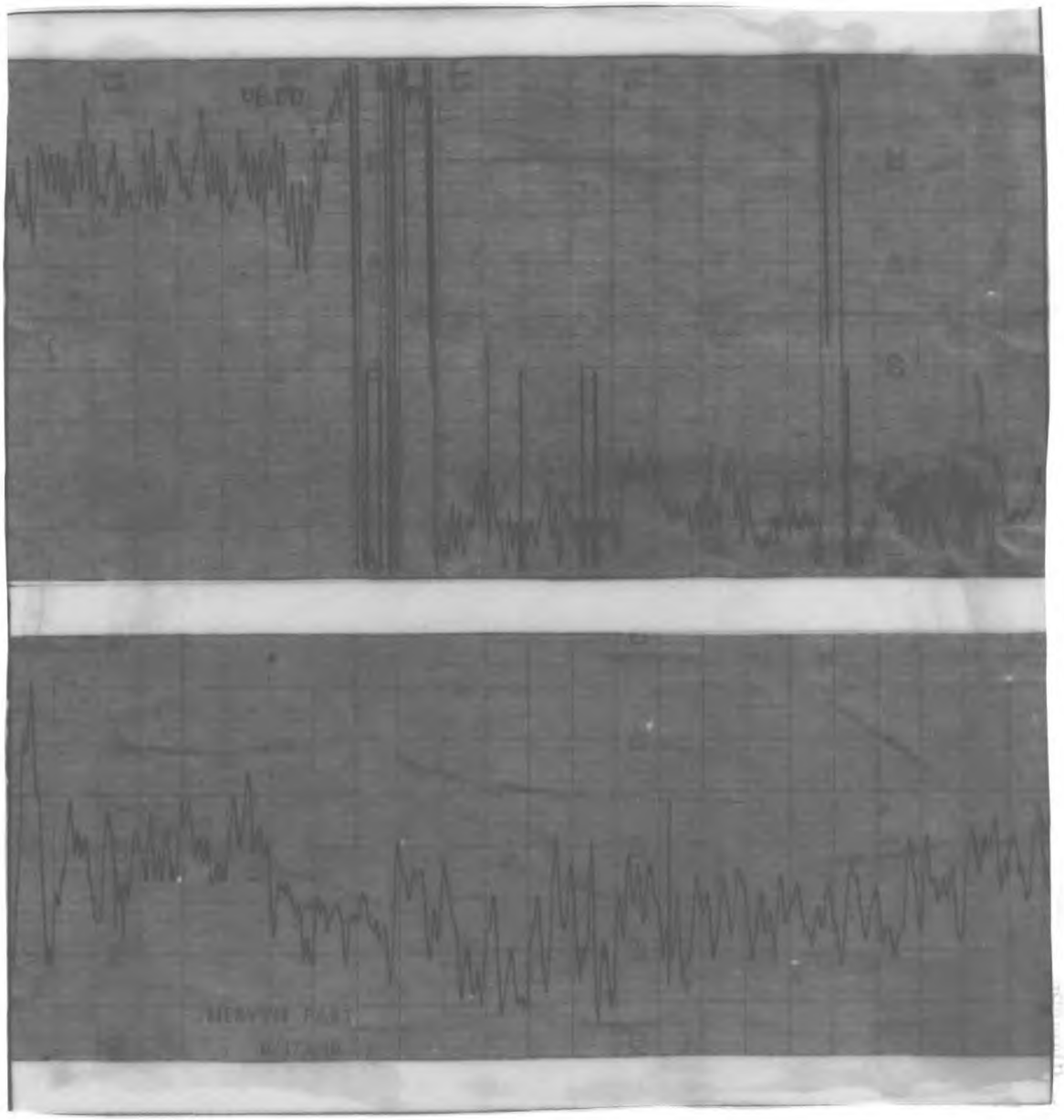

Fig. 7.7. Two almost consecutive sections of record showing
a) period change from 30 seconds to 60 seconds within an hour.
b) Intermodulation of frequencies, including harmonic modulation.

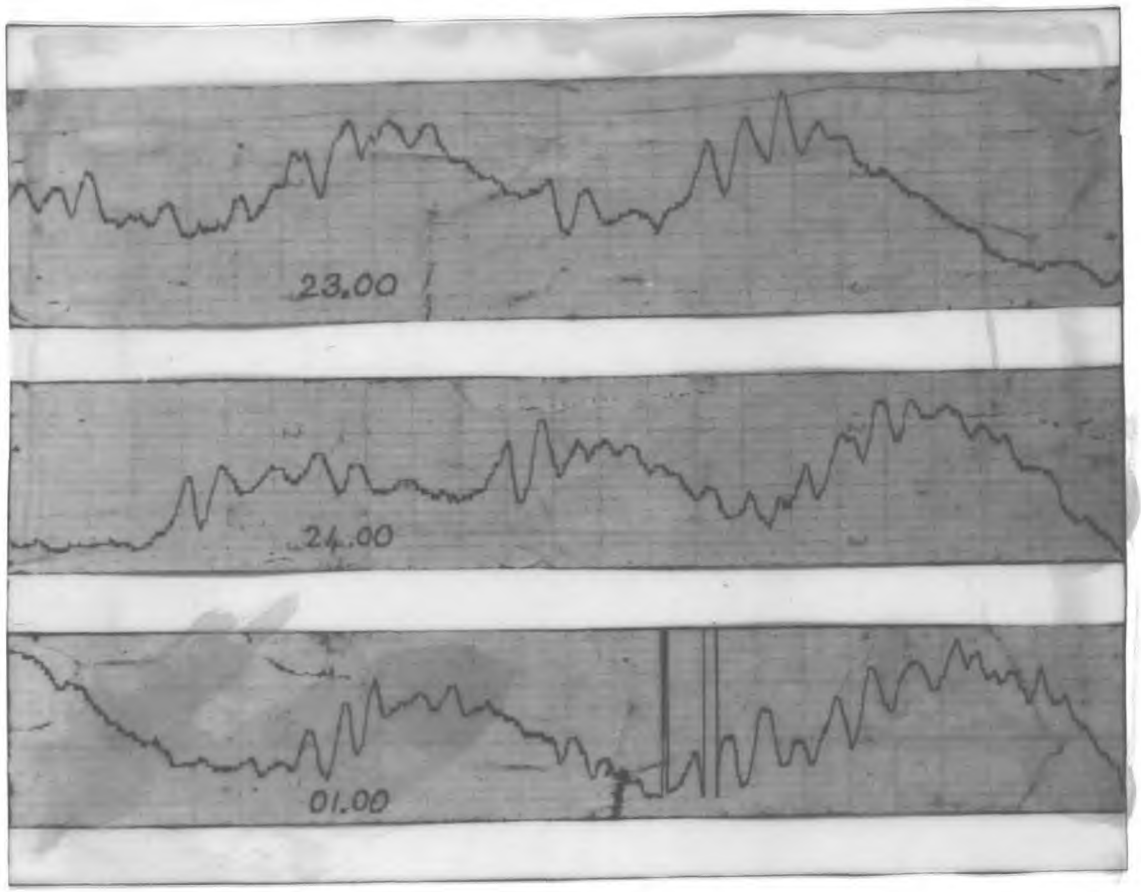

Fig. 7.8. Three consecutive sections of records showing amplitude modulation of waves of 120 seconds period associated with a long period field fluctuation.

Amplitude modulation of continuous activity is frequently observed. Fig. 7.9 shows two consecutive sections of record occurring at about 03.00. The chart speed here is indicated by the timing marks, which occur at five minute intervals. The period of the activity is 45 seconds and that of the modulation envelope is about 5 minutes.

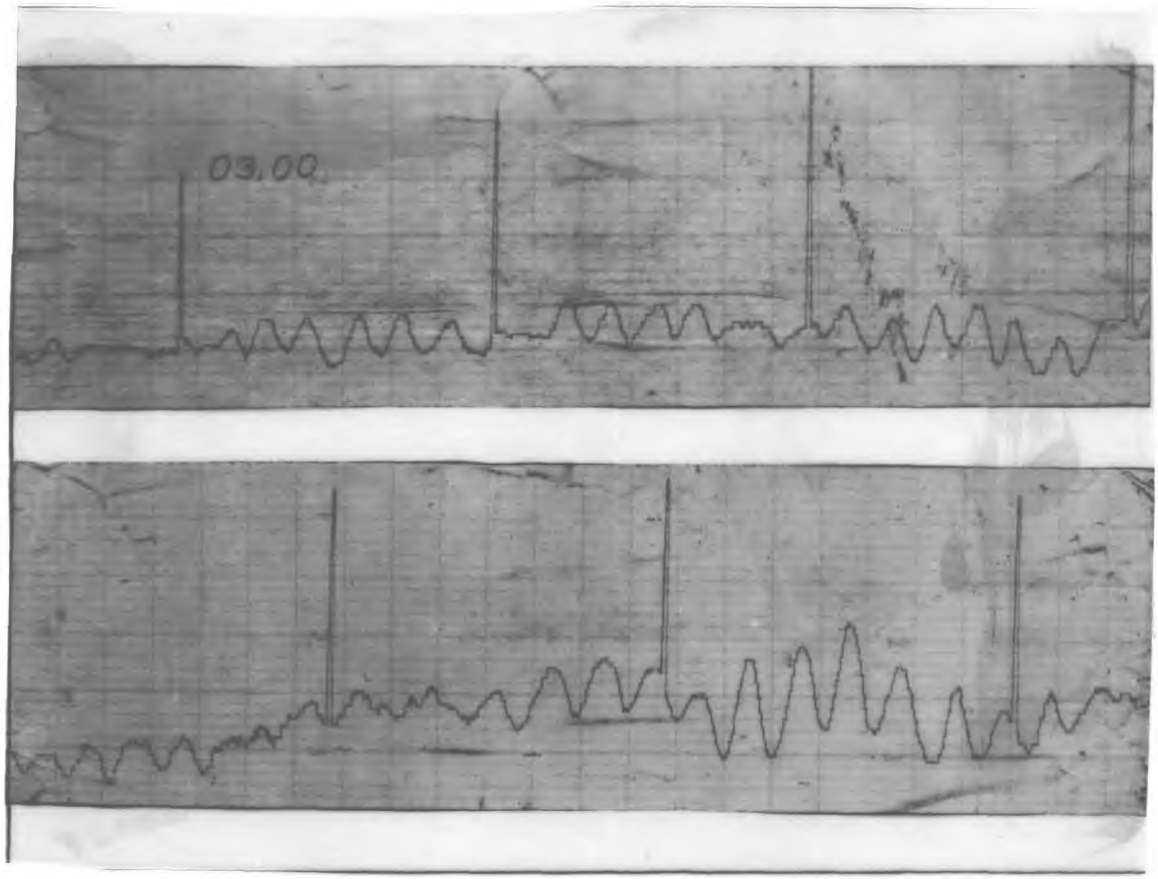

Fig. 7.9. Consecutive sections of record showing amplitude modulation of waves (period 42 seconds). Modulation period approximately 5 minutes.

Both Fig. 7.8 and Fig. 7.9 are examples of the type of night time activity which, at Lerwick, was classified by the value 1 in the Pc analysis.

Because of the variability of period within a day's continuous activity and between consecutive days it has not been possible to compare events in the specific way that was hoped. Fig. 7.10 shows three sections of record taken at

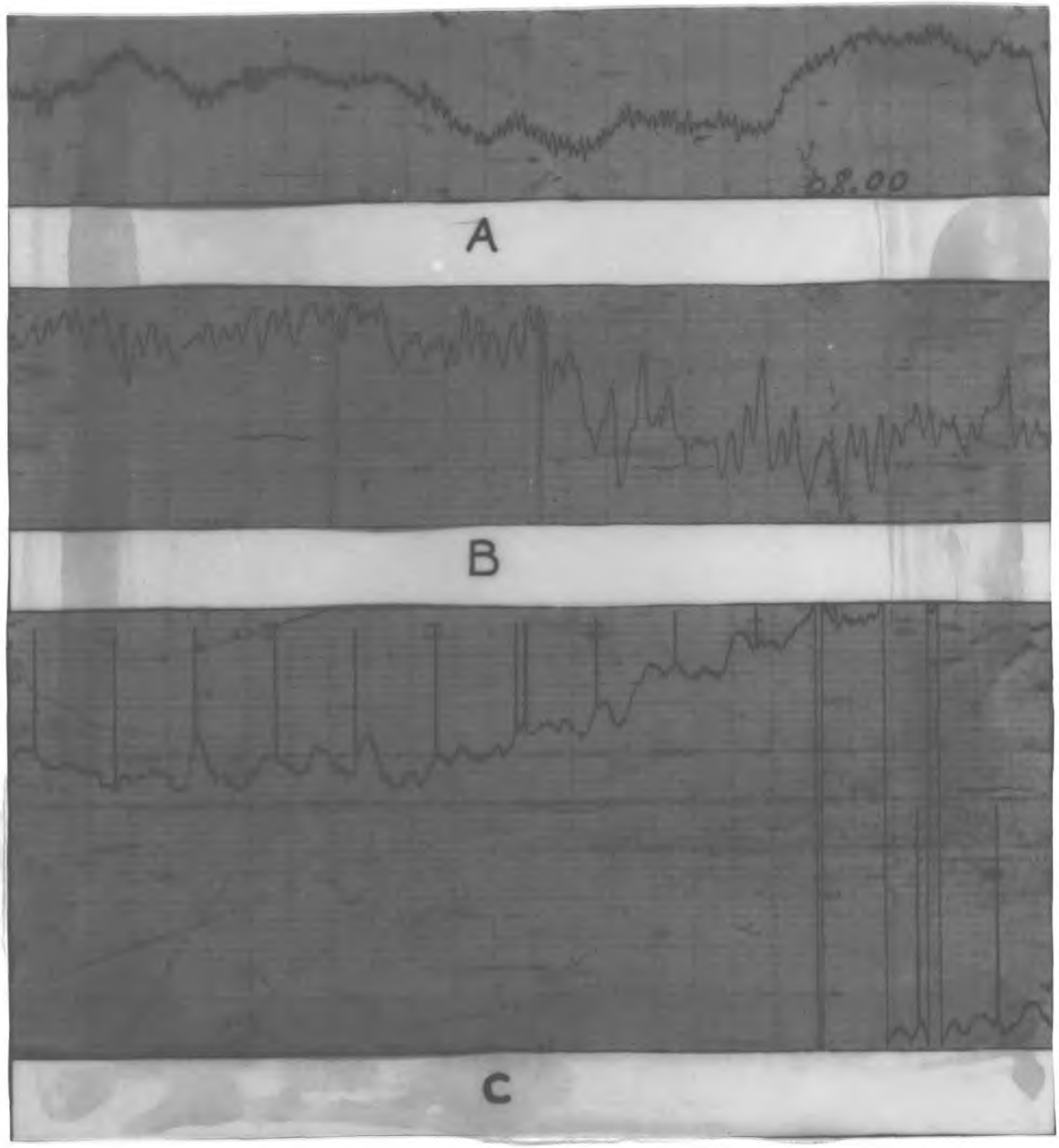

Fig. 7.10. Three sections of record showing the variability of Pc period at the same time of day at the same station.

Eskdalemuir within a week and covering approximately the same time of day. Each record shows distinctly different period from the others. The periods displayed are 20 seconds and 50 seconds in A and B respectively and 90 and 180 seconds in C. In each case the time scale is the same, and is illustrated by the 5 minute timing marks in C.

It was found in some cases that an increase in the period of the predominant continuous pulsations occurred during the course of the forenoon. Two examples are shown in Fig. 7.11

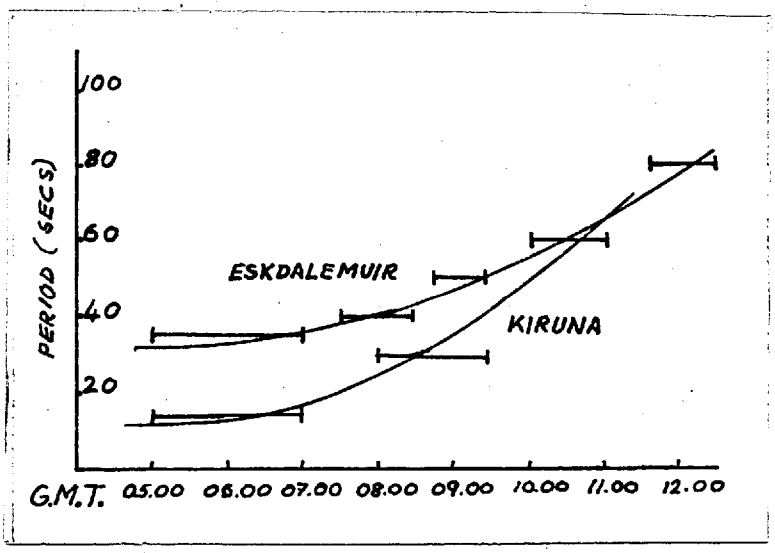

Fig. 7.11. Some examples of the observed increase in Pc period during the morning.

where the average periods of Pc activity are plotted against time of occurrence. It was not possible to demonstrate this property more generally, because of the uncertainty of

measurements and the spread of periods encountered.

The harmonic structure of the spectrum of micropulsation activity would appear to confirm the resonant origin of the phenomenon. Inspection of the records during the compilation of the general analysis showed a great number of periods of good quality events and, in particular, periods which recurred during the observations were 30, 45, 60, 90, 120 and 180 seconds. A further period of 240 seconds occurred, although with less frequency than the higher order periods. The values given to the lower periods are very approximate due to the number of values which occurred. Consider the two harmonic series 240, 120, 80, 60, 48, 40, 34, 30 seconds and 180, 90, 60, 45, 36, 30, 26, 22½ seconds. It is clear that these two series are sufficient to explain the periods observed, and the number of higher harmonics in the low period range agrees well with the uncertainty encountered in attempting to detect a single specific value to the events of this period. The question of false peaks caused by the intermodulation of harmonically related wave trains may exclude the necessity for requiring two series to explain the observed results.

Detailed examination of the periods of Pc activity is obviously required in order to indicate the precise harmonic series occurring, and in particular to resolve the components between 20 and 50 seconds.

The significant conclusion to be drawn from the foregoing remarks is that the fundamental period of Pc activity may be longer than that previously suggested from the direct measurement of Pc events. A fundamental of 180 seconds or 240 seconds is indicated, perhaps suggesting that the origin of pulsations is located near the magnetosphere boundary.

Such values for the period of the fundamental mode of oscillation may invalidate the reasons given by Kato for considering a low altitude resonant cavity. The period of 240 seconds, occurring over the range of latitudes covered does not agree with Dungey's analysis. However the values suggested by Westphal and Jacobs, when the compression of the dipole field and the particle density of the exosphere are taken into account, are in reasonable agreement with a period between 120 seconds and 240 seconds.

Two reservations about the validity of such a simple picture must be remembered. Firstly the period of the longer pulsations are not easy to estimate by virtue of their line width, and the relative shortness of a wave train. A greater volume of data will be necessary before the values of the longer periods which occur can be determined with confidence. Secondly the manner in which harmonics were displayed often suggested that the fundamental and its first and/or second harmonic occurred together, as illustrated in Fig. 7.6, 7.7

and 7.10. While this may not alter the suggested pattern to any great extent, it may indicate, on further study, that the fundamental period of oscillation is itself variable.

Since the E-W component of micropulsations is observed to have a similar magnitude to the N-S at Kiruna, it is not possible to exclude toroidal vibrations from the possible modes of origin, particularly when it is remembered that activity is detected in the vertical component during highly disturbed times. It is observed that during undisturbed times the sequence of activity occurs in a generally similar form in both N-S and E-W components, while within the individual bursts of pulsation the traces do not necessarily correspond. This has been suggested as a possible cause of the incoherence of the total field record, and may represent an intermixing of modes at the same frequency. The wide diurnal range of occurrence is, however, not directly compatible with the conditions imposed in the theoretical treatment of toriodal resonance, where interaction between adjacent lines of force is zero, limiting consequent activity on the ground to the regions corresponding to excited lines of force.

The form of the diurnal spectral distribution of period (Fig. 7.1) is in agreement with the general concept of the deformed magnetosphere, where the confining effect of the solar wind may be expected to reduce the resonant periods in the day time hemisphere. The indicated increase in period

during the course of the day (Fig. 7.11) does not fit this model, since the reverse trend should be indicated. This may be due to lower modes of activity being excited by the more direct action of the solar wind, or to the diurnal variation of such a low altitude resonant cavity as suggested by Kato, due, perhaps, to a diurnal variation of particle density in the lower atmosphere, or to such a daily variation in the density distribution of the exosphere as would affect the calculations of Westphal and Jacobs.

P_t Analysis

Fig. 7.12 shows a comparison of P_T events between Lerwick and Hartland. Evening events at Kiruna were masked by disturbances and few P_T8s were observed at Eskdalemuir. In the analysis events were classified with the value 1 or 2 to distinguish clearly defined transient pulsations from short bursts of pulsation. The graph was plotted using the totals of the designated numbers.

The frequency spectra shown are approximately normalised and indicate a difference in period. The observed period of 120 seconds at Lerwick agrees with the predicted values of the compressed dipole field taking particle density into account, but the Hartland value of 90 seconds does not agree with any expected period.

Fig. 7.13 shows a comparison of the occurrence of P_ts

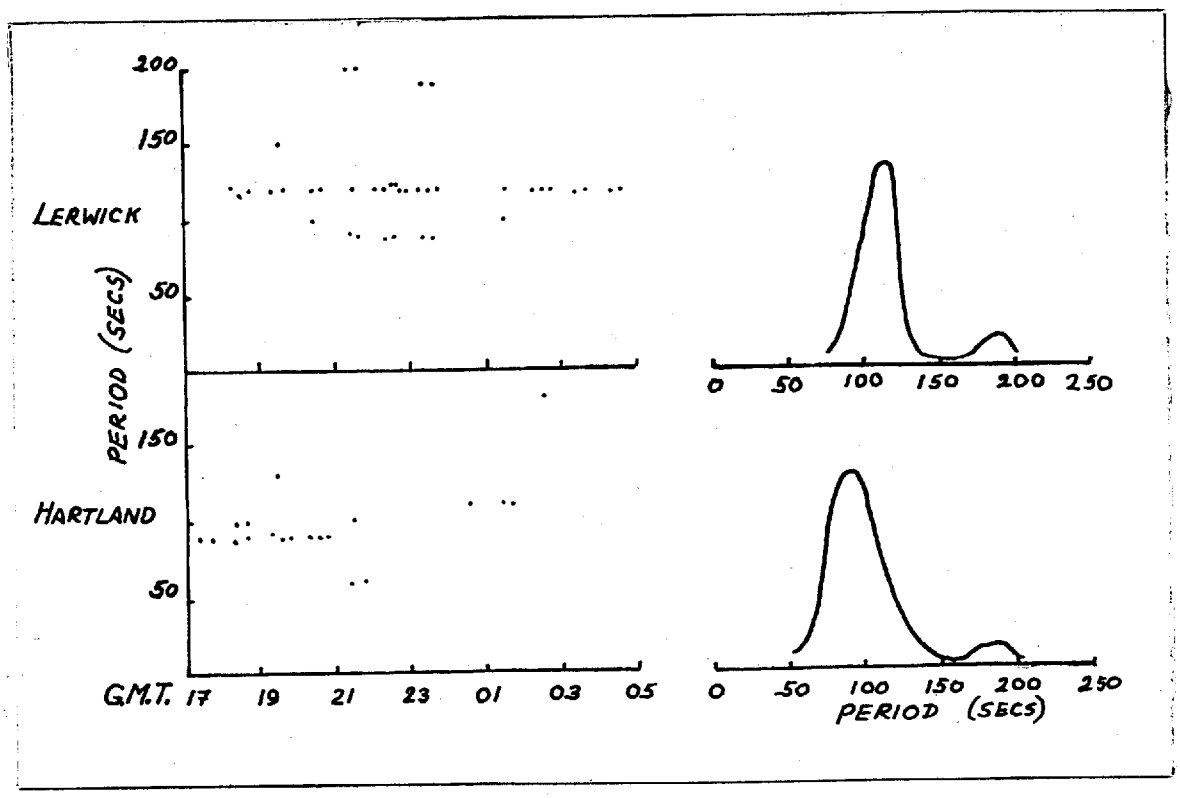

Fig. 7.12. Analysis of P_T events observed at Lerwick and Hartland.

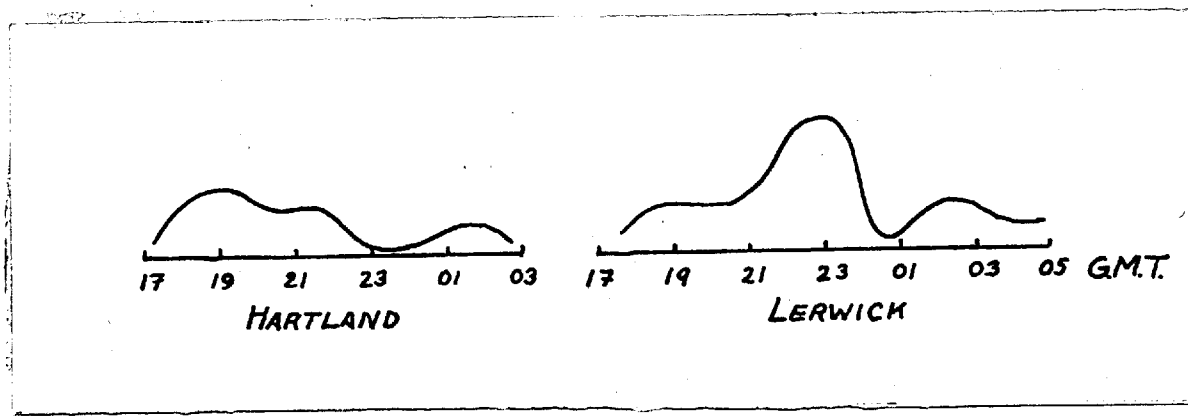

Fig. 7.13. Occurrence of P_T events at Lerwick and Hartland.

at Hartland and Lerwick. The range of occurrence is between 17.00 hours and 03.00, and is seen to be generally complimentary to the range of Pc occurrence. The reduction of activity somewhere between 23.00 and 01.00 is displayed at both stations.

The lack of statistical mass of information about P_Ts hampers any conclusions to be drawn from the analysis.

Fig. 7.14 illustrates three transient pulsations which occurred on different nights at Lerwick. The time scales are all approximately the same and are indicated by the five minute timing marks on A. A and B show periods of 230 and 120 seconds respectively and may be taken to indicate a harmonic structure in the periods of P_ts. They occurred between 22.00 and 23.00, where the peak of P_t activity at Lerwick was observed. Fig. 7.14C shows a transient type event which occurred at 03.30. The period of 30 seconds corresponds to that of Pc's observed at that time. Beyond the record shown in C there occurred two more transient events of the same period, the last one developing into continuous activity.

Large Pulsations

Pulsations with periods in the range 5 minutes to over an hour were observed at all stations visited. At the stations south of the auroral zone the amplitude of such

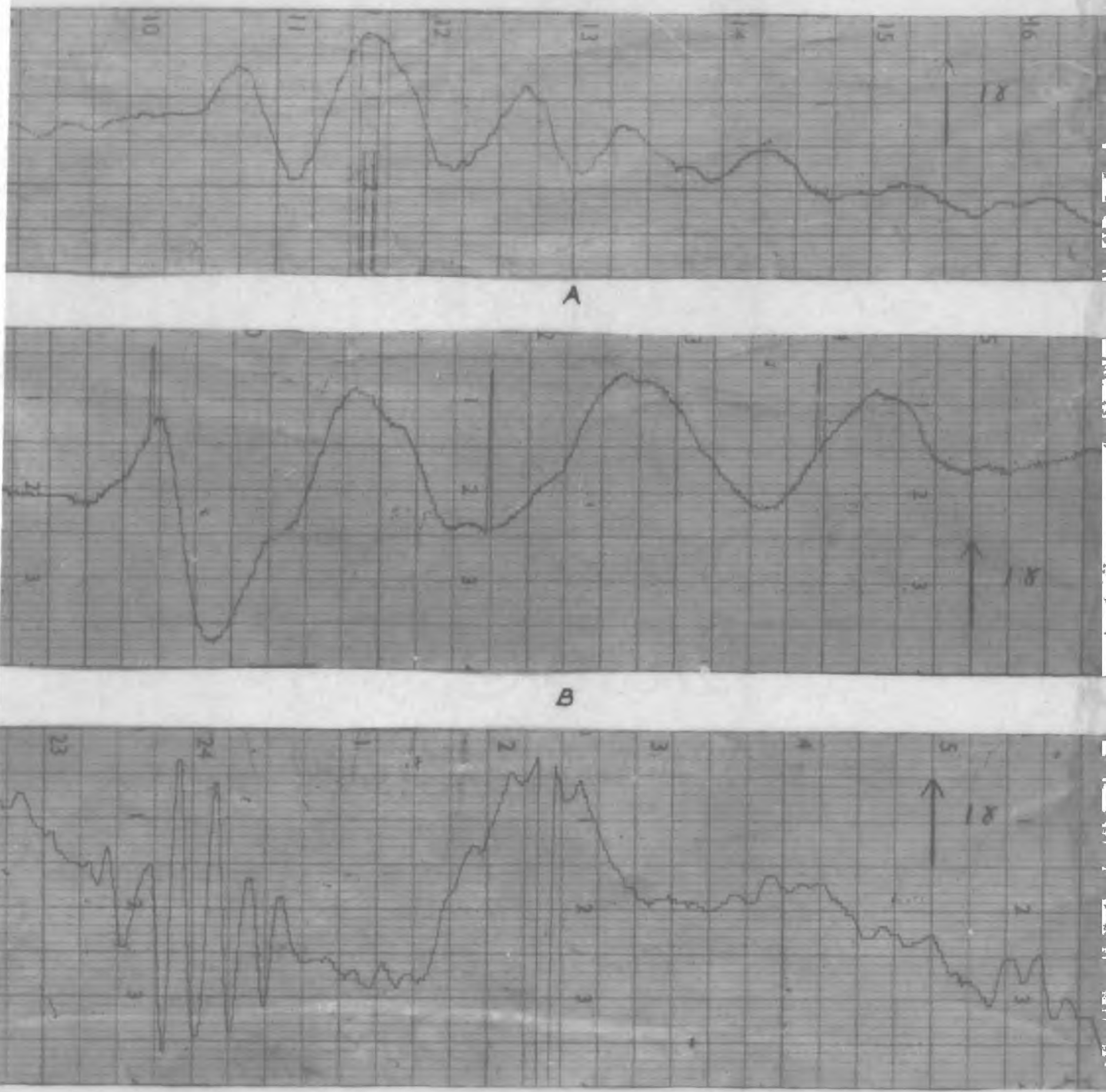

FIG. 7. 14

events was usually less than one gamma. Their occurrence was mainly at night, although long period fluctuations were apparent throughout the day. Fig. 7.8 shows long period fluctuations which are typical of those observed at the lower latitudes, and several other illustrations are to be found in the recordings shown.

At Kiruna, which is almost exactly underneath the nodal point of the auroral current system (Hultqvist and Gustaffson), large amplitude pulsations occurred in the period range 5 - 10 minutes. These occurred mainly at night in association with auroral disturbances, although they often recurred well into the morning. Fig. 7.15 shows an example of this

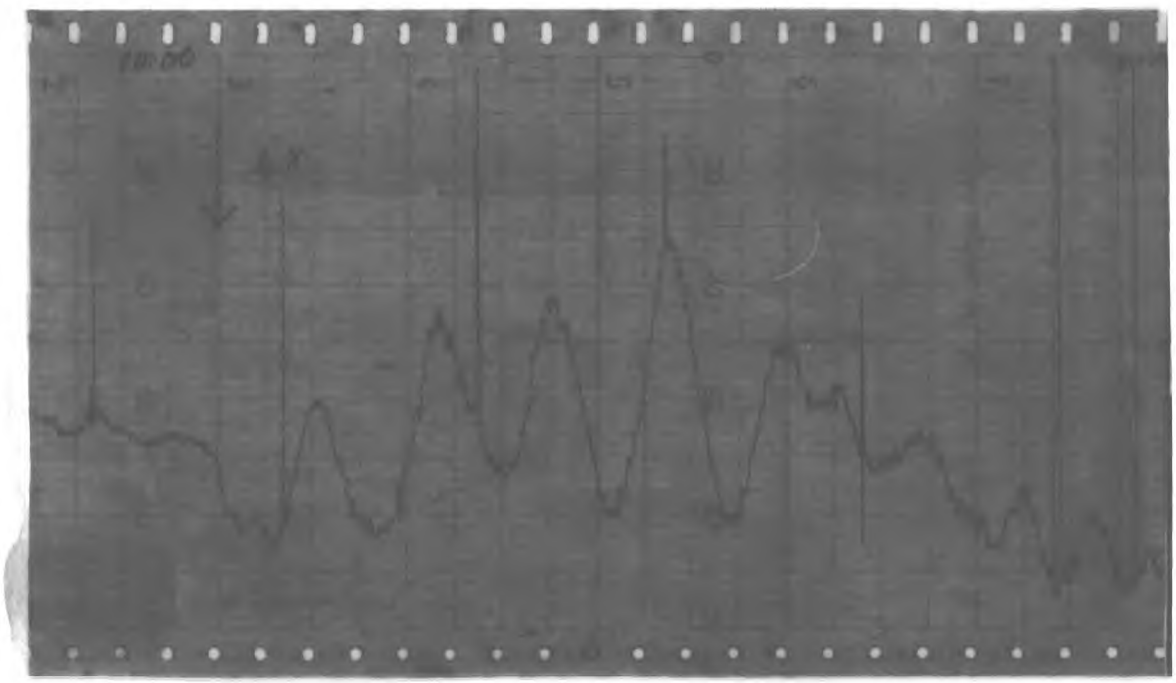

Fig. 7.15. A long period event observed at Kiruna (Period approximately 5 minutes).

activity which occurred at 10.00. The period of the event is approximately 6 minutes and its peak amplitude is 10 gamma. The amplitude increases with time and it starts and ends abruptly. The spikes on the record are spurious counts thought to be due to the proximity of the electronic apparatus to the sensor.

Study of the observatory magnetograms showed that such long period pulsations displayed a strong component in the vertical direction, and at least one case was observed where the event occurred in the vertical component alone. The period corresponds well with the theoretical values and it is of note that Dungey's values agree closely with those of Westphal and Jacobs at auroral latitudes.

Magnetometer and Instrumentation

Sensor: The sensor configuration is considered to be satisfactory for use in ground instrumentation. The sensor was transported in its assembled form in a packing case with other heavier equipment, and on at least one occasion was dropped from a height of two feet to the floor. Having survived these rigours without noticeable effect some confidence may be expressed concerning the robustness of the configuration.

Lamp: The modified lamp design has now been operated continuously for over 4,000 hours and has shown no detectable change in performance. During this time it has been subjected to switching off and on associated with tests of the instrumentation which have taken place. Design work is being undertaken in order to find a sufficiently rigid bulb enclosure and mounting to satisfy the rigorous envirnomental conditions of a rocket launch.

While the valve oscillator is thought to be in every way satisfactory, the use of transistors may have advantages when the total instrumentation requirements of a satellite are considered. The valve oscillator requires 110 - 120 v. H.T. supply which necessitates a multiplier to convert the voltage from the satellite supply, which is typically 30 v. Transistors operating directly from the satellite supply may be preferable. However, it is not clear whether transistor efficiency will be satisfactory when operated at 100 Mc/s nor whether the voltage swing in the exciting coils in a transistor circuit operating from a 30 volt supply will be sufficient to maintain the discharge.

A possible development, which is not essential in most of the magnetometer's applications, is that of isolating the lamp oscillator from the bulb. Such a design would greatly reduce the dimensions of the sensor unit and eliminate magnetism from the lamp circuit. However it is not likely

that this practice will be resorted to unless its necessity is dictated by experimental requirement.

Monitoring System

The performance of the counting and decoding apparatus was satisfactory with the exception of a thickening of the trace, thought to be a ±1 count deviation caused by the magnetism of the energised relays. An example of this form of interference is shown in Fig. 6.10C where the thickening of the trace corresponds to a ±1 count variation. Because of this effect, and the large current required by the decoding relays it has been suggested that transistorised switching circuits might be used in the decoding system. Such an arrangement may be powered from the counter's internal power supply, and would not require a long display time for latching purposes. Thus it is possible to maintain the present magnetic field resolution while eliminating the 1 second display time of the counter to increase the time resolution of the system. It will then be possible to use a $\frac{1}{2}$ second counting time to produce a field resolution of 0.1 gamma and a pulsation resolution upper limit of $2\frac{1}{2}$ seconds.

Resolution.

In Chapter 6 the resolution of the counting system was shown to be $F/10^6T$ gamma, where T is the time in seconds

over which the count is made, and F, in gamma, is the field represented. The examples given were of measuring a 50,000 gamma field to an accuracy of 0.05 gamma with a 1 second counting time. The inverted system of counting was adopted to make full use of the 1 μsec resolution of the available counter.

The above formula indicates that as F decreases, the fractional accuracy to which it can be measured increases. The limit of sensitivity occurs when the indeterminacy of the magnetometer signal frequency is reached due to the noise level.

Consider the case of a sinusoidal wave of peak amplitude S and peak to peak noise N. The uncertainty $d\lambda$ to which a wavelength (or period) may be measured is given by the 'thickness' of the noise measured across the wave in the direction of the θ coordinate (Fig. 7.16). $d\lambda$ at any point on the wave is given by

$$d\lambda_\theta = \frac{N}{\tan I},$$

where I is the slope of the curve.

Hence, assuming a sine wave

$$d\lambda_\theta = \frac{N}{\frac{d}{d\theta}(\sin\theta)}$$

$$= \frac{N}{\cos\theta}$$

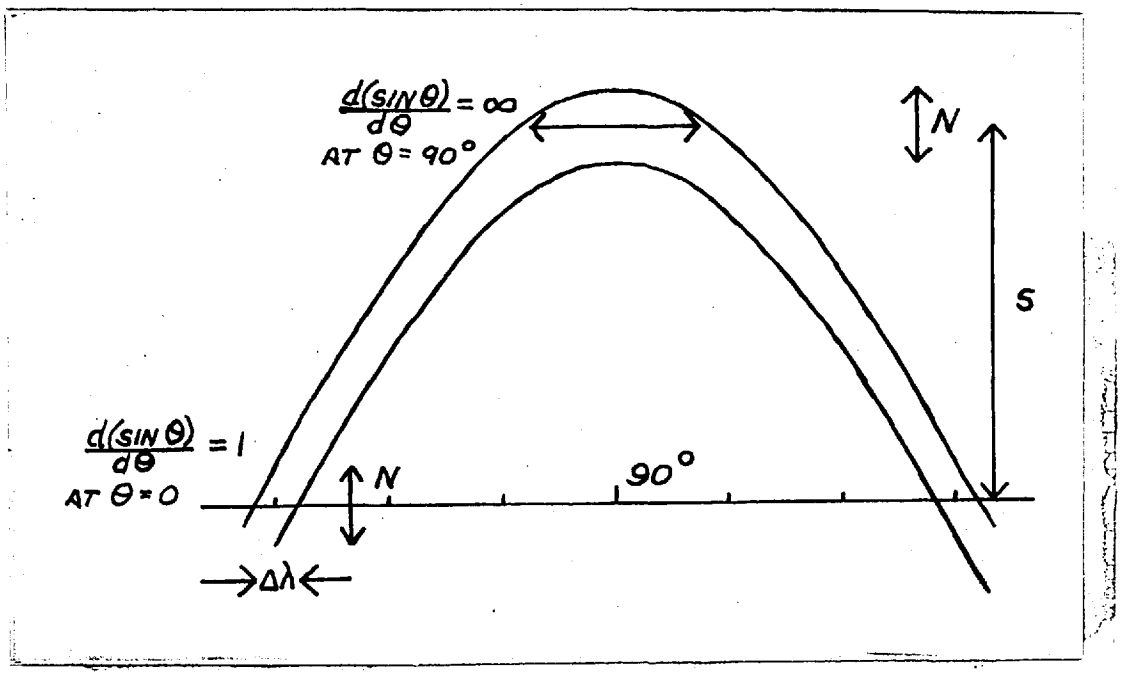

Fig. 7.16 Illustrating the time resolution in a measurement of the period of a noisy sine wave.

The coordinate system is one where the peak amplitude of the wave, S, is of equal magnitude to 1 radian on the θ axis.

Thus $$\frac{d\lambda}{\lambda} = \frac{N}{2\pi S \cos\theta}$$

In counting techniques it is usual to arrange that, in effect, the point at which a wave triggers the gate of the counting scheme is the crossover point, where the error due to signal to noise ratio is least. Thus it is permissable to take $\theta = 0$, whence $\lambda/d\lambda = 2\pi S/N = A$, for convenience in what follows. The value of A represents the ultimate

resolution to which measurements of the magnetometer frequency can be made.

In a counting system the maximum efficiency is reached when the resolution of the magnetometer is equal to that of the frequency standard. If N is the number of periods used to gate the counting of the standard oscillator frequency, then the error in time due to N is 1/f.A, with f = magnetometer frequency and N = f.T.

Where the maximum time resolution is 1μsec then f(= 10^6/A) is the field frequency at which the maximum sensitivity is attained. Thus for a one second count, if A has a value of 25, corresponding to a magnetometer signal to noise (= 2S/N) ratio of 8, f is 40 Kc/s, a field value of 8 x 10^3 gamma. The resolution obtained is 8 x 10^3/ 10^{-6} gamma, i.e. less than 0.01 gamma.

Two further features pertain to this discussion. Firstly, at the low frequencies indicated a signal-to-noise ratio of 30/1 has been observed, and secondly, the addition of a tuned amplifier to the Earth's field instrument improved its signal-to-noise ratio by a factor of five. Thus it is possible by utilising A values of the order of 60 which are available, to measure field variations with a sensitivity as high as 0.005 gamma with a 1 second count, or 0.05 with a 0.1 second count.

In order to improve the resolution of measurement of the

magnetometer two possible methods are available, (1) the use of a frequency greater than 1 Mc/s as the standard (2) the use of biassing coils to reduce the magnitude of the measured field. The use of a higher standard frequency is not discussed further.

The use of biassing fields is illustrated in Fig. 7.17

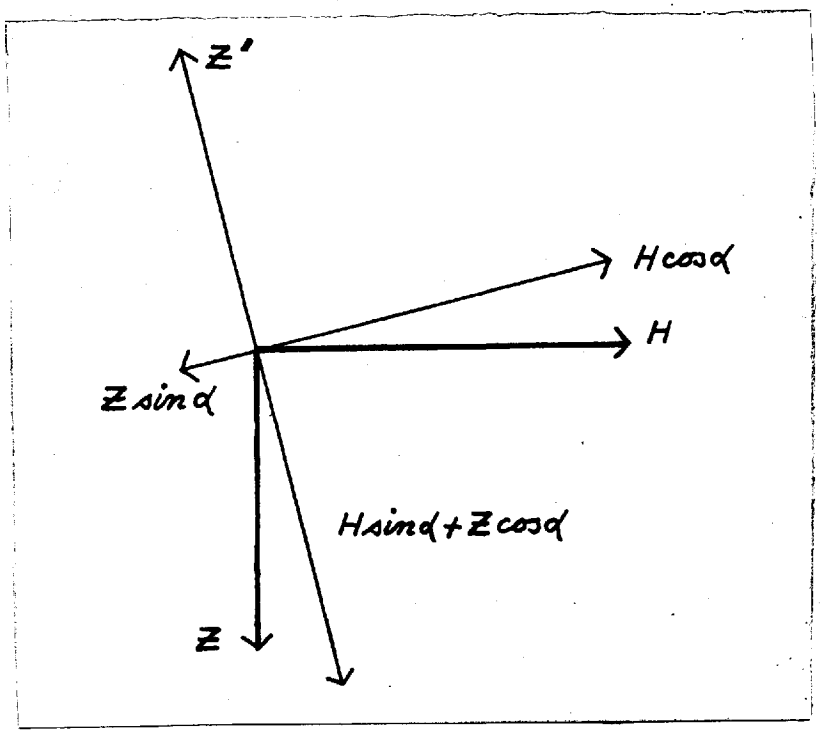

Fig. 7.17

where the vertical component of the total force Z is to be balanced by a bias field Z^1, which in practice is inaccurately aligned with Z. For simplicity the angular inaccuracy is taken to be in the meridian plane.

Then $R^2 = (N - Z^1 \sin\alpha)^2 + (Z - Z^1 \cos\alpha)^2$

$$\frac{dR}{dZ^1} = 0$$

when $Z^1 = H \sin\alpha d\alpha + Z \cos\alpha$

Thus a minimum field value exists, when the resulting field is perpendicular to Z^1 and has a value $H \cos\alpha - Z \sin\alpha$ In the case where α is small the direction of the field to be measured is thus effectively that of H.

For the stability of the reduced field it is necessary to consider the effect of variations δZ^1 of Z^1. The components of δZ^1 along and perpendicular to the H direction are $\delta Z^1 \sin\alpha$ and $\delta Z^1 \cos\alpha$, respectively, and their effect upon the magnitude of the resultant is given by $Z^1 \sin\alpha$, and $(\delta Z^1 \cos\alpha)^2 / 2H$.

If H is similarly reduced by a field H^1, which may have an angular inaccuracy β the variations in the resultant may be referred to the same coordinate system, for simplicity. They are $\delta H^1 \cos\beta$ along the resultant direction and $(\delta H^1 \sin\beta)^2/2(H - H^1)$. Table 7.1 shows the permitted deviations to each component to produce a measured field variation of 1 gamma. The conditions chosen for their calculation were $Z = 5 \times 10^4$ gamma, $Z^1 = 5 \times 10^4$, $H = 2 \times 10^4$, $H^1 = 10^4$ and $d = \frac{1}{2}^o$. Allowable variations are calculated for measurements with and without the use of the biassing field H^1.

It is clear that the greatest stability is required of the bias field acting in the direction of the measured field. It remains a matter for experiment to discover to what extent biassed fields may be used in the study of micropulsations.

The comparatively low stability required for a bias field perpendicular to the direction along which observations are to be made suggests, without direct reference to resolution, that some form of component studies may be undertaken by the rubidium magnetometer, merely, by eliminating either the horizontal or vertical components of the total force.

Conclusions

The dual object of the field study was to determine the capability of the self-oscillating rubidium vapour magnetometer in the measurement of rapid variations of low amplitude of the geomagnetic field, and to provide preliminary information and experimental familiarity with micropulsation phenomena.

The instrumental system has been shown to be reliable in operation over long periods of time, and has provided satisfactory observations of the micropulsations which occurred. Comparison with the variometer at Kiruna showed that apart from that due to the rapid large scale fluctuations, the magnetometer recorded pulsation activity without noticeable

loss. The loss of information due to the scalar form of the measurement is largely overcome by the high sensitivity of which the instrument is capable. This, together with the unrestricted response to low frequency variations have permitted significant results to be made available. The value of the instrument in synoptic observations of micropulsations, and in particular within the frequency domain has been established.

Techniques have been suggested which may be used to increase the resolution of the magnetometer system in both time and magnetic field. The biassed form of the instrument, which may add to the capability of the system requires to be investigated in the field, where the difficulties to be encountered due to the misalignment of the coils and the stability of the biassing currents may be assessed.

It has not been possible to resolve the question of the latitude dependence of micropulsation period, or to indicate in any confident way the mode of excitation of their vibration. However, the harmonic content of the observed pulsations leads to longer periods of the fundamental mode of oscillation than had previously been considered appropriate, and a general agreement with the work of Westphal and Jacobs has been found. The complimentary form of the diurnal range of Pc and P_t activity, together with the harmonic structure shown by each type and the overlapping of

their forms, indicated in Fig. 7.13, may indicate that they differ only in their mode of excitation. It has been shown that during the times when their occurrence overlaps it is possible to have clearly defined transient events with periods corresponding to those of Pc's and almost continuous events at periods corresponding to P_t's. Holmberg has indicated that the observed decay rate of transient pulsations corresponds to the excitation, by a single pulse, of a resonator having the same bandwidth as observed Pc activity. Holmberg's value of bandwidth has been confirmed, but it has not been possible to arrive at a value for the decay rate.

The apparent variation of P_T period with latitude is in general agreement with the ideas of the intuitive model. It is clear that the form of the daily occurrence of P_T's and their period structure must be investigated in some detail, using a much greater amount of data, in order to establish their source and the mechanism of their excitation.

The existence, over the range of latitude studied, of long period pulsations may be related to the higher order modes of the mathematical analysis, or the high altitude poloidal mode. Dungey) did not calculate the periods for such events in detail; however, he did indicate that one hour was the order of magnitude of the period to be expected.

The observations have established the existence of 'pearl' type of phenomena within the period range 30 to 120 seconds and, in one example shown, indicate a relationship between such events and a long period field fluctuation. The pearls discovered by Mm. Troitskaya and investigated by Tepley and Heacock occurred at periods less than 4 seconds and are thought to be caused by 'bunches' of trapped electrons shuttling to and fro between mirror points. The period of the observed micropulsations are taken to represent the 'bounce' period of the electron bunch between the mirror points, and since the velocity of such a bunch is expected to be greater than the velocity of sound in the corresponding region of the exosphere, it is thought that the shock wave associated with the motion produces the hydromagnetic disturbance. The observations made using the rubidium magnetometer indicate pearl type activity requiring a 'bounce' period up to 40 times as long. The extreme value may correspond to the case where proton bunches are involved.

However, it is not established that the amplitude modulation observed in the longer period range has the same significance as the pearls of Mme. Troitskaya. The association of the event with a longer period disturbance may suggest an entirely different cause, based on a stimulus, of some undefined form, acting upon a damped resonator at regularly

repeating intervals. The existence of the damping of the resonance is demonstrated directly by P_t's. The association with the long period fluctuation may suggest that either the long period wave contains the stimulus, or acts as a shutter, which impedes the exciting stimulus, e.g. dilating the field around the area resonating at the higher frequencies. It is possible, also, that a variable transmission of shorter period waves may be set up in the exosphere associated with the long period fluctuation, resulting in a simple amplitude modulation of the short period event. However, since an example is shown where pearl type events occur without any association with long period events further speculation is unwarranted without a greater mass of information.

Several conclusions may be drawn from the described observations which will be used in the planning of future studies of the subject.

1. Any attempt to detect period differences between pulsations occurring at different latitudes must use coincident methods. Coincident measurements at a chain of stations at approximately the same longitude will allow detailed measurement of the period variation of individual events, and will allow observations of the extent of their simultaneous occurrence to be made. A suitably placed

station at a different longitude will provide additional information on the daily occurrence, which may be important in locating the source of P_t's.

2. In general manual analysis of the records is considered to be preferable to machine analysis, because of the detailed inspection which is required in the identification of events and the large range of activity which occurs. Machine analysis is not expected to be available because of the amount of the data to be examined, and an automatic system of recording in digital form would therefore be wasteful. However, it is possible that machine analysis may be employed to provide detailed examination of specific events and of the periods involved in intermodulating trains, e.g. to determine the line width of events, and the decay constants of P_t's.

3. In order to resolve some of the questions of mode and propagation it is necessary it provide detailed information about the vector properties of the vibrations. It is not expected that the rubidium magnetometer will provide this information completely in the short period range. Vector information may allow a determination of the plane of polarisation, if it exists, and the direction of rotation of the vibration vector.

In conclusion it must be admitted that the statistical data used in this analysis is limited by the number of days spent at each station and some of the results, and the conclusions drawn from them, must be confirmed by a substantially increased amount of data. However, the very high resolution in time and magnetic field allowed every pulsation which occurred to be inspected, a feature which is not common on some previous analyses of micropulsations.

TABLE 7.1

	$\left(\frac{\delta Z^1 \cos\alpha}{2H}\right)^2$	$\delta Z \sin\alpha$	$\delta H \cos\beta$	$\left(\frac{\delta H \sin\beta}{2H}\right)^2$
	$\frac{\delta Z^1}{Z^1}$	$\frac{\delta Z^1}{Z^1}$	$\frac{\delta H^1}{H^1}$	$\frac{\delta H^1}{H^1}$
without H^1	$\frac{1}{250}$	$\frac{1}{500}$	-	-
with H	$\frac{1}{360}$	$\frac{1}{500}$	$\frac{1}{10^4}$	$\frac{1}{200}$

ACKNOWLEDGEMENTS

The author wishes to express his thanks to the following individuals and groups for their contributions to this research.

1. His supervisor Professor J.McG. Bruckshaw, for advice and discussion throughout.
2. His colleagues, Drs. S.H. Hall and M.J. Usher, whose cooperation was invaluable.
3. The National Aeronautics and Space Agency (N.A.S.A.) for the opportunity to work at the Goddard Space Flight Centre for a year (1961) during which time many valuable discussions took place with Dr. Heppner, Dr. Ness, and the staff of the Magnetic Fields Section.
4. Varian Associates, Palo Alto, California, for their assistance in the provision of sensor components and information on the operation of the magnetometer.
5. G.E.C., Hirst Research Centre, Wembley, Middlesex, for the manufacture of sensor glassware, and for their cooperation in the development of the enclosed bulb.
6. The superintendants of the four observatories, their staffs, and their respective governing bodies, for the use of the facilities and their assistance in carrying out the field work.
7. The British National Committee for Space Research under

the auspices of the Royal Society, and D.S.I.R., who supported the development of the magnetometer.

8. Shell Research Ltd., who provided funds which were needed for the field equipment.

REFERENCES

Beard, D.B., J.G.R. Vol. 65, p.3559 (1960).

Bell, W.E. & A.L. Bloom, Phys. Rev. No. 107, p.1559, (1957).

Bender, P.L., Ann Arbor Conference on Optical Pumping, University of Michigan (1959).

Bloom A.L., Ann Arbor Conference on Optical Pumping, University of Michigan (1959).

" " Scientific American, October 1960.

" " Applied Optics, Vol. 1, No. 1 (1962).

Bridges H.S., Kyoto Conference on Cosmic Rays and Earth Storms (1961).

Cahill L.J., and J.A. Van Allen, J.G.R., Vol. 63, p.547 (1956).

" " State Univ. of Iowa (1958).

Cahill L.J. and P.G. Amazeen, J.G.R. Vol. 68, p.1835 (1963).

Cain J.C., I.R. Shapiro, J.D. Stolorik and J.P. Heppner, J.G.R., Vol. 67, p.5055 (1962).

Coleman P.J., L. Davis and C.P. Sonnet, Phys. Rev. Letters, Vol. 5 p.43 (1960).

Dehmelt H.G., A. Phys. Rev. 105, p.1487 (1957).

B. Phys. Rev. 105, p.1924 (1957).

Dungey J.M., A. Penn. State University Sci. Reps. No.57 (1954)

B. Pen.. State University Sci. Reps. No. 69 (1954).

Franzen W. and A.D. Little, Ann Arbor Conference on Optical Pumping (1959).

Heacock R.R., J.G.R. Vol. 68, p.589, (1963).

Heppner J.P., T.L. Skillman & J.C. Cain, International Space Science Symposium, COSPAR, Florence (1961).

Jacobs J.A., Utrecht Symposium on Rapid Magnetic Variations (1961).

Jacobs J.A., and K.O. Westphal. "Physics and Chemistry of the Earth", Vol. 5, Pergammon Press.

Kastler, A., J. Phys. Radium, Vol. 11, p.255 (1950).

Kato Y., Utrecht Symposium on Rapid Magnetic Variations, 1961.

" Sci. Rep. of Tohoku University (1961).

Kopferman H., 'Nuclear Moments' Academic Press Inc. New York 1958.

Meredith L.H., L.R. Davis, J.P. Heppner and O. Berg, Rocket Auroral Investigations U.S. Naval Res. Labs (1958).

McNicol R.W.E., J.S. Mainstone and J.R. Wilkie, Imperial College on the Ionosphere (1962).

Ness N.F., Kyoto Conference on Cosmic Rays and Earth Storm (1961).

Parsons L.W. and Wiatr Z.M. Jour. Sci. Inst. Vol. 39, p.292 (1962).

Rabi I.I., N.F. Ramsey and J. Schwenger, Rev. Mod. Phys. Vol.26 p.167 (1954).

Siebert M., Planetary and Space Science, Vol. 12, p.137 (1964).

Singer S.F., E. Maple and W.A. Bowen, J.G.R. Vol. 56, p.265, (1951).

Singer S.F. Trans. A.G.U. Vol. 38, p.175 (1957).

Shapiro I.R., J.D. Stolarik and J.P. Happner, J.G.R. Vol. 65, p.913 (1960).

Skillman T.L. and Bender P.L. J.G.R. Vol. 63 p.513. (1958).

Tepley L.R., J.G.R. Vol. 66, p.1651 (1961).

Triotskaya V.A., J.G.R. Vol. 66 p.5 (1961).

" Utrecht Symposium on Rapid Magnetic Variations (1961)

Watanabe T., Sci. Reps. of Tohoku Univ. (1961).

Westphal K.O. and J.A. Jacobs, Geophys. Jour. R.A.S. Vol. 6, p.360 (1962).

Zmuda A.J., J.G.R. Vol. 63, p.477 (1958).

De Zafra R.L., American Jour. of Phys. Vol. 28, p.646 (1960).